DOCTOR OF ENGINEERING (ENGD)

Analysis and Mitigation of the Low Inertia Challenges Due to the High Renewable Penetrations

Bian, Yuankai

Award date:
2019

Awarding institution:
University of Bath

Analysis and Mitigation of the Low Inertia Challenges Due to the High Renewable Penetration

submitted by

Yuankai Bian

for the degree of Doctor of Philosophy

of the

University of Bath

Department of Electronic and Electrical Engineering

September 2018

Abstract

The power system inertia refers to the stored kinetic energy in all synchronous rotating elements, which determines the stability of system frequency as it is the initial resistance to any frequency deviations caused by the generation failure, generation shortfall, a sudden load increase. The integration of the asynchronous renewable generations reduces the overall system inertia thus introduces new challenges for maintaining the stability of system frequency. For a conventional generation dominated system, frequency stability is ensured by the adequate frequency response. However, for a renewable dominated system, the same frequency response reserve is unable to guarantee the frequency stability due to the reduced inertia. When there is a sudden load/generation imbalance, the consequences of the reduced inertia on the system operation are the rapid change in frequency, the potential hazards of the higher rate of change of frequency (ROCOF) to trip the ROCOF-based protection relays for the distributed generators, and the significant frequency drop causing unintentional low-frequency demand disconnection.

Due to the reduced inertia, the system operation planning is shifting from efficiency driven to the balance between efficiency and stability, which is commonly investigated in the unit commitment (UC) to determine the optimal generation scheduling. The existing research in addressing the reduced inertia issues from the perspective of UC optimisation only considers the ROCOF requirements for inertia and ignores the requirements for the maximum frequency drop allowed due to the lack of the representation for the frequency dynamics. The UC is a mixed-integer problem and the transcendental relationship between inertia and the minimum frequency raises the difficulty to not only implement the inertia-related constraint into the UC consideration but also solve the mixed-integer nonlinear-constrained problem. Further challenges from considering the inertia-related constraints into UC is to bring finical incentives for the generator with low output and high inertia contributions. For the current practice, the inertia is provided voluntarily and the significance of inertia is not reflected and rewarded.

This thesis aims to address the challenges of the system operation planning and the market incentives. For the operation planning perspective firstly a frequency mathematical model is proposed that can analyse the representation of the frequency transient dynamics for the initial ROCOF, the minimum frequency and the quasi-steady-state frequency during contingencies; secondly the frequency-related constraints are incorporated into the UC generation scheduling problem for the system operation planning while ensuring the stability of system frequency.

Finally, an inertia market is developed for the inertia providers to reward with an incentive for the provision of inertia based on the UC optimisation results. The major contributions of this work are listed below:

1. The frequency mathematical model in the existing research neglects the demand frequency sensitivity and the primary frequency response speed, thus causing inaccuracy in frequency transient dynamics. This research brings the two into the scope and presents an aggregated mathematical approach by solving the piecewise continuous differential equation set to model the frequency dynamics after a sudden load/generation imbalance according to the primary frequency response availability, which enables the inertia-dependent frequency-related constraints to be implemented in the practical power system operation planning.
2. The demand side inertia contributions are often being overlooked for inertia quantifications due to its minimal effect in the conventional generator dominated system. This research develops a method to quantify the demand side inertia contributions by using linear regressions to separate the generation side inertia contribution from the total system inertia based on the historical data of frequency outage events and consider the power/frequency ratio as an indicator to the inertia contribution in spinning reserves.
3. The inertia-dependent frequency-related constraints, derived from the frequency mathematical approach, are incorporated into the consideration of the frequency constrained UC (FCUC) optimisation. The non-linear frequency-related constraints are implemented through the two-layer heuristic update criteria for the Lagrange multipliers. The pricing for the provision of inertia is obtained through the marginal price reflecting the necessity and availability of providing the additional inertia.

Acknowledgements

First and foremost, I would like to express my deepest gratitude to my supervisor, Prof. Furong Li, who has provided me with valuable and enlightening guidance, impressive kindness and patience.

I shall extend my thanks to other academic staffs in Department of Electrical and Electronic Engineering for their willingness to share knowledge with me. I would like to thank all my colleagues and friends in the University of Bath for their support over the years. I would also like to thank the colleagues and friends of the 2 East fitness team, for helping me find my six pack.

In addition, I am sincerely grateful to the University of Bath for providing me with not only the scholarship but most importantly the opportunity to meet my life-long partner, Chi Zhang.

Last but not least, I would like to express my ultimate gratitude to my beloved parents, who give me endless support and encouragement.

Contents

List of Figures

List of Tables

List of Abbreviations

AC	Alternating Current
ACE	Area Control Error
AGC	Automatic Generation Control
AGR	Advanced Gas Reactor
BESS	Battery Energy Storage System
BMU	Balancing Mechanism Unit
CCGT	Combined Cycle Gas Turbine
CHP	Combined Heat And Power
DC	Direct Current
DFIG	Doubly-fed Induction Generator
DSR	Demand Side Response
ED	Economic Dispatch
EFR	Enhanced Frequency Response
ENCC	Electricity Network Control Centre
ENTSO-E	European Network of Transmission System Operators for Electricity
FFR	Firm Frequency Response
FS	Frequency Support
HFR	High Frequency Response
HIE	Hidden Inertia Emulator
HVDC	High Voltage Direct Current
LFC	Load Frequency Control
LFDD	Low Frequency Demand Disconnection
LOM	Loss of Mains
MFR	Mandatory Frequency Response
MIQP	Mixed Integer Quadratic Programming
ODE	Ordinary Differential Equation
PFR	Primary Frequency Response
PMU	Phasor Measurement Unit

PVPP	Photovoltaic Power Plant
PWR	Pressurised Water Reactor
ROCOF	Rate of Change of Frequency
RPM	Revelution per mimunites
SFR	Secondary Frequency Response
SQSS	Security and Quality of Supply Standard
TSO	Transmission System Operator
UC	Unit Commitment
UFLS	Under Frequency Load Shedding
UK	United Kingdom
VFD	Variable Frequency Drive
VS	Vector Shift
WAMS	Wide Area Monitoring System
WECC	Western Electricity Coordination Council
WTG	Wind Turbine Generator

List of Symbols

E_{KIN}	Stored kinetic energy in the generator
α	Additional inertia contribution from partially-loaded spinning reserve
$B_{i,t}$	Start-up signal of the generator i at time t
ΔD	Response from frequency-sensitive demand
ΔE_t	Mismatch of the inertia requirement
$\Delta P_{D,t}$	Mismatch of the power balance constraint
ΔPFR	Response from the generating units
ΔPFR_t	Mismatch of the PFR requirement
ΔR_t	Mismatch of the spinning reserve constraint
D_{f_N}	Total system demand
D_{f_n}	Total system demand in p.u.
DP_i	Governor droop of the generator i
E_{dem}	Inertia contribution from the demand
E_{gen}	Inertia contribution from the generation
$E_{gen,\alpha \cdot K}$	Inertia contribution from the spinning reserve
$E_{gen,output}$	Total generation side inertia estimation considering the generation outputs of d
E_i	Stored kinetic energy of the machine
$E_{i,t}$	Inertia contribution of the generator i at time t
$E_{Req,t}$	System inertia requirement at time t
E_{sys}	Stored kinetic energy of the system
$f(t)$	System frequency in p.u.
f_0	System frequency prior to the event in p.u.
f_{base}	Frequency base
FC_i	Fuel cost of generator i
f_{limit}	Frequency nadir requirement in p.u.
f_{min}	Minimum frequency in p.u.
f_N	Nominal frequency in p.u.

f_n	Nominal frequency in p.u.
f_{qss}	Quasi-steady-state frequency requirement in p.u.
f_{SL}	Statutory limit of the system frequency, i.e. 49.5hz.
h_{dem}	Demand side inertia constant
H_i	Averaged inertia constant of a particular generation type
H_{sys}	Inertia constant for the power system
i	Generator index
K	Power/frequency ratio
k	Iteration index
k_{DFR}	Demand frequency ratio
k_{dfr}	Demand frequency ratio in p.u.
${\lambda_t}^D$	Lagrange multiplier for power balance constraint
${\lambda_t}^E$	Lagrange multiplier for inertia constraint
${\lambda_t}^{PFR}$	Lagrange multiplier for PFR constraint
${\lambda_t}^R$	Lagrange multiplier for spinning reserve constraint
N	Total number of generators
ω_N	Rated angular velocity of the generator
P_D	Total system demand
$PFR_{i,t}$	PFR contribution of the generator i at time t
$PFR_{Req,t}$	System PFR requirement at time t
P_i^{max}	Maximum generation output of generator i
P_i^{min}	Minimum generation output of generator i
$P_{i,t}$	Generation of the generator i at time t
$P_{D,t}$	System demand at time t.
P_{loss}	Sudden active power imbalance
P_{ni}	Actual generation output of a particular generation type
P_{PFR}	PFR reserve
r	PFR ramp rate
RC_i	PFR providing cost of generator i
${r_i}^d$	Ramp down rate of the generator i
${r_i}^{sd}$	Shut-down rate of the generator i
${r_i}^{su}$	Start-up rate of the generator i
${r_i}^u$	Ramp up rate of the generator i
r_{opt}	Minimum PFR required for frequency nadir
R_t	System reserve requirement at time t
S_{base}	Power base
SD_i	Shut down cost of generator i

S_N	Rated apparent power of the generator
ST_i	Start-up cost of generator i
T	Total number of demand settlements
t	Settlement index
t_1	Time of primary frequency response start
t_2	Time primary frequency response reaches maximum
${t_i}^d$	Minimum downtime of the generator i
$T_{i,off}$	Consecutive time of generator i at off-state
$T_{i,on}$	Consecutive time of generator i at on-state
${t_i}^u$	Minimum up time of the generator i
t_{min}	Time to reach frequency nadir
$U_{i,t}$	On-off states of the generator i at time t
$X_{i,t}$	Shut-down signal of the generator i at time t

Chapter 1

Introduction

THIS chapter describes the background, motivations, objectives, challenges and contributions of this work. The outline of the thesis is presented at the last.

1.1 Research Background

1.1.1 Power System Frequency

The power system frequency is a significant parameter regarding the operation of the power grid which directly indicates the active power balance between the generation and consumption. Any mismatch between the two will cause the frequency to deviate from the nominal value. The system frequency will rise if electricity generation exceeds consumption and vice versa [1].

Several frequencies were used in the late 19^{th} and early 20^{th} centuries when the commercial use of the electricity developed dramatically. The frequency standardisation gradually evolved into two camps: 50 Hz for Europe and 60 Hz for the United States. Now the two frequencies coexist with no clear desire for a global standardisation due to the lack of strong technical evidence to prefer the one over the other [1, 2].

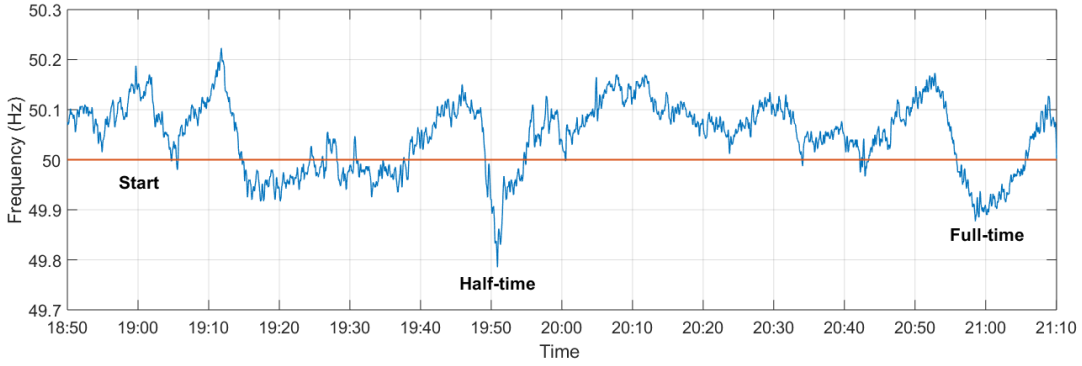

Figure 1-1: Frequency oscillations on 18^{th} of June 2018 [3]

The frequency standard in the United Kingdom (UK) is 50Hz. The unified frequency makes the formation of the power grid possible by connecting all the generators synchronously and delivering the power to the end users through transmission and distribution networks. To achieve a continuous operation of the power grid, the frequency stability requirements for the normal operating condition and during contingencies needs to be met. For the normal operating condition, the electricity generations and consumptions are rarely perfectly balanced, resulting in frequency oscillations. Figure 1-1 shows the frequency oscillations of the UK power system on the evening of June 18, 2018 [3]. However, as long as the frequency deviations are within the operational limits, the power system can endure the oscillations without interrupting the continu-

ous operation of the power system. As shown in Figure 1-1, there were two frequency dips around 19:50 and 21:00, which match the halftime and finish time of the football match between England and Tunisia during the 2018 FIFA World Cup. As observed, a sudden change in electricity consumption by users will lead to frequency changes. To keep the frequency oscillations within the operational limit, the traditional method is to guarantee that generation follows demand. As for the system contingencies, such as generation loss, frequency responses are deployed to return the frequency back to the designed nominal value.

1.1.2 Power System Inertia

The system inertia refers to the stored kinetic energy in all rotating components such as the rotors, shafts, gears that are synchronously connected to the system [1, 4, 5]. The transmission-connected conventional fossil-fired generators, containing a large weight of rotating masses, are the main inertia providers [4, 5]. Being synchronised to the system, the stored kinetic energy is able to perform as the resistance to any change in machine speed triggered by the change in the electrical power imbalance, such as the generation failure, generation shortfall, transmission failure, a sudden increase in load [1]. In the case of the demand exceeding the generation, the system frequency decreases, and the stored kinetic energy in the synchronous rotating elements will be released into the system to compensate the power mismatch, thus resisting the frequency reduction. When the generation is more than the demand, the system frequency increases and the synchronous rotating elements are able to resist the frequency rising by storing extra kinetic energy. Hence, the total system inertia provides initial resistance to any frequency deviations, which is the indicator of the robustness and stiffness in terms of the stability of the system frequency.

High levels of inertia reduce the difficulty for the system to handle the transient changes in system frequency. Lower system inertia levels increase the possibility of rapid change in frequency and a small disturbance could result in severe system faults such as the loss of generation or demand. The risk of low inertia increasingly becomes prevalent as the power industry is undergoing a decarbonisation transition, conventional generation plants increasingly being replaced by renewable generations, substantially reducing the inertia providers in the system [4, 5].

1.1.3 Decarbonisation of the Power Industry

Climate change is one of the biggest crises people are facing in the 21st century. Studies show that the world is one degree Celsius warmer than the pre-industrial average temperature back in the period between 1850 and 1900 [6]. Greenhouse gases, i.e. carbon dioxide, emitted by the burning of fossil fuels is the predominant cause for not only global warming but also the other climate issues such as the rising sea levels, ice mass reduction and frequent extreme weather events. In order to mitigate climate change, legislations have been established to limit greenhouse gas emissions. The Kyoto Protocol was signed in 1997, which stipulated the emission reduction assignments for developed countries [7]. The Copenhagen Summit in 2009 was a follow up to the Kyoto Protocol due in 2012, but there were no legally binding agreements. In 2015, the Paris Agreement was proposed to limit the global average temperature increase within 2 degrees Celsius above the pre-industrial level and strive to reduce this number to 1.5 degrees Celsius [8]. In the meantime, the European Union and the UK government have created their own emission reduction targets stated in European Union Climate and Energy Package and the UK Climate Change Act 2008 to achieve 20% greenhouse gas emission reduction from the 1990 level by 2020 for EU [9] and 80% greenhouse gas emission reduction from the 1990 level by 2050 for the UK [10].

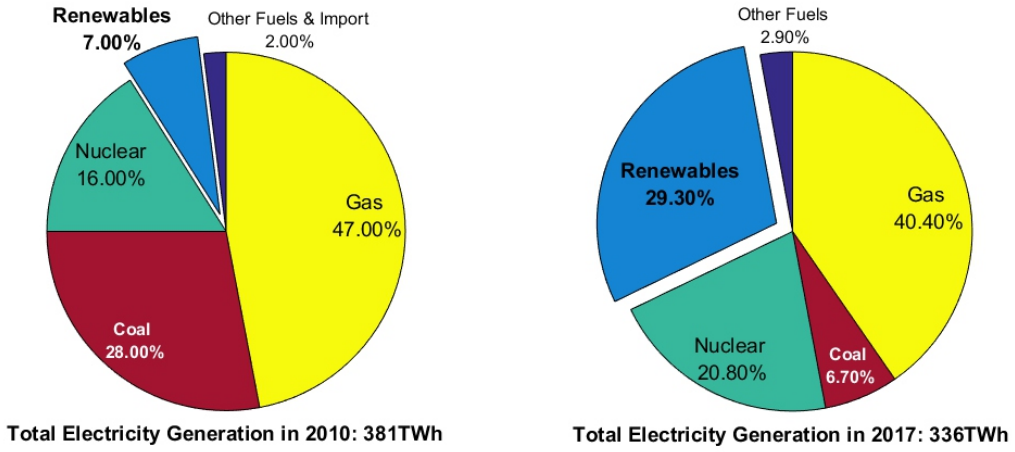

Figure 1-2: Shares of electricity generation by fuel types in 2010 and 2017 [12, 13]

The power industry is one of the largest sources of greenhouse gases emissions. The electricity generation was responsible for 42% of the world's total CO_2 emissions in 2015 [11]. Therefore, the decarbonisation of the power industry is imperative. Both the environmental and economic benefits of the zero-emission non-fuel renewable energy

have rose their popularity worldwide. Thanks to the legislations and the state-of-the-art low-carbon technologies, some progress can already be seen regarding the environmental concerns. For example, 2015 was the first year since the 1990s that the global CO_2 emissions from fuel combustion had not grown while the global economy kept growing [11]. Figure 1-2 shows the changes in the electricity generation shares by fuel types for the UK power system in 2010 and 2017 [12, 13]. Due to the improved efficiency and the increasing contributions from the embedded generators, the total electricity generation reduced from 381 TWh in 2010 to 336 TWh in 2017. However the share of renewables increased from 7% in 2010 to 29.3% in 2017 while the share of traditional fossil-fuel (coal and gas) reduced from 75% in 2010 to 47.1% in 2017 [12, 13].

The increasing popularity of renewable generation reduces the carbon emissions while it brings new challenges for the frequency stability in terms of the reduced system inertia.

1.1.4 New Challenges for Frequency Control

As the adoption of intermittent, low carbon renewable generation increases, system inertia decreases significantly and poses a major threat to the system frequency stability. The reduced system inertia would amplify the degree of frequency deviations for any possible contingencies and a relatively small disturbance could result in large frequency excursions from the nominal. The majority of the renewable generators, such as the variable speed wind turbines, are asynchronous with the system. The turbine is de-coupled from the grid to extract the maximum wind power, such that the inertial energy stored in the turbine is disabled [14, 15]. For photovoltaic power plants (PV-PPs), there is no inertial energy due to the lack of rotating components. Other challenges in the large-scale adoption of renewable energy generation are the generation scheduling with the intermittent nature of wind and solar, affecting the cycling of the conventional generators.

From an economic point of view, renewable generators are expected to produce as much electricity as possible to take full advantage of wind and solar power; otherwise, it would be a waste of energy. For a system with large adoptions of renewable generation, they must be de-loaded by letting go a certain amount of wind energy or shading the PV-PPs to provide frequency response [16, 17, 18, 19], which violates the economic purpose of renewable generation. The work in this thesis addresses the challenges of the reduced inertia raised by the adoption of the renewable generation from the perspective of system operation planning and market incentives to achieve a balance

between efficiency and frequency stability.

1.2 Research Motivations and Objectives

The total power system inertia is decreasing as the consequence of the increasing penetration of renewable energy. The problems of the reduced system inertia are the rapid change in frequency, such as the greater initial rate of change of frequency (ROCOF) and the significant frequency drop followed by a generation/consumption mismatch. The potential hazards of the higher ROCOF and the lower frequency nadir are the miss-trip of the ROCOF-based protection relay for distributed generators and the unintentional low-frequency demand disconnection (LFDD), respectively [20, 4, 5]. The size of the power system determines the severity of the low inertia challenges. For the UK power system, the trend of decreased system inertia is an inevitable obstacle on the path to low carbonisation.

1.2.1 Motivations

As a system dominated by the synchronised conventional generation naturally has sufficient inertia, the current practice of frequency regulation focuses on ensuring that sufficient frequency response is available in the system from the conventional generators to compensate the largest potential generation loss [20]. However, the situation is not the same for a future system dominated by renewable generation with a low system inertia. Due to the response deadband, the frequency might deviate beyond the limit of LFDD even if sufficient frequency response is available. The frequency problem transforms from a one-dimensional problem only considering the frequency response into a two-dimensional problem considering both the frequency response and inertia. Therefore, a representation of the relationship between inertia and frequency response is required to analyse the frequency dynamics.

Inertia, as a valuable asset to the frequency stability, is not considered in the current system operation planning. To meet the inertia requirements, the conventional generators are required to de-load in order to bring more inertia-providing generators online. The lack of appropriate incentive schemes for inertia may no longer provide sufficient returns for the inertia-providing generators to service.

To address the frequency stability challenges in a renewable dominated system, the motivations of this research work are listed below:

- **Lack of the representation of the relationship between inertia and frequency response.**

The total system inertia and frequency response are equally important for the frequency restoration after a system contingency. The minimum frequency in a frequency drop event is determined by both the total system inertia and the frequency response reserves. The current practice only ensures the sufficient frequency response is available in the system from the conventional generators to counter for the largest potential generation loss, which will address the inertia issue for a conventional power system. However, in a future low carbon system, the sufficient frequency response is unable to guarantee that the minimum frequency will satisfy the requirements due to low inertia reserves. There is a lack of critical analyses that would lead to a representation of the relationship between inertia and frequency response for the frequency transient dynamics. With such representation, the frequency response and the matched inertia can ensure the maximum frequency deviation within the requirements, thus avoiding the LFDD caused by the excessive drop in frequency for a low inertia system.

- **Lack of the comprehension for the demand side inertia contribution.**

For a potential future low-inertia system due to the increasing utilisation of renewable generation, the demand will become a significant inertia provider. However, the demand side inertia contributions are often being overlooked in inertia quantifications due to their relative small effects in the conventional generator dominated system. Understanding the ability to provide inertia from demand is essential to the analysis of future low-inertia power system frequency dynamics and frequency control.

- **Lack of the consideration for inertia constraints in the system operation planning.**

The inertia requirements are currently not considered in the system operation planning. Since the inertia affects the initial ROCOF and the minimum frequency during a frequency contingency, the consequences of lacking the inertia constraints on the system operation are the potential hazards to trip the ROCOF-based protection relays for the distributed generators, and LFDD caused by the significant frequency drop. For the purpose of enhancing frequency stability, the system operation planning must bring the inertia constraints into the scope.

- **Lack of an effective reward system for inertia to incentivise inertia providers**

Unlike frequency response, inertia currently is provided voluntarily by the conventional

generators and energy/frequency based payments may no longer provide sufficient returns for their services. There is also lack of incentives for renewable generation to invest in state-of-art technology to perform an inertia-like response to compensate the reduced inertia, such as the synthetic inertia from wind turbines [21, 22, 23]. The lack of appropriate incentive schemes for inertia could limit conventional generators' ability to contribute to system inertia, and the renewable generation's will to address the problem. The rewards for the provision of inertia can thus not only bring incentives for renewable generators to install new technologies, but also to increase the competitiveness and willingness of conventional generators to perform low generation outputs with high inertia contribution.

1.2.2 Objectives

The research work aims to provide a new perspective to look into the inertia problem on the system operation planning and the market incentives. The main research objectives of this work are summarised as:

- Present a systematic analysis of the relationship between the total system inertia and frequency response to investigate the impact of inertia on the frequency requirements for maintaining system stability.
- Investigate the ability of demand to provide inertia as the demand contribution becomes important in a low inertia system, and incorporate the demand contributions into the scope of the system operation planning.
- Develop new formulation for inertia constraints based on the frequency requirements in order to be represented in the frequency-constrained unit commitment (FCUC) problem.
- Develop an inertia pricing criteria to reward inertia providers with an incentive for the provision of inertia for both conventional and renewable generators.

1.3 Research Contributions

The contributions of this work are listed below:

- **Present an aggregated mathematical approach to relate the system frequency dynamics with system inertia for a low carbon system**

The principle of the mathematical approach is to investigate the influence of inertia on the frequency dynamics through the differential equation set describing the accumulated effects of the power mismatch on the frequency behaviour. The aggregated model is divided into three stages depending on the primary frequency response (PFR) availability which is further used to quantifies the inertia-related constraints associated with frequency. The constraints, affected by the ROCOF and frequency nadir requirements, are stipulated based on the frequency requirements during contingencies to ensure the constant operation of the system.

The equivalent PFR to the system inertia can also be acquired through the analysis of the mathematical approach of the frequency dynamics. The inertia-PFR relationship is transcendental. Therefore polynomial fitting is applied to provide a high-quality estimation for the implementation of the inertia-related constraints in the unit commitment (UC) consideration.

- **Develop a method to quantify the inertia contributions from the demand side based on the past frequency outage events.**

The principle of the demand side inertia contribution quantification method is to separate the generation inertia contribution from the total system inertia by using linear regressions based on the historical data of frequency outage events and to consider the power/frequency ratio as an indicator of the additional inertia contribution in spinning reserve. The proposed method is also able to estimate the averaged generation loading level for the conventional fossil-fired generators.

The proposed method is demonstrated using fifteen frequency outage events in 2010, and the results are further used to analyse the inertia profiles in relation to the demand profile. The resultant inertia profile suggests demand levels primarily decide the amount of inertia in the system under the current renewable and variable frequency drive (VFD) penetrations. A hidden benefit of shifting the demand from peak to trough is to shift the redundant inertia in the safe period to the weak period, thus improving the system frequency stability.

- **Incorporate the inertia-related constraints into the UC generation scheduling optimisation problem.**

Unlike the conventional UC which is a mixed integer linear problem, the inertia constraints are affected by the PFR reserves, which makes the FCUC a mixed integer with a transcendental nonlinear-constrained problem. The modified Lagrange relaxation is adapted to covert the nonlinear constraints into a two-layer heuristic update criteria

for the Lagrange multipliers, and the two layers are associated for the conventional UC constraints and the frequency constraints respectively.

Since the demand for conventional UC optimisation is the target generation amount to be met by generators, the demand inertia and demand frequency sensitivity are being ignored [24, 25, 26, 27]. This work brings the demand frequency characteristics into the consideration and updates the UC problem accordingly.

- **Propose the pricing criteria for the provision of inertia based on the FCUC.**

The pricing for the provision of inertia is obtained through the marginal price, which indicates the necessity and availability of providing the additional inertia, based on the economic meaning of the Lagrange multipliers in the Lagrange relaxation FCUC optimisations since they represent the marginal price of satisfying the associated constraint.

The marginal price of inertia reflects the inertia requirements which are constrained by the ROCOF and the minimum frequency requirements. With the implementation of inertia-related constraints, the frequency transient stability can be enhanced to withstand the largest generation loss with minimum generation cost increase.

- **Publications**

The outputs of this research work merged into three journal publications and several conference publications. For the journal publications, one accepted by the IEEE transactions on power system and the other two are currently under review.

1.4 Thesis Outline

The layout of the rest of the thesis is organised as follows:

Chapter 2 briefly explains the power system frequency control basics. Then a comprehensive overview of the current inertia problems for the UK power system due to the increasing penetration of renewable generators is presented.

Chapter 3 proposes a mathematical approach to simulate the system frequency dynamics after a sudden load/generation imbalance. The model is based on the synchronous generator swing equation and divides the frequency curve into three stages depending on the PFR availability. The impacts of total system inertia and PFR are

investigated using the mathematical model representing the key system parameters regarding frequency stability.

Chapter 4 presents a solution to stipulate the constraints for both the total system inertia and frequency response to ensure the frequency requirements are satisfied for the UK power system. The initial ROCOF, quasi-steady-state frequency and frequency nadir are inertia only, PFR only and inertia plus PFR constraints, respectively. The relationship between total system inertia and PFR reserve is also investigated.

Chapter 5 introduces a novel method to estimate the inertia contribution from the demand side based on the limited publicly available information on past frequency outage events. The estimation is implemented by separating the generation inertia contribution from the total system inertia. Moreover, a correction factor is introduced during the estimation, linked with the power/frequency ratio, to convert the actual generation outputs into the connected rated capacity which required for the inertia calculation.

Chapter 6 firstly proposes a method to incorporate the frequency-related constraints into the generation scheduling UC problem to assess the influence of the frequency constraints on the system operational cost. Secondly, the pricing for inertia is analysed based on the economic meaning of the Lagrange multipliers in the Lagrange relaxation UC optimisations.

Chapter 7 concludes the thesis by outlining the major contributions, the key findings and the potential future improvements of the research work.

Chapter 2

An Overview of the Frequency Regulations and the Inertia Problems in the UK Power System

THIS chapter provides a comprehensive review on the frequency regulation basics and the current inertia problems for the UK power system due to the increasing penetration of renewable generation.

2.1 Introduction

This chapter briefly explains the power system frequency control basics. Then a comprehensive overview of the current inertia problems for the UK power system due to the increasing penetration of the renewable generations is presented.

For the purpose of ensuring frequency stability, the adequate frequency response and system inertia are the key elements in frequency stability management. This chapter reviews methods for applying frequency-related constraints to improve system frequency stability during system contingencies. The gaps in the current research have been pointed out and will be addressed in the rest of the thesis.

2.2 Power System Frequency Control

The power system is a complex network composed of innumerable components such as generators, motors, transmission lines, transformer and protection equipment. The continuous operation of the power system requires the coordination of electricity generation, transmission, and distribution to the electricity consumers. It is crucial for consumers to have a reliable power grid that also operates as efficient as possible. Therefore, a stable system frequency is the key to the system reliability.

2.2.1 Power System Frequency Basics

The power system frequency is described by the number of complete cycles per second in the alternating current (AC) direction, with the unit of Hertz, and is a significant parameter of power system operation [1, 28, 29]. The physical meaning of the power system frequency indicates the active power balance between the electricity generation and consumption [1, 28]. Any mismatch between the two will cause the frequency to deviate from its designed nominal value. Two nominal frequencies are commonly used worldwide 50 Hz for the United Kingdom, Europe, China; and 60 Hz for the United States, western Japan. There is no fundamental difference between the two nominal frequencies except for the nominal settings for generators and power equipment [1, 28].

Power System Synchronisation

Under normal operating conditions, all generators rotate synchronously and the power system frequency is equal to the nominal value. However, the synchronisation does not mean that all generators spin at the same angular velocity. Instead, the angular velocity of the generator is determined by its number of pole pairs [1]. There is a strict relationship between the generator's rotor velocity and the system frequency:

$$f = \frac{pn}{60} \tag{2.1}$$

where,

- p is the number of pole pairs of the synchronous generator,
- n is the generator rotor speed in revolutions per minute (RPMs),
- f is the system frequency in Hz.

When the balance between the electricity generation and consumption is interrupted, from the perspective of the generator, the balance between the input mechanical power of the prime mover and the output electric power to the grid is also interrupted. The power mismatch will cause the angular acceleration to change the rotor rotational speed, in turn affecting the system frequency. Since the inertia of the rotating elements prevents the speed from changing, the frequency stability is related to the amount of inertia in the system.

System Inertia

System inertia represents the robustness and stiffness of the system when there is an imbalance between generation and demand [1, 28, 29]. In addition, system inertia can also help to damp small oscillations. The concept of inertia from a single machine is the summation of the kinetic energy stored in all rotating components, while the total system inertia reflects the summation of the inertia provided by generators, motors and embedded generators which are directly connected to the system. For ease of calculation, inertia is usually measured by the means of inertia constant, which is the ratio between the total stored kinetic energy and the nominal apparent power [1, 21, 30]. For the current system configuration, the conventional fossil-fired power plants, containing the heavy weight of rotating components, are the main inertia providers in the system.

System inertia has a significant impact on the initial ROCOF and the frequency under system frequency contingencies. Low system inertia, i.e. high ROCOF, has the potential hazard to cause the tripping of the frequency-sensitive protection relays, i.e. the ROCOF-based relay for the embedded generators, which might result in the cascaded loss of generation and further frequency deviations when the system encounters a large disturbance. Although high system inertia slows the frequency recovery as the inertia is resistant to frequency changes [31], a higher inertia level is still beneficial to the system compared to low inertia.

Centre of Inertia

The development of global positioning systems allow the measuring of frequencies at different locations on a synchronous time. This opens up a new field to investigate the system frequency behaviour. For different locations of the power system, the local frequency is not always the same, especially for a system with loose connections or a system with inner interconnections [32, 33, 34]. When a network contingency occurs at a certain location in the power system, the frequency disturbance propagates from the specific location to the periphery region in the form of an electromechanical wave. Studies indicate the electromechanical wave propagates at 400 to 600 miles per second for the United States Eastern Interconnection and Western Interconnection [34, 35]. The potential reason for the propagation of the frequency is that disturbance changes of the power flow in the tie-lines connecting different areas.

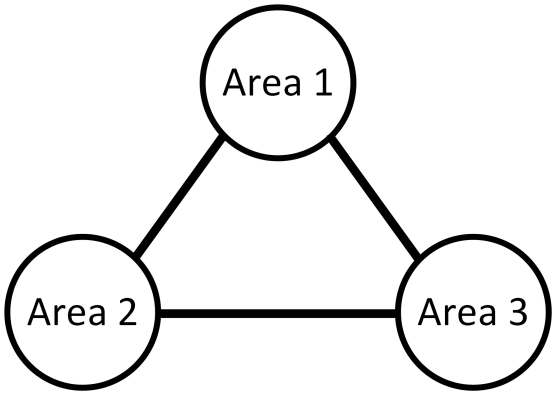

Figure 2-1: Three-area test system

The variations of frequency in different areas are tested based on a three-area system shown in Figure 2-1. The frequencies are denoted as f_1, f_2 and f_3 for Area 1, 2 and 3, respectively. A 0.02 p.u. disturbance of generation loss is applied to Area 1 and 3

at 2 seconds. The parameters of the test system are shown in Appendix A1. As can be seen in the Figure 2-2, the frequency in Areas 1 and 3 drops immediately after the disturbances while there is a delay for the frequency drop in Area 2. This is caused by the change in the tie-line power exchange, which also leads to the inter-area oscillations.

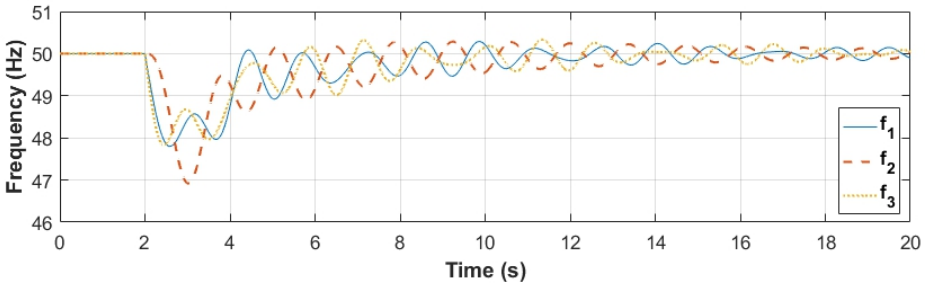

Figure 2-2: Frequency oscillations for the three-area system

To analyse the system frequency for the case of inter-area oscillations, it is assumed that the system is aggregated into a one-bus power system. The frequency of the aggregated system is called centre of inertia frequency. This is defined as [30]:

$$f_{COI} = \frac{\sum_{i=1}^{N} E_i f_i}{\sum_{i=1}^{N} E_i} \tag{2.2}$$

where,

- f_{COI} is the centre of inertia frequency,
- E_i is the inertia of area i,
- f_i is the frequency of area i.

Figure 2-3 illustrates the centre of inertia frequency for the three-area test system, which can be seen as the frequency at which the three-area are aggregated into single-area. Figure 2-3 shows the comparison between the centre of inertia frequency and the single-area frequency. The results indicate that the centre of inertia frequency is a relatively accurate representation of the frequency dynamics of the whole system.

For a system that is highly meshed the frequency differences at each bus-bar are relatively small. Therefore, considering the size and typology of the transmission network in the UK, a single bus-bar system is a reasonable representation for the analysis of the frequency dynamic in the UK power system [36, 37].

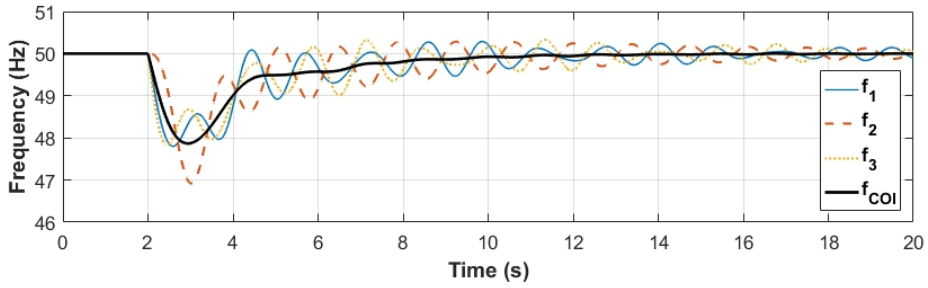

Figure 2-3: Centre of inertia frequency for three-area system

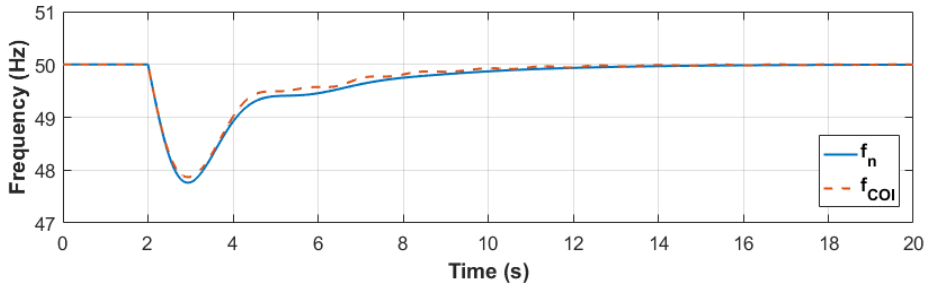

Figure 2-4: Centre of inertia frequency and single-area frequency

2.2.2 Principles of Frequency Response

Frequency response services are used to bring frequency back to the nominal value when there is a mismatch between generation and consumption. Figure 2-5 shows a typical frequency recovery process after a generation loss, which can be divided into three stages depending on the response time frame:

- **The inertia response** is the initial resistance to the frequency drop by releasing the stored kinetic energy.
- **The primary response** typically starts within 10 seconds. It represents the governor reaction to the frequency deviation to arrest the frequency drop and to stabilise the frequency at a quasi-steady-state frequency.
- **The secondary response** has a longer response time. It brings the frequency from quasi-steady-state frequency back to the nominal value by increasing the total generation.

The mechanisms of the primary and secondary responses are the main tools to maintain the frequency, which can be explained in more detail by the droop characteristic of the generator and demand.

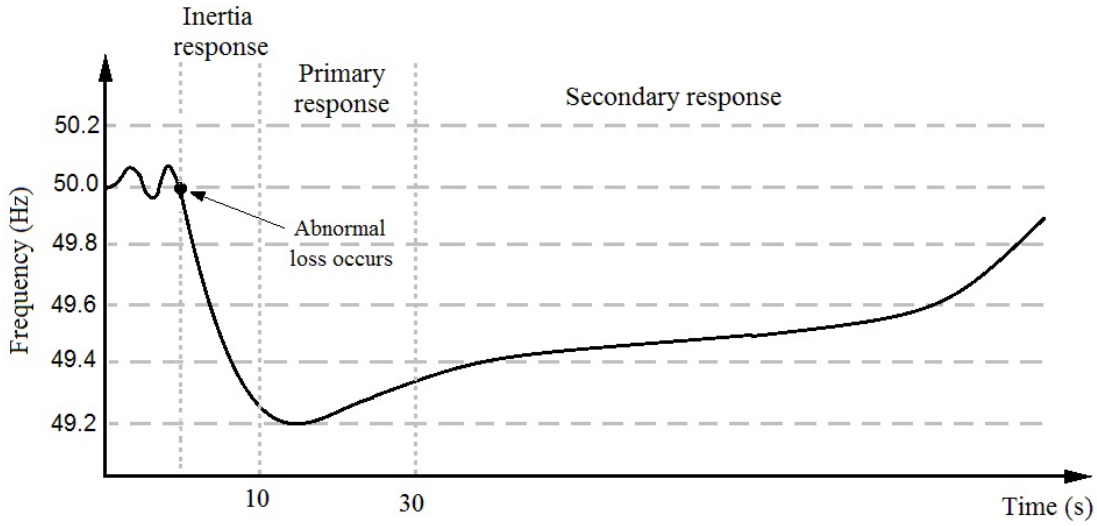

Figure 2-5: Frequency responses mechanism

Droop Characteristic

The droop characteristic describes the relationship between power and frequency for both generators and demand, as the generator/load can react to the frequency change by changing the active power generated/absorbed [38].

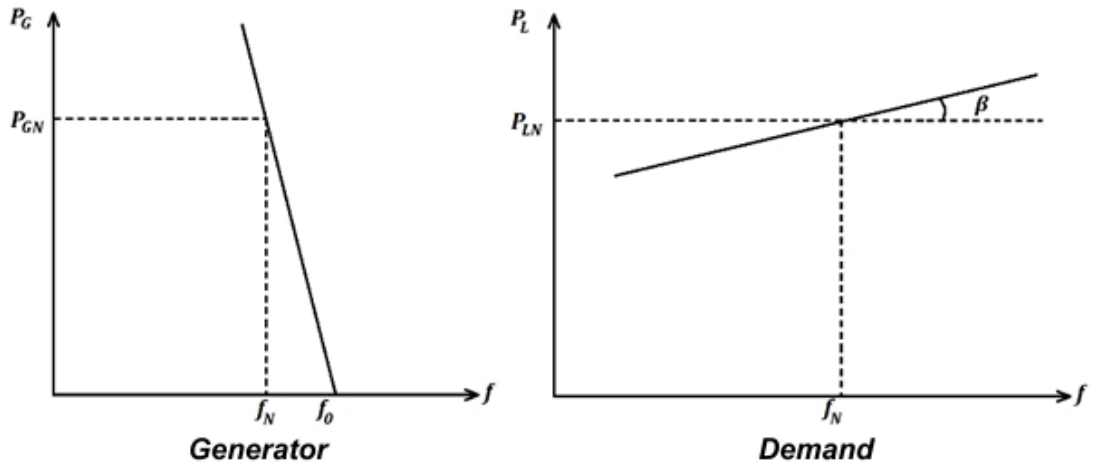

Figure 2-6: Typical droop characteristics for demand and generator [1, 38]

Figure 2-6 illustrates the typical power-frequency curves for the generation and demand, respectively. The droop characteristic of the generator represents the speed control mechanism from the prime mover governor. The power entering the prime mover

is controlled in response to the change in load, which will result in a change in the frequency. Any increase in load will lower the frequency and extra power will enter the prime mover to keep the frequency at the set point. Any reduction in load will cause the increase in frequency and the power entering the prime mover will be lower to maintain the frequency at the set point. The droop reference setting of a generator, G_{Droop}, is obtained using the no-load speed and the full load speed as:

$$G_{Droop} = \frac{v_{No} - v_{Full}}{v_{No}} = \frac{f_0 - f_N}{f_0} \tag{2.3}$$

where,

- v_{No} and v_{Full} are the no load speed and full load speed, respectively;
- f_0 and f_N are the no load frequency and full load (nominal) frequency, respectively.

The generator droop allows all the generators in the system to share the imbalance between generation and consumption. The power-frequency characteristic of the generator is defined according to the slope:

$$K_G = \frac{P_{GN} - 0}{f_N - f_0} = -\frac{P_{GN}}{\Delta f} \tag{2.4}$$

The droop characteristic of demand represents the combined effects of the loads with different relationships between power absorbed and frequency. The loads can be classified into the following categories [1]:

(a) Not affected by frequency changes, e.g. purely resistant load such as lighting.

(b) Proportional to the frequency changes, e.g. ball crusher, stock-removing machine, compressor.

(c) Proportional to the square of the frequency changes, e.g. transformer's eddy current loss.

(d) Proportional to the cube of the frequency changes, e.g. ventilator.

(e) Proportional to the higher power of the frequency changes.

Hence, the droop characteristic of demand can be expressed as:

$$P_L = c_a P_{LN} + c_b P_{LN} \left(\frac{f}{f_N}\right) + c_c P_{LN} \left(\frac{f}{f_N}\right)^2 + c_d P_{LN} \left(\frac{f}{f_N}\right)^3 + \cdots \tag{2.5}$$

where,

- f_N is the nominal frequency,
- P_L is the demand at frequency f,
- P_{LN} is the demand at frequency f_N,
- c_a, c_b, c_c and c_d are the percentage of each type of load, with $c_a+c_b+c_c+c_d+\cdots = 1$.

The power system frequency deviations are relatively small, normally smaller than 0.01 p.u., the loads proportional to the square or higher power of the frequency changes are negligible [39], and therefore the demand droop characteristic can be treated as the linear relationship shown in Figure 2-6. The slope of the power-frequency characteristic for demand is obtained by:

$$K_L = \tan\beta = \frac{\Delta P_L}{\Delta f} \tag{2.6}$$

The typical value of the demand droop is 1-3%, indicating 1% change in frequency will cause 1-3% change in demand [38]. The demand droop has no influence on the initial ROCOF but affects the frequency nadir and quasi-steady-state frequency for frequency events.

Primary Frequency Response

The PFR, shown in Figure 2-5, is the response to frequency deviations that prevents the system frequency from further deviations. Generator governor response, load droop characteristic and other devices capable of providing an immediate response based on local control are the main PFR contributors [1, 28, 29, 38]. Defined by the response speed, PFR refers to the additional power injected into the system in response to frequency drop within 10 seconds and sustainable for another 20 seconds [40].

Figure 2-7 illustrates the mechanism of PFR with the example of a sudden load increase. Before the sudden load increase, the system is balanced at point A, with the frequency equal to f_1 and the power flow equal to P_1. The generation and load power-frequency characteristics before the load sudden increase are shown as $P_G(f)$ and $P_L(f)$, respectively. After the sudden load increase of ΔP, the load power-frequency curve moves up to $P_L{}'(f)$ and the new cross point of the generator and load power-frequency curves is

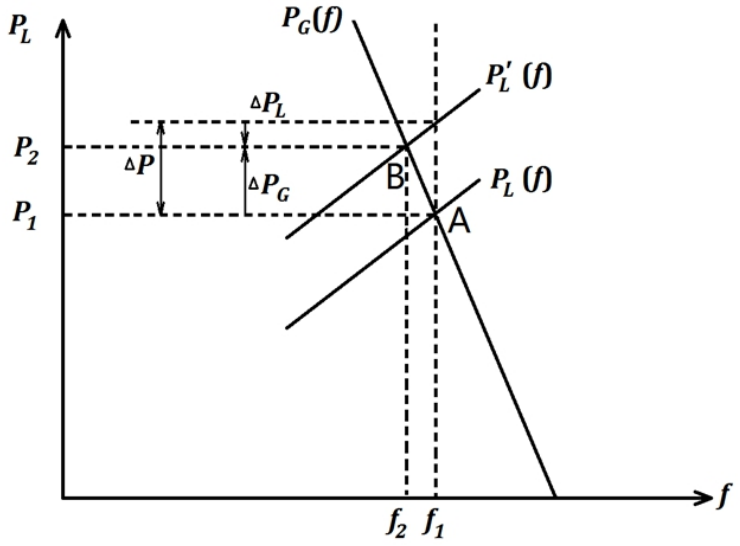

Figure 2-7: Primary frequency response mechanism [38]

point B, with the quasi-steady-state frequency equal to f_2 and the power flow equal to P_2. Due to the increase of load the system is re-balanced with a power flow equal to P_2, and P_2 is smaller than the load increase ΔP. As the generation is unable to meet the demand, the frequency starts to drop from f_1 to f_2. Meanwhile, as the frequency decreases, both generation and load react to the frequency decrease by increasing the generation by governor control and reducing the load absorbed by the demand droop. The changes for generation and demand in response to the frequency drop are ΔP_G and ΔP_L respectively, which are the PFR in this case. The frequency reaches steady state at f_2. The power increment of generation and demand can be described using vectors:

$$\overrightarrow{\Delta P} + \overrightarrow{\Delta P}_L = \overrightarrow{\Delta P}_G \tag{2.7}$$

Substituting by the generation and demand power-frequency characteristics:

$$\Delta P = \Delta P_G - \Delta P_L = -(K_G + K_L) \cdot \Delta f = -K \cdot \Delta f \tag{2.8}$$

where K is the coefficient of the system overall power-frequency characteristic.

To sum up, the features of PFR are listed below:

- PFR is the cornerstone of system frequency stability, as it arrests and stabilises the frequency deviations.

- The sources of PFR are the generator governor response, load droop characteristic and any devices that could provide an immediate response. The typical time window for PFR is within 10 seconds.
- PFR is shared among all generators agreed to provide this service depending on the generator droop setting.
- PFR could stabilise the frequency at a quasi-steady-state frequency. To restore the system frequency back to nominal value secondary frequency response (SFR) is required.
- PFR can damp small oscillations in the system effectively; however, the regular load variations, i.e. domestic and industry load profiles, requires the generation scheduling to compensate.

Secondary Frequency Response

The purpose of the SFR is to bring the quasi-steady-state frequency stabilised by the PFR back to the nominal frequency. Figure 2-8 shows the basic concept of the SFR mechanisms. Since the generation cannot meet the demand, to restore the nominal frequency generation needs to increase. Taking the example of a sudden load increase, in order to lift the frequency from f_2 back to f_1, the generation curve needs to move from $P_G(f)$ to $P_G{}'(f)$ with the total generation increase equal to ΔP, which matches the demand increase. The system is re-balanced at point C with the system frequency back to f_1 and the power flow equals to $P_1 + \Delta P$.

In terms of the response time, SFR refers to the additional power injection within 30 seconds after the contingency and sustainable for another 30 minutes. To provide SFR, the system requires spinning reserve from generators to increase their production when called upon. Hence, the sufficient system reserve is crucial in the frequency recovery process. The notable features of SFR are summarised below [1, 29, 38]:

- The purpose of SFR is to bring the system frequency from a quasi-steady-state value back to nominal.
- SFR is a system-level response to the frequency deviation instead of a device-level response.
- The response speed of the SFR is slower than the PFR, with the typical response time window of 30 seconds to 30 minutes [40].

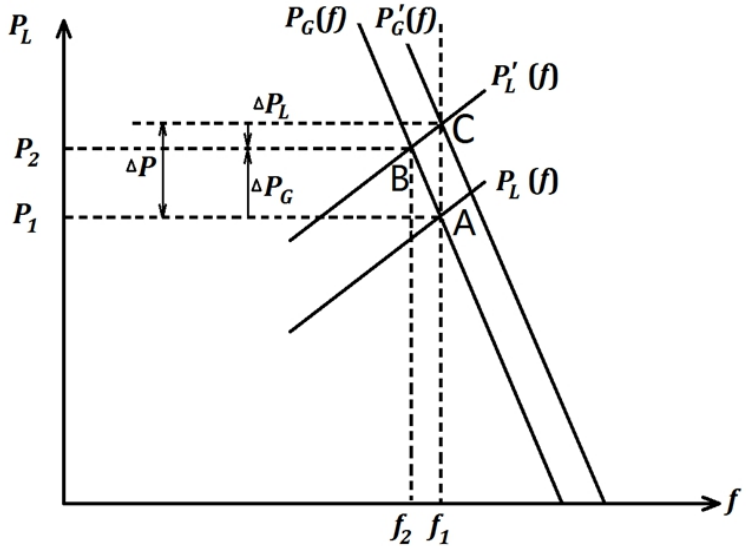

Figure 2-8: Secondary frequency response mechanism [38]

- SFR cannot replace PFR solely since the PFR arrests and stabilises the frequency drop to allow the SFR to bring frequency back to the nominal frequency. In the absence of the PFR, the frequency will drop to the limit of under frequency load shedding way before the SFR takes place.

- The amount of the SFR each generator should provide is usually determined by the economic dispatch (ED).

High Frequency Response

High frequency response (HFR) refers to the generation reduction when frequency exceeds the upper boundary of the operational limit of 50.2 Hz. HFR is required to be provided within 10 seconds and sustained infinitely [40].

According to the one-second interval frequency data for the year from 2014 to 2016 released by National Grid, high-frequency events (i.e. frequency rises above the upper operational limit) are considerably more frequent than low-frequency events (i.e. the frequency drops below the lower operational limit) [3]. Therefore, during the normal operation of the system, generation tends to over-committed than under-committed and HFR is essential to reduce the generation when necessary.

2.2.3 Development of Frequency Control

The main objective of a power system is to deliver a constant supply of electricity to all consumers with a satisfactory quality regarding voltage and frequency. The voltage and frequency stability are determined by the reactive power and active power, respectively. The imbalance of reactive power will affect the voltage but has no influence on the system frequency; while the imbalance of active power will affect the system frequency only and leaves voltage unaffected. The longer time duration of frequency deviations from the nominal value will affect the system operation and lower the system efficiency, security and reliability. The consequences might be damaged equipment, degraded load performance, overloaded transmission lines and increased potential of triggering protection devices. The balance of reactive and active power is regulated by the automatic voltage regulator and the load frequency control (LFC) respectively. The Transmission Network Operator (TSO), managing the operation, development and maintenance of the transmission system, is responsible for balancing the generation and demand at the national level for the frequency stability. As the power system continuous expanding in size and complexity, methods to balance the active power have been developed over the past few decades.

A Brief History and Current Status Quo

The frequency control problem can be interpreted as the problem of turbine-generator speed control, as the power produced by generators is primarily determined by the generator rotational speed. Therefore, a governor mechanism was added into the turbine-generator to adjust the fuel input valve in order to track the load change and keep the frequency at the nominal level. However, without the secondary control, the system lacks the ability to return to the nominal frequency after large disturbances [1, 29, 38].

In the 1960s due to the development of transistors and integrated circuits, the active power balance and system frequency control mechanism moved from analogue toward digital. Since the 1970s, the booming computer technology facilitated the online automatic generation control (AGC) and ED from the centralised control centre. After the 1980s, the AGC was developed and widely used and the standards for the frequency control and AGC were established in various regions [41, 42]. In the early 1990s, the power system began to enter the market-oriented era and the frequency control became one of the main parts of the ancillary services market. Recently, owing to the development of artificial intelligence, artificial neural networks, genetic algorithm and fuzzy

logic methods were synthesised with frequency control [43, 44, 45, 46].

Regarding the regional difference, SFR or secondary control in the US is called LFC, which is the primary function of AGC. The US transmission system is formed of two major networks, the Western Interconnection and the East Interconnection, and three minor networks, the Quebec, Alaska and Texas Interconnections. The priority target of LFC is to maintain the regional frequency stable and then help the whole system frequency to return to its nominal value among all controlled regions based on a signal called area control error (ACE), which indicates the share of the responses each control area should contribute. In Europe, the synchronous grid of continental Europe is under-regulated by the European Network of Transmission System Operators for Electricity (ENTSO-E), which covers 43 TSO from 36 countries [47]. Although the frequency regulations vary from one TSO to another, they are obligated to help the interconnected systems operated by other TSOs [42]. The transmission system in the UK is not as robust as the synchronous grid in continental Europe, because all the interconnectors with neighbouring countries are all high voltage direct current (HVDC) lines and sufficient domestic frequency responses are required at all time.

Frequency Services in the UK

The UK transmission system is formed of three transmission networks: the England and Wales network owned by National Grid Electricity Transmission plc, the southern Scotland network owned by Scottish Power Transmission Limited, and the network for the northern Scotland and the Scottish islands groups owned by Scottish Hydro Electric Transmission plc. These three regional operators are responsible for the development and maintenance of their own transmission networks. However, the system as a whole is operated by one TSO, National Gird, to ensure the stable and reliable operation of the entire transmission system in the UK [48]. Figure 2-9 illustrates the frequency balancing services in the UK power system. There are three types of frequency response service currently being used: the mandatory frequency response (MFR), firm frequency response (FFR) and enhanced frequency response (EFR).

- **Mandatory Frequency Response**

The MFR is an automatic response obliged for all large generators connected to the transmission system to adjust their output power in response to the frequency deviations. The classification criteria for large generators in the three transmission systems are shown in Table 2.1. The MFR covers the PFR, SFR and HFR, and the generators

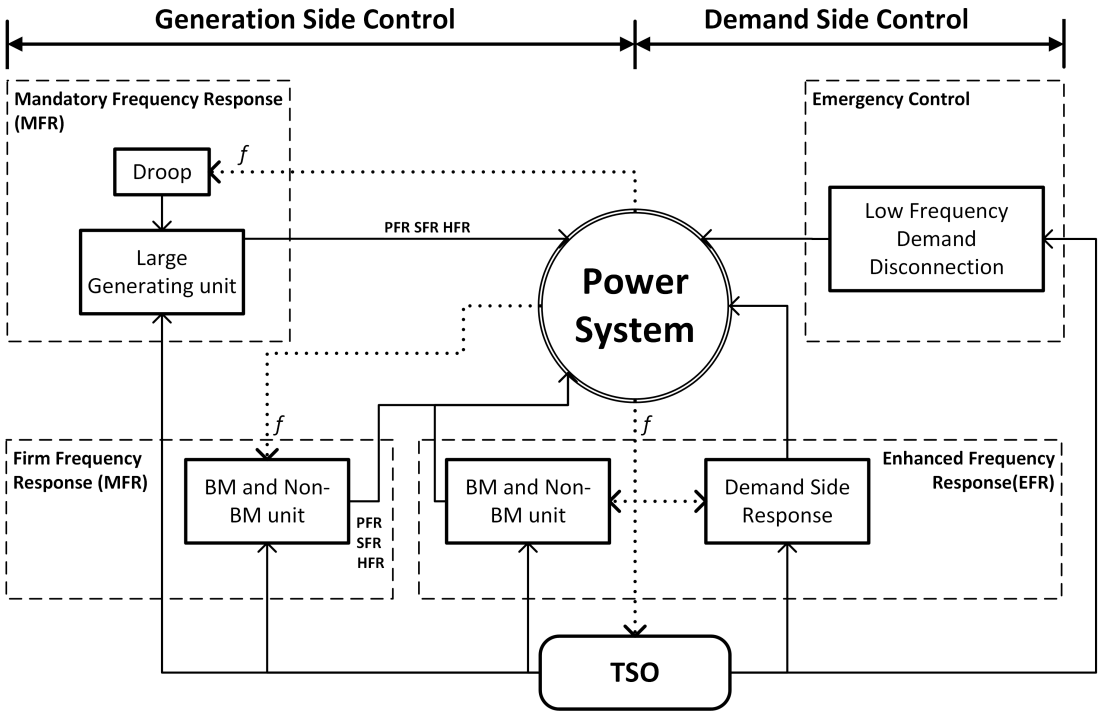

Figure 2-9: The UK frequency response services

are allowed to provide other services if the obligations of MFR are met [49].

Table 2.1: Generation unit classification criteria [49]

	National Grid Electricity Transmission	Scottish Power Transmission	Scottish Hydro Electric Transmission
Small	$<$ 50 MW	$<$ 30 MW	$<$ 10 MW
Medium	50 MW - 100 MW	N/A	N/A
Large	$\geq$ 100 MW	$\geq$ 30 MW	$\geq$ 10 MW

- **Firm Frequency Response**

The FFR opens the market for response providers inaccessible to the MFR. The FFR providers could be a Balancing Mechanism Unit (BMU) or a non-BMU and deliver a minimum of 1 MW response energy as a single generator or a Power Park Module (a group of generators). The frequency response in FFR service includes the dynamic PFR, SFR and HFR as well as the non-dynamic static SFR triggered by target frequencies. A monthly tender process is conducted for the FFR for all potential providers

[50].

- **Enhanced Frequency Response**

The EFR is an automatic dynamic service targeted for the BMUs and non-BMUs as well as the aggregated demand side response and the storage owners. The EFR providers are required to deliver a minimum of 1 MW and maximum of 50 MW response within one second to the frequency deviations. The EFR belongs to the fast frequency response according to the technical requirements, which is ideal for an inertia-less system to fill the system imbalance before massive frequency deviations. A monthly tender process is conducted for the EFR for all potential providers [51].

- **Low Frequency Demand Disconnection**

The LFDD is the final option to prevent the further frequency drop and system collapse by disconnecting the load from the faulted area to the adjacent area. The LFDD is triggered by large generation loss as a result of rapid frequency drop. In the UK, the LFDD starts when frequency drops to 48.8 Hz [20].

2.3 Frequency Regulations in the UK

This section summarises the frequency limits and generation loss types in the UK. The frequency regulations involve the frequency requirements for normal operation and under contingencies which will be used to stipulate the requirements for total system inertia and PFR in the next section.

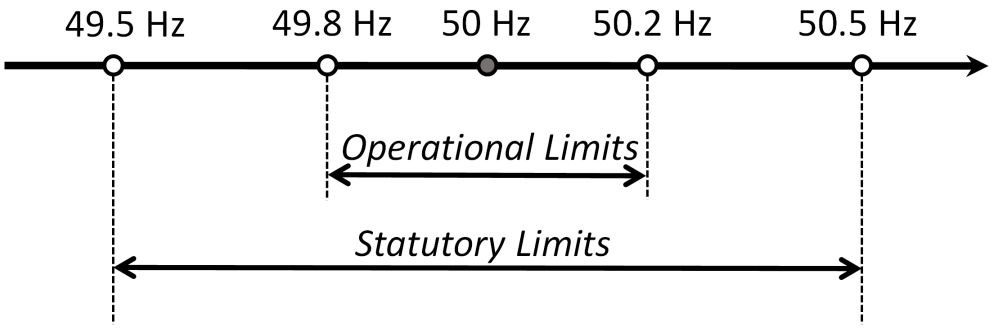

Figure 2-10: Frequency limits in the UK

2.3.1 Frequency Limits

The UK power system transmission network operator, National Grid, specifies the frequency limits into the **Operational limit** and **Statutory limit** as shown in Figure 2-10. The **Operational Limit** is ±0.2 Hz to the nominal frequency of 50 Hz, which defines the range of system frequency in normal operation situations. While **Statutory Limit** refers to the frequency deviation of ±0.5 Hz to the nominal frequency, which outlines the maximum frequency deviations under intermediate quasi-steady-state.

Besides the frequency limit, National Grid also specifies the maximum ROCOF allowed in the system. The initial ROCOF is the largest ROCOF during a frequency excursion which is entirely dependent on the total system inertia. For the safety of the equipment and personal, all the embedded generators with a rated capacity greater than 50 MW must installed the ROCOF protection relay just in case forming an islanding distribution network. If the island remains electrified, it will become a potential hazard to the nearby embedded generators and the repair workers. The maximum allowed ROCOFs of the UK power system is increased to 0.5 Hz/s from 0.125 Hz/s under the new requirements started from the year of 2016 due to the inevitable inertia decrease as a consequence of increasing penetration of inertia-less renewable generations [52, 53].

2.3.2 Potential Generation Loss

Currently, the largest infeed generator in the UK is a coal power station at Drax with maximum 1320 MW capacity. This number will increase to 1800 MW as a result of the new constructed nuclear power plants at Hinkley Point C [20]. National Grid, divides the potential generation losses into three categories and the frequency-related requirements for each type of loss are summarised in Table 2.2.

Table 2.2: Frequency requirements under contingencies

Type of loss	Amount of loss	ROCOF	Frequency Nadir	Quasi-steady-state Frequency
Small disturbances	≤300 MW	0.5 Hz/s	49.8 Hz	49.8 Hz
Significant Loss	300 MW - 1000 MW	0.5 Hz/s	49.5 Hz	49.5 Hz
Abnormal Loss	≥1000 MW	0.5 Hz/s	49.2 Hz	49.5 Hz

- For the generation loss less than 300 MW, the lowest frequency nadir allowed is the **Operational Limit**, i.e. 49.8 Hz.
- For the generation loss between 300 MW and 1000 MW, defined as **Significant Loss**, the lowest frequency tolerated is the **Statutory Limit**, i.e. 49.5 Hz.
- For the generation loss greater than 1000 MW, defined as **Abnormal Loss**, the lowest frequency nadir permitted is 49.2 Hz but must recover to the **Statutory Limit** within 1 minute.

2.4 Inertia Problems in the UK Power System

In November 2011, the Grid Code and Balancing Services Standing Group in National Grid drafted a Frequency Response Technical Sub-Group Report to address the problems and mitigation methods regarding the reduced system inertia. Together with the Future Energy Scenarios created by National Grid to reflect different possible future system configurations, a clearer picture of the inertia problems could be obtained.

2.4.1 Background

Conventional synchronous generators, containing large-weight of rotating masses, are sensitive to the frequency variations. Whenever a generation loss occurs, the kinetic energy stored in the rotating masses can be released into the system to narrow the power mismatch temporarily. However, renewable generation is largely inertia-less, such as the variable speed wind turbines, which lack the ability to support the frequency during transient. Figure 2-11 shows the growth of offshore wind farms in the UK from 2010 to 2017 [54]. Compared with 2010, the share of renewable generation increased from 7% to 29.3% in 2017, while the share of traditional fossil-fuel (coal and gas) reduced from 75% in 2010 to 47.1% in 2017 [12, 13].

As the penetration of renewable generation is growing, the inertia problem gradually becomes a major issue. Besides, the Security and Quality of Supply Standard (SQSS) redefines the largest infeed generation loss from 1320 MW to 1800 MW after 2014 [20]. In the future, the predicted total installed capacity of wind generation around 2050 can meet the current peak system demand for the Two Degrees future projection, representing the highest level of green ambitious and financial ability to promote green technology, as shown in Figure 2-12 [55, 56]. The increased potential generation loss and

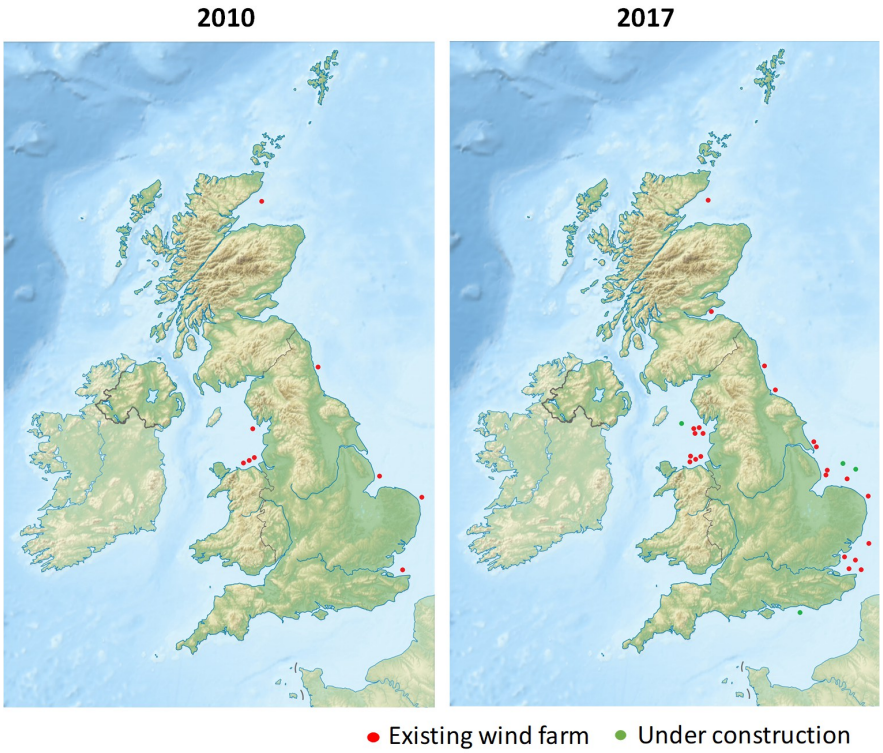

Figure 2-11: The growth of offshore wind farms in the UK [54]

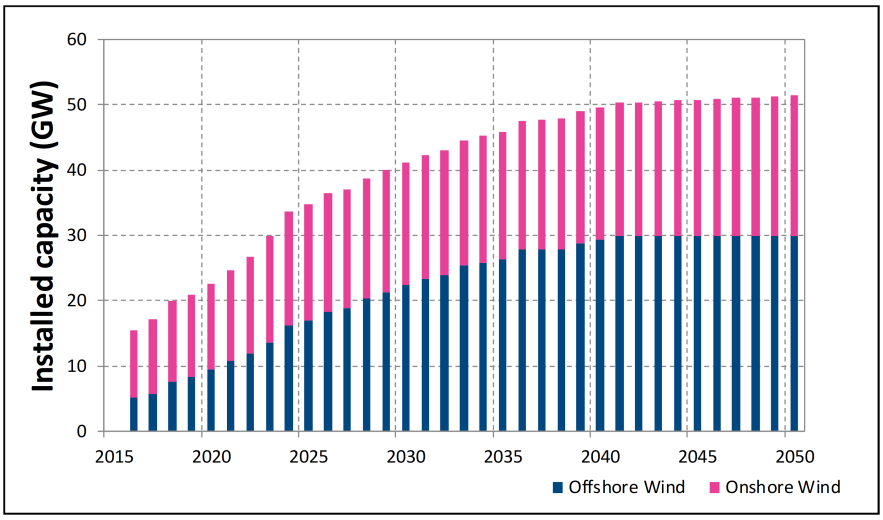

Figure 2-12: Wind installed capacity prediction for the Two Degrees Scenario [55]

the reduced system inertia bring new challenges to the system frequency stability. The most challenging cases are during low demand period since the renewable generation are associated with higher priority order in the scheduling.

2.4.2 Rate of Change of Frequency Problems

In the event of a generation loss, the first impact related to low system inertia is the high ROCOF. The Distribution Code in the UK states the setting for ROCOF loss of mains (LOM) protection relay of distributed generators is 0.125 Hz/s before 2014. The reason for installing ROCOF LOM relays for distributed generators is to prevent the formation of electrical islands in the distribution network. If a part of the power distribution network is disconnected from the mains and becomes an isolated island, all the distributed generators must be taken offline for safety issues. The potential hazards of the island distribution network remaining energised is the high risk for the people near the island network and damaging synchronous distributed generators. However, as the inertia continuous decreasing, a large disturbance of generation loss might exceed the 0.125 Hz/s limit and cause the disconnection of distributed generators. The miss-tripping of distributed generators exacerbates the deficit between generation and demand, leading to the further decline of frequency.

The initial ROCOF in the event of generation loss can be expressed as:

$$ROCOF = \frac{\Delta P}{2 \cdot E_{sys}} \cdot f_0 \tag{2.9}$$

where,

- ΔP is the generation loss,
- E_{sys} is the total system inertia,
- f_0 is the system frequency prior to the generation loss.

The current largest infeed generator is 1320 MW which can be considered as the largest potential generation loss. To prevent the ROCOF exceeding 0.125 Hz/s, the system must have at least 264 GW·s inertia.

$$E_{sys} = \frac{1320 \text{ (MW)}}{2 \cdot 0.125 \text{ (Hz/s)}} \cdot 50 \text{ (Hz)} = 264 \text{ (GW·s)} \tag{2.10}$$

Figure 2-13 shows the percentage distribution of the total system inertia for the year 2015 according to the generation profile [57]. There is a significant part of the time that the system inertia is insufficient to meet the inertia requirement. Considering the increase to the largest infeed generation by the SQSS, the minimum inertia required for the ROCOF limit is 360 GW·s.

There are three possible solutions to mitigate potential high ROCOF issues.

1. Increasing the total system inertia.
2. Part-loading the largest generator to reduce the largest potential generator loss.
3. Relaxing the ROCOF LOM protection relay setting for distributed generators.

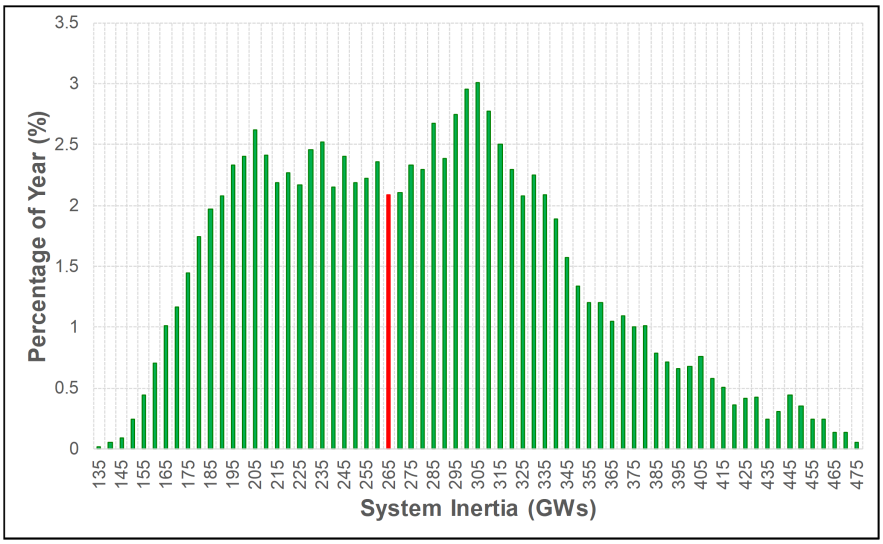

Figure 2-13: Distribution of the total system inertia for 2015 [57]

Solution 1, increasing the total system inertia, requires more participation from the conventional generators, which is against the decarbonisation trend in the power industry. Considering the prospective largest generator in the future is a nuclear power plant, it is uneconomical and impractical to part-load the generator as solution 2. Therefore, solution 3 is the most promising mitigation for the ROCOF problem. Table 2.3 shows the minimum inertia required for different generation loss level and ROCOF limits.

Table 2.3: Minimum inertia for different generation loss and ROCOF requirements

Generation Loss	0.125 Hz/s	0.5 Hz/s	1 Hz/s
1320 MW	264 GW·s	66 GW·s	33 GW·s
1800 MW	360 GW·s	90 GW·s	45 GW·s

Actions have been conducted by National Grid to relax the ROCOF relay settings to avoid miss-tripping of the distributed generators. The initial modification proposal for

the Distribution code in 2014 targeted for the distributed generators of 5 MW or larger to change the ROCOF LOM relay setting as [52]:

- 1 Hz/s for all existing and new non-synchronous distributed generators, as well as new synchronous distributed generators commissioned after 1 July 2016.
- 0.5 Hz/s for all existing synchronous distributed generators and all new synchronous generators commissioned before 1 July 2016.
- All existing distributed generators should have made the change before 1 July 2016.

Besides the ROCOF LOM protection, vector shift (VS) protection is also permitted in the UK power system. In 2017,the Distribution code was updated with two main aspects [58]: (i) specified the new ROCOF setting for distributed generators smaller than 5 MW, and (ii) removed the VS LOM protection. The updates of the proposal are as follows:

- The ROCOF LOM protection setting for distributed generators smaller than 5 MW changes to 1Hz/s with a 500 ms definite time delay, the changes should be made before 1 February 2018.
- The distributed generators commissioned on or after 1 February 2018 can no longer use the VS protection.

With the new settings of the ROCOF relay for distributed generators, the ROCOF problems have been alleviated. However, for the future largest infeed generator loss, 1800 MW, the minimum inertia required for 0.5 Hz/s and 1 Hz/s is 90 GW·s and 45 GW·s respectively, which is still quite challenging for the future renewable dominant power system.

2.4.3 Frequency Containment

The frequency containment in the UK power system refers to the actions made by the TSO to counter the frequency change due to a generation loss or a load sudden increase and keep the frequency deviations within the allowed limit. In the event of a large generation loss, the maximum frequency deviations allowed are 0.8 Hz, but these must be back within a 0.5 Hz range in 60 seconds. However, with the increasing popularity of renewable generation, the frequency containment is facing challenges of ensuring sufficient frequency response is in place to meet the above requirements. The

challenges are threefold:

- The reduced inertia due to the utilisation of renewable generation rises the ROCOF. In the event of a generation loss, the frequency drops to 49.2Hz with less time.
- The largest infeed generation loss that the system should withstand increases from 1320 MW to 1800 MW. Therefore, more frequency response is required to arrest the frequency drop for the worst scenario.
- The amount of frequency response available in the system is decreasing due to the fact that renewable generation is unable to provide the frequency response with the same way conventional generation does.

Table 2.4 shows the required response ramp rate for the largest potential infeed generation loss, i.e. 1800 MW, with different inertia levels. As the inertia reduces, the total required response and response ramp rate increase dramatically; however, the displacement of the conventional generators poses a major threat to the frequency containment of ensuring enough response available.

Table 2.4: Required response ramp rate for 1800 MW loss

Inertia (GW·s)	Time to reach 49.2 Hz (s)	Response required (MW)	Response ramp rate (MW/s)
264	9.9212	1012.5	126.6
220	8.0049	1331.1	166.4
170	5.8159	2092.2	261.5
120	3.5984	5005.8	625.7

The results in Table 2.4 assume the governor reaction delay is 2 seconds. During the governor reaction deadband the frequency decrease is purely dependent on the total system inertia. The consequence of low inertia is the rapid drop in system frequency during the governor deadband and lifting the requirement for the response ramp rate. The mitigation to the frequency containment problem with low inertia requires a faster response to arrest the frequency drop before massive frequency deviations. EFR services are still under development in the UK, which require the response being delivered within 1 s after the event. The main sources of the EFR services are the converter-related technologies such as the wind turbine generators [59, 60, 61, 62],

HVDC interconnectors [63, 64, 65, 66, 67] and battery storage through the demand side management [68, 69, 70, 71].

2.5 Power System Frequency Dynamics Management

The power system frequency stability management focuses on maintaining the system frequency following large disturbances, i.e. a significant imbalance between generation and demand. The main objectives are ensuring the adequate available frequency responses and minimising the unintentional loss of load for any possible system contingencies. The main challenge of power system frequency stability management is associated with the rising popularity of renewable generation. From the perspective of the TSO, the large displacement of the conventional generations by the renewables reduces the total system inertia and limits the amount of frequency response, making the frequency containment more and more challenging [4, 5, 55, 56]. In this section, a literature review regarding the management of power system frequency dynamics is presented.

2.5.1 Estimation of System Inertia

The system inertia plays a crucial role in the frequency stability since it is the initial resistance against all frequency deviations. The frequency dynamics management relies on the accurate quantification of the total system inertia. From the perspective of a TSO, the accurate estimation of the total system inertia can stipulate the requirements for response in relation to the frequency deviations and the time window for deploying the frequency response [72].

The methods for quantifying the inertia contribution from a single machine, to a large extent, depend on the specific generation technology and its designed parameters, e.g. the moment of inertia of the turbine-generator and all the synchronous rotating elements and the designed rotating speed:

$$E_{Machine} = \frac{1}{2} J_{Machine} {\omega_{Machine}}^2 \tag{2.11}$$

where,

- $E_{Machine}$ is the inertia of the machine in terms of stored kinetic energy,
- $J_{Machine}$ is the moment of inertia of all the synchronously rotating elements,

- $\omega_{Machine}$ is the designed rotating velocity of the machine.

As for the total system inertia, it is unrealistic to summarise the inertia contributions of all synchronously connected machines. Therefore, the quantification methods for the total system inertia are mainly based on the analysis of the frequency dynamics in frequency outage events. This is known as post-mortem analysis. The required data are the size of the imbalance ΔP, the initial ROCOF and the system frequency prior to the event f_0:

$$E_{System} = \frac{\Delta P}{2 \cdot df/dt} \cdot f_0 \tag{2.12}$$

The accuracy of the estimation depends on the measurement of the frequency dynamics, especially the derivative of the frequency. In the early stages of quantifying the system inertia reserve, due to the limitations in frequency measurements, estimations were based on the recorded frequencies. The authors in [24] investigated the total system inertia constant and the capacity of the spinning reserve by the polynomial approximation on the measured frequency transient waveform. Since the inertia contribution of the demand was neglected, the resulting inertia constant found was slightly less than the real value. A similar study was conducted on the Western Electricity Coordination Council (WECC) with more frequency outage events [73]. With the development of the data acquisition technology, wide area monitoring system (WAMS) was introduced to the frequency measurement. Using WAMS to collect information about system frequency and power for each generator for the purposes of inertia estimation was investigated in [74, 75, 76]. However, this method was limited by the size of the power system, since it is unrealistic to obtain all the required information for a large power system due to the complexity. The studies for the regional inertia based on the phasor measurement units (PMUs) as the frequency measurements were performed in [77, 78]. The authors in [77] investigated the regional inertia for the WECC system by reducing the system configuration into five single-machine areas with the frequency data observed via PMUs. The authors in [78] estimated the regional inertial response from different generator clusters by strategically allocating the PMUs. The estimation of the total system inertia in the UK based on PMUs was presented in reference [79] by summarising the regional inertia contributions.

The learnings from the previous research suggest two aspects of the total system inertia estimation have often been overlooked:

- The inertial contribution of a single machine is determined by the rated capacity

rather than the actual operating conditions, which is the value typically used to calculate the total system inertia.

- The total system inertia should consider all the inertia providers in the system, including the inertia contributions from the generation side (including distributed generators) and the demand side. However, the contribution from the demand side is often overlooked.

The above two aspects will lead to an inaccurate estimate of the total system inertia that either generation side or demand side inertia contributions are underestimated.

The synchronous load in the demand side will become a significant inertia provider to ensure the system frequency stability, as the increasing penetration of inertia-less renewable generation increase the lack of inertia. It is essential to understand the quantity of inertia that demand could contribute to assist the frequency containment management. Therefore, Chapter 5 proposes a novel method for estimating the demand side inertia contributions based on the limited public information about the frequency outages events.

2.5.2 Implementation of Frequency Constraints

The main objective of frequency stability management is to keep the frequency deviations within the acceptable limits when subjected to large disturbances. Therefore, the key elements that need to be managed are listed below:

- **The worst scenario of frequency contingency**

  Frequency contingencies are triggered by the imbalance between generation and demand, e.g. loss of a generation unit and a sudden load increase. The worst scenario of the potential contingency must be identified, namely the loss of the largest infeed generator, loss of the HVDC interconnection. The contingency plans for the worst scenario are necessary; otherwise, the worst scenario should be avoided, e.g. de-loading the largest infeed generator to reduce the largest potential generation loss.

- **Frequency dynamics during contingency**

  The management of the frequency dynamics during contingency is to avoid violating the requirements for the frequency transients. The requirements include the ROCOF, the frequency nadir and the quasi-steady-state frequency.

- **Frequency containment during contingency**

  To keep the frequency dynamics within the requirements, the management of frequency containment ensures that sufficient actions are in place. The actions include the deployment of frequency response and the low frequency demand disconnection when it is necessary.

- **System Inertia**

  The total system inertia is a vital index indicating the robustness of the system. However, the consequence of the increasing penetration of renewable generation is the reduced system inertia. Frequency stability requires sufficient inertia in the system. In some cases, the curtailment of renewable generation is necessary to bring the inertia-providing conventional generators online.

To fulfil system frequency stability, significant research has been conducted. The early attempts to ensure the frequency stability were based on the PFR reserve constraint in ED [80, 25]. The reserve was calculated from the largest infeed generator to avoid unintentional load shedding. Investigation regarding the PFR constraints in operation was presented in [26], which considered the physical constraints of the generators to provide the PFR. The PFR constraints associated with the wind generations were studied in [81, 82, 83] , the curtailment of wind generation was considered when the system required more PFR reserve.

With the development of frequency characteristics of the modern power system, two new constraints were added to the system operation planning, namely the ROCOF constraint and frequency nadir constraint. The largest ROCOF during a frequency drop event is the initial ROCOF. Therefore the requirement for the ROCOF constraint is to ensure that the initial ROCOF does not exceed the maximum ROCOF tolerance [27, 84, 85, 86].

However, the frequency nadir is determined not only by the total system inertia but also by the PFR, which makes the frequency nadir constraint more complex than the ROCOF constraint. The authors in [27] used a black box representing the frequency dynamics, and regressions were applied to find the parameters between the response reserves and frequency deviations. In [87], the authors firstly expressed the relationship between maximum frequency deviation and the PFR by first-order transfer functions; secondly used the relationship to get the nonlinear constraint of PFR to satisfy the frequency nadir requirements; finally, a piecewise linearisation was applied to linearise the frequency nadir function. The authors in [88] brought the under frequency load shed-

ding (UFLS) into the frequency nadir constraint, allowing UFLS to be activated when necessary. The battery energy storage was added into the consideration of frequency nadir constraint by the studies in [84]. Mathematical approaches for the frequency dynamics were proposed by Chavez *et al.* [85] and Teng *et al.* [86] to derive the frequency nadir. However, the method proposed by Chavez *et al.* did not consider the demand damp while the method proposed by Teng *et al.* did not consider the PFR ramp rate.

Chapter 3 in this thesis proposes a mathematical approach to simulate the frequency dynamics, considering the PFR ramp rate and the demand damp to improve the representation of the system behaviour. The mathematical approach is further investigated into the frequency-related constraints in the system operation in Chapter 4.

2.5.3 Unit Commitment

The UC algorithm solves the problems of the operation and planning of generators, which decides the optimal operation schedule for the generating units to meet the predicted demand profiles under different technical and environmental constraints [89]. The UC has the potential to manage the low-inerita challenges caused by the utilisation of renewable generation on the perspective of system planning. The system reliability requires the UC decision to be robust, in term of the frequency stability, the robustness means adequate PFR and inertia in place to counter the largest potential system contingency.

The UC optimisation is a mixed-integer non-linear problem, and the optimal UC decisions can be acquired through enumerations. However, the non-deterministic polynomial-time hard (NP-hard) nature of the UC problem brings excessive computational burden to the problem-solving process. A variety of methods have been proposed to solve the UC problem including stochastic system scheduling [86, 90, 91], mixed-integer linear programming [26, 87, 84, 27], particle swarm optimisation [92, 93, 94], Lagrange relaxation [95, 27, 96, 97]. Since the Lagrange multiplier reflect the marginal price to satisfy the associated constraint, Lagrange relaxation is selected for this research [95, 27, 96, 97].

2.6 Chapter Summary

This chapter begins with an overview of the power system frequency basics and the problems raised by the utilisation of inertia-less renewable generations in the UK. The

main problems for the reduced inertia are the high ROCOF triggering the protections of distributed generators and the necessities for fast frequency response.

For the purposes of the frequency stability, adequate frequency response and the system inertia are the key players in the frequency stability management. This chapter provides a review regarding the methods of applying the frequency-related constraints in the system operations to improve the system frequency stability. The gap in the existing research is the lack of a systemic model to assess the relationship between the frequency dynamics and the frequency containments to incorporate the frequency-related constraints.

Inertia, as a scarce property in the renewable dominated systems, is currently voluntarily provided by conventional generators. However, the significance of the total system inertia is not reflected in the current ancillary services market mechanism. This thesis fills the gap regarding the pricing methods for inertia providers. That will not only bring incentives for the potential inertia providers but also improve the competitiveness of the conventional generators.

Chapter 3

Mathematical Approach for Analysing System Frequency Stability

THIS chapter identifies the key elements in maintaining system frequency depending on the mathematical representation of the frequency deviations.

3.1 Introduction

The power system frequency indicates the dynamic balance of active power between generation and consumption. Any mismatch between the two will cause the system frequency to deviate from its nominal value. The simulation of power system frequency is largely adopted from the swing equation of a synchronous generator which considers the rotor angle change due to the power deficit between input and output power from the perspective of the rotor shaft. The electricity demand will exceed the electricity generation followed by a generation failure. On rotor shaft, the input mechanical torque from prime mover is insufficient for the output electricity torque to the power system. Therefore, all the rotor shafts of the synchronous generators are forced to slow down, ending up in a decline of power system frequency.

The majority of the research for power system frequency simulation is done through the closed-loop control mechanism based on the transfer functions in the Laplace domain, which emulates the behaviour of the generator's governor and turbine for the PFR and the supplementary control for the SFR. However, the definition of PFR and SFR has been relaxed from its response mechanism into a more time-specific concept. Any response satisfying the time requirements for PFR can be categorised into PFR no matter of the response sources. The other drawback of the transfer function based frequency simulation is the difficulties of adopting the recent fast frequency response technology from wind turbines and batteries into the system.

The work in this chapter introduces a mathematical approach to simulate the system frequency behaviour after a sudden load/generation imbalance. The model is based on the synchronous generator swing equation and divides the frequency curve into three stages depending on the PFR availability. The impact of total system inertia and PFR are investigated using the mathematical model representing the key system parameters regarding frequency stability.

The rest of the chapter is organised as: Section 3.2 introduces the mathematical approach to simulate and study the frequency behaviour. Section 3.3 investigates the impacts of the frequency behaviour regarding the following aspects: the total system inertia, the PFR availability, the PFR delivery time and the load frequency-sensitivity. Section 3.4 summaries the chapter by presenting the key findings and key learnings of this chapter.

3.2 Mathematical Model for Frequency Response

For the security of the power system frequency stability, it is essential to investigate the behaviour of the system frequency immediately after a sudden generation/load imbalance. The trigger of the imbalance includes, but is not limited to: generator outage, transmission failure, loss of interconnecting tie-line, and the sudden connection of a large demand.

3.2.1 Swing Equation

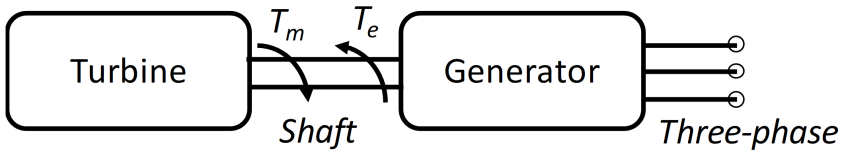

Figure 3-1: Generator shaft

The swing equation describes the position of the rotor axis reflecting the deceleration or acceleration of rotor speed depending on the active power mismatch. The generator shaft is a rotational reference frame and the mismatch between the input mechanical torque and output electrical torque cause the shaft to accelerate/decelerate. The angular acceleration can be expressed as [1]:

$$A = \frac{T_M - T_E}{J} = \frac{T_A}{J} \tag{3.1}$$

where,

- A is the angular acceleration in rad/s^2,
- T_M is the input mechanical torque in N·m,
- T_E is the output electrical torque in N·m,
- T_A is the accelerating torque in N·m,
- J is the moment of inertia in kg·m^2.

Note that the moment of inertia J contains all the synchronous rotating elements including the turbine, generator, shaft and gears.

The acceleration torque will cause the rotor angular velocity ω_R to change based on:

$$T_M - T_E = A \cdot J = J\frac{d\omega_R}{dt} \tag{3.2}$$

The definition of inertia constant is the ratio between stored kinetic energy to the machine rated apparent power:

$$H = \frac{E_{KIN}}{S_N} = \frac{\frac{1}{2}J{\omega_N}^2}{S_N} \tag{3.3}$$

where,

- H is the inertia constant of the generator in s (second),
- E_{KIN} is the stored kinetic energy in the generator in MW·s,
- ω_N is the rated angular velocity of the generator in rad/s,
- S_N is the rated apparent power of the generator in MVA.

Substituting the moment of inertia in (3-2) by the inertia constant (3-3) get:

$$T_M - T_E = H \cdot \frac{2S_R}{{\omega_N}^2} \cdot \frac{d\omega_R}{dt} \tag{3.4}$$

The basic relationship between the torque and power is $P = \omega_N \cdot T$. As the speed deviation is relatively small, by replacing the torque by power, equation (3.4) represents the relationship between the ROCOF and active power mismatch in per-unit form.

$$\begin{aligned} \frac{\omega_N T_M - \omega_N T_E}{S_R} = 2H \cdot \frac{d(\frac{\omega_R}{\omega_N})}{dt} = 2H \cdot \frac{d(\frac{2\pi f_R}{2\pi f_N})}{dt} \\ P_m - P_e = 2H \cdot \frac{df}{dt} \end{aligned} \tag{3.5}$$

where,

- P_m is the input mechanical power in p.u.,
- P_e is the output electrical power in p.u.,
- f_R is the generator frequency in Hz,
- f_N is the generator rated frequency in Hz,
- f is the generator frequency in p.u.

The swing equation (3.5) is a non-linear differential equation describing the dynamics of the rotor swing caused by the power exchange between the mechanical power from the prime mover and the electric power to the power grid. The inertia can be considered as the resistance to any speed changes by releasing/adsorbing the stored kinetic energy.

For the simplicity of the calculation and deduction, power system analysis usually employs a per-unit form. The base values of the deduction are listed below:

- Frequency base f_{base}: the nominal system frequency f_N,
- Power base S_{base}: the total system demand D_{f_N}.

3.2.2 Load Frequency Response

The frequency variation is caused by the interaction between electricity generation and demand; however, generation is not the only element to react to frequency deviations, but also frequency-sensitive loads. An example of the frequency damping provided by the frequency-sensitive load is addressed in [98]. A generation loss of 1050 MW occurred on 19:04 p.m. 19^{th} of April 2005 in Scotland with total system demand at 45 GW. As shown in Table 3.1, the frequency services only cover 64.7% of the imbalance, with the remaining 35.3% countered by the frequency sensitivity of the demand.

Table 3.1: Demand contribution to frequency deviation

Total generation loss	1050 MW
Frequency services:	
Spinning reserve	500 MW
Demand-side response	80 MW
Total	680 MW
Demand contribution	370 MW

The sensitivity of the demand against frequency is fundamentally dependent on the percentage of motor-type loads. As the electricity absorbed by the motor is primarily determined by the rotation speed which is aligned with the infeed electricity frequency, when frequency drops the absorbed electricity power declines simultaneously and vice

versa (when the frequency rises the demand also inclines). The auto-adjustment of system demand against the frequency deviation is a self-regulating process which provides a considerable part in the total frequency responses to counter the generation/demand deficit and helps the system restoring frequency stability [98].

The Great Britain Transmission Network Operator, National Grid, estimates the load frequency sensitivity is 2.5%, indicating 1 Hz frequency deviation from the nominal frequency leads to a 2.5% change in the system demand [99]. The response from frequency-sensitive load ΔD can be expressed as:

$$\Delta D = D_{f_n} \cdot k_{DFR} \cdot f_N \cdot [f_n - f(t)] = k_{dfr} \cdot [f_n - f(t)] \tag{3.6}$$

where,

- D_{f_n} is the system demand at the nominal frequency in p.u.,
- f_N is the system nominal frequency, i.e. 50 Hz,
- f_n is the system nominal frequency in p.u.,
- k_{DFR} is the demand frequency ratio, i.e. 2.5%,
- $k_{dfr} = D_{f_n} \cdot k_{DFR} \cdot f_N$, representing the per-unit demand change against the per-unit frequency change.

3.2.3 Three Stages of Primary Frequency Response

The system overall frequency performance after a loss of a generator unit is a combination of the responses from the frequency-sensitive load and the responses supplied by generating units. The majority of the responses are delivered by the generation side in the form of frequency responses, i.e. PFR and SFR. The purpose of PFR is to arrest the frequency drop to a quasi-steady-state frequency, while the SFR is to bring the quasi-steady-state frequency back to nominal value. The mathematical model of system frequency only concerns on the transient performance of the system frequency, which is primarily dominated by the total system inertia and PFR; hence, the SFR is neglected for simplicity. Depending on the amount of the PFR availability in different time frames, the frequency curve after a generation loss can be split into three stages shown in Figure 3-2.

Stage 1 (0 to t_1) represents the inertial response period where no PFR is provided due to the generator governor response deadband for frequency deviations. The PFR start

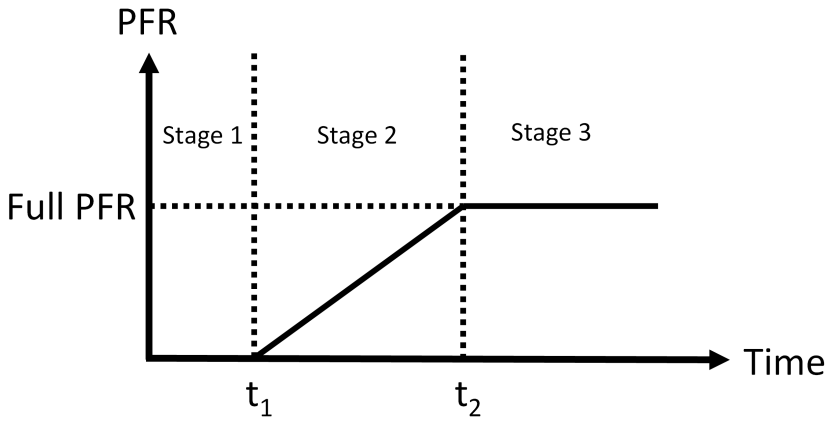

Figure 3-2: Frequency responses time frames

Table 3.2: PFR availability in different time frame

	Stage 1	**Stage 2**	**Stage 3**
Time frame	0 to t_1	t_1 to t_2	After t_2
PFR availability	Governor deadband, no PFR	PFR rising from 0 to full	Full PFR

time is noted as t_1.

Stage 2 (t_1 to t_2) indicates the period in which the PFR start to respond until the full PFR is delivered. At time t_2, the maximum amount of PFR is fully injected. Assuming the PFR rises linearly, the PFR ramp rate can be expressed as:

$$r = \frac{P_{PFR}}{t_2 - t_1} \tag{3.7}$$

where,

- P_{PFR} is the full PFR in the system in p.u.,
- r is the PFR ramp rate in p.u.

At **Stage 3** (after t_2) the full available PFR is injected into the system. The system frequency will be re-stabilised at a quasi-steady-state before the SFR brings the frequency to its nominal value.

The change of injected PFR over time for three stages can be summarised as:

$$\Delta PFR = \begin{cases} 0, & \text{for } 0 \leq t < t_1 \\ r(t - t_1), & \text{for } t_1 \leq t < t_2 \\ P_{PFR}, & \text{for } t_2 \leq t \end{cases} \tag{3.8}$$

3.2.4 Frequency Deviations Based on Swing Equation

Due to the fact that the scale of the Great Britain power system is relatively small compared with continent Europe or the United State of America or China. The regional frequency difference can be neglected, and the whole system is assumed to have a unified system frequency equal to the frequency at the centre of inertia. Aggregating the system into one single generator shaft, the frequency deviation in the Great Britain power system is, therefore, determined by the active power mismatch between the overall system demand and the total system generation.

Assume the initial frequency is the nominal system frequency, i.e. 50 Hz. According to the swing equation (3.5), the dynamic frequency change is affected by the responses from both the generation unit and frequency-sensitive load. Hence, the frequency curve can be generalised as:

$$\frac{df(t)}{dt} = \frac{-P_{loss} + \Delta D + \Delta PFR}{2H_{sys}} \tag{3.9}$$

where,

- $f(t)$ is the system frequency in p.u.,
- P_{loss} is the sudden active power imbalance, in p.u., e.g. loss of generation,
- ΔD is the response from frequency-sensitive demand in p.u.,
- ΔPFR is the response from the generating units in p.u.,
- H_{sys} is the inertia constant for the power system in s.

Assuming the system frequency before the event is the nominal system frequency, the

change of system frequency is expressed piecewise for three stages shown as:

$$\begin{aligned}
\frac{df_1(t)}{dt} =& \frac{-P_{loss} + k_{dfr} \cdot [f_n - f_1(t)]}{2H_{sys}}, && \text{for } 0 \leq t < t_1 \\
\frac{df_2(t)}{dt} =& \frac{-P_{loss} + k_{dfr} \cdot [f_n - f_2(t)] + r \cdot (t - t_1)}{2H_{sys}}, && \text{for } t_1 \leq t < t_2 \\
\frac{df_3(t)}{dt} =& \frac{-P_{loss} + k_{dfr} \cdot [f_n - f_3(t)] + P_{PFR}}{2H_{sys}}, && \text{for } t_2 \leq t
\end{aligned} \tag{3.10}$$

where,

- $f_1(t)$ is the frequency expression against time for $0 \leq t < t_1$ (**Stage 1**),
- $f_2(t)$ is the frequency expression against time for $t_1 \leq t < t_2$ (**Stage 2**),
- $f_3(t)$ is the frequency expression against time for $t_2 \leq t$ (**Stage 3**).

As shown in the Figure 3-2, the available PFR injected into the system is not linear but continuous against time. Therefore the piecewise differential equations are continuous for all three stages and at the PFR start time t_1 and PFR fully deployed time t_2.

$$\begin{aligned}
\frac{df_1(t)}{dt} =& \frac{df_2(t)}{dt}, && \text{for } t = t_1 \\
\frac{df_2(t)}{dt} =& \frac{df_3(t)}{dt}, && \text{for } t = t_2
\end{aligned} \tag{3.11}$$

At **Stage 1**, the initial ROCOF is the frequency dropping rate when $t = 0$. At the initial time the system frequency has not change:

$$\Delta D = k_{dfr}[f_n - f_1(0)] = 0 \tag{3.12}$$

Hence, the initial ROCOF is purely dependent on the total system inertia for a certain generation loss:

$$\left.\frac{df}{dt}\right|_{t=0} = \frac{-P_{loss}}{2H_{sys}} \cdot f_N \text{ (HZ/s)} \tag{3.13}$$

3.2.5 Frequency Expressions for Three Stages

This section proposes a mathematical approach to model the frequency behaviour followed by an active power deficit between electricity generation and consumption. The system frequency is described by the differential equation set, indicating the ROCOF,

which is based on the swing equation at the rotor shaft point of view. The solutions to the differential equation set (3.10) can be found in Appendix A2. The continuity of frequency (f) and the ROCOF (df/dt) are both taken into consideration for all three stages.

The complete frequency functions are listed below:

$$f_1(t) = \left(f_n - \frac{P_{loss}}{k_{dfr}}\right) + \left(f_0 - f_n + \frac{P_{loss}}{k_{dfr}}\right) \cdot e^{-\frac{k_{dfr}}{2H_{sys}}t}$$

$$f_2(t) = a_1 + a_2 \cdot e^{-\frac{k_{dfr}}{2H_{sys}} \cdot t} + \frac{r}{k_{dfr}} \cdot t$$

$$f_3(t) = a_3 \cdot e^{-\frac{k_{dfr}}{2H_{sys}}t} + a_4$$

where,

- $a_1 = \left(f_n - \frac{P_{loss}}{k_{dfr}}\right) - \frac{2H_{sys} \cdot r}{{k_{dfr}}^2} - \frac{r \cdot t_1}{k_{dfr}}$ (3.14)
- $a_2 = \left(f_0 - f_n + \frac{P_{loss}}{k_{dfr}}\right) + \frac{2H_{sys} \cdot r}{{k_{dfr}}^2} \cdot e^{-\frac{k_{dfr}}{2H_{sys}}t_1}$
- $a_3 = \frac{2H_{sys} \cdot r}{{k_{dfr}}^2} \cdot \left(e^{\frac{k_{dfr} \cdot t_1}{2H_{sys}}} - e^{\frac{k_{dfr} \cdot t_2}{2H_{sys}}}\right) + \left(f_0 - f_n + \frac{P_{loss}}{k_{dfr}}\right)$
- $a_4 = f_n + \frac{P_{PFR} - P_{loss}}{k_{dfr}}$

The mathematical model is the foundation of the works presented in Chapter 4 and 6 as the frequency constraints are generated based on the mathematical model.

3.3 Key Elements Affecting Frequency Performances

Since the electricity generation and consumption are rarely balanced, the system frequency is always fluctuating around the nominal frequency. However, as long as the system frequency stays in the Operational Limit, the tiny frequency fluctuations will cause no trouble to the power system stability. Major frequency deviations are generated by the instant large power deficits. National Grid specifies the frequency limits for Significant Loss and Abnormal Loss. To maintain the system frequency within acceptable limits and avoiding the under frequency load shedding, the combined support from several deciding elements such as the total system inertia and frequency responses is required. This section investigates the influences on the frequency performance from the total system inertia, the amount of PFR the PFR response speed and the load

frequency-sensitivity.

3.3.1 System Inertia for Frequency Performance

The system inertia accounts for all synchronous rotating elements in both generating units and demand equipment. However, the main inertia providers are still traditional fossil-fired power stations such as coal and gas. In Great Britain power system, the demand variation is fundamentally countered by the gas-fired power station, hence, the inertia difference is quite significant between the demand peak and trough time due to the inertia contributions from the gas-fired power stations.

The influence on the frequency curve from the inertia point of view is studied based on a 40 GW system. A 1320 MW generation loss is applied at 5 seconds and the system has 1000 MW frequency response available to be called upon. The typical values for inertia constant of different types of generators are between 3 s to 7 s [1, 29]. Therefore, three scenarios are being tested with the total system inertia constant equals to 3 s, 5 s and 7 s in the total system demand base respectively. Results are shown in Figure 3-3 and Table 3.3, which indicate the system inertia affects the initial ROCOF, the maximum ROCOF in an event; and the frequency nadir, the minimum system frequency in an event.

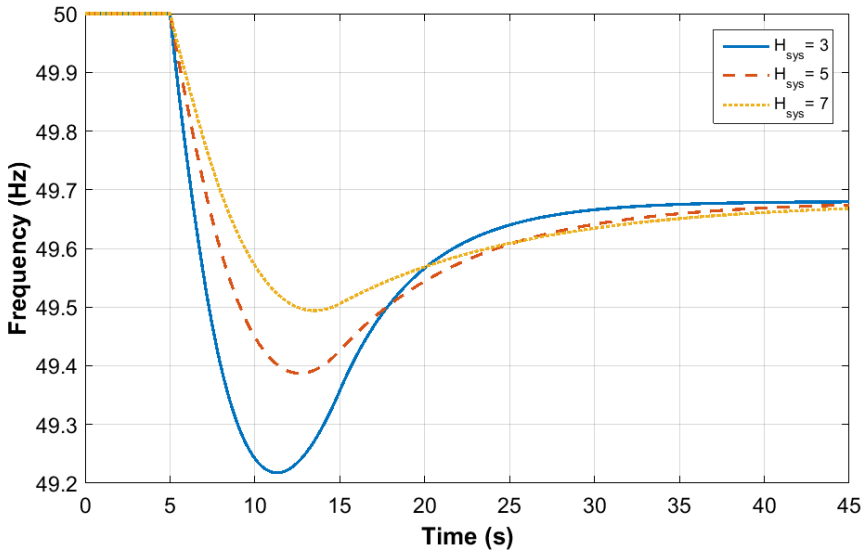

Figure 3-3: Frequency curves for different inertia levels

As the total system inertia increases, the initial ROCOF reduces from 0.275 Hz/s for

Table 3.3: Results of different inertia levels

System inertia constant H_{sys}	3s	5s	7s
Initial ROCOF (Hz/s)	0.275	0.165	0.118
Frequency nadir (Hz)	49.22	49.39	49.49

the system with 3 s inertia constant to 0.118 Hz/s for the system with 7 s inertia constant. To avoid part of a distribution network becoming isolated and energised, all the distributed generators above a certain size are equipped with a ROCOF relay to protect the equipment and personal. The initial ROCOF is the maximum value which will appear in a frequency drop event which is the most possible trigger for the ROCOF relays. The more inertia in the system, the lower the initial ROCOF will appear, hence reducing the possibility of unnecessary tripping of distributed generators after a major frequency deviation.

The total system inertia also helps to resist the frequency dip. The more inertia in the system, the less frequency will deviate from the nominal frequency. The frequency nadir for the same generation loss with the total system inertia constant at 3 s, 5 s and 7 s are 49.22 Hz, 49.39 Hz and 49.49 Hz, respectively, according to Figure 3-3. If frequency drops below 48.8 Hz, the automatic under frequency load shedding will start to prevent further frequency decreasing. Hence, the total system inertia is of great importance regarding the frequency nadir allowed for a frequency contingency.

However, the system inertia not only resists the frequency from decreasing but also resists the frequency restoring process. As shown in Figure 3-3, the frequency rises more quickly with less total system inertia, i.e. 3 s inertia constant, for the same amount of generation loss.

The system inertia is a vital system property regarding frequency stability which helps to reduce the initial ROCOF and lift the frequency nadir. The only side effect of inertia is slowing down the frequency restoration process, but the initial ROCOF and frequency nadir are more important for the system operation. However, typically renewable generation are decoupled from the main grid through power electronic devices to extract the maximum wind power and solar panels lack the ability to provide inertia naturally. Therefore, the total system inertia is decreasing in recent years due to the increasing penetration of renewable generation [4, 5, 100, 101].

3.3.2 Primary Frequency Response Availability for Frequency Performance

PFR is implemented through the generator governor control. The role of PFR is to arrest the frequency drop, hence the frequency will not re-stabilise at the nominal frequency but at a quasi-steady-state frequency. The impact of different levels of PFR availability is investigated for a system with 40 GW demand. A 1320 MW generation loss is applied at 5 seconds and the system inertia constant is 5 s in the base of total system demand.

The influence of PFR availability is tested in three scenarios, i.e. 700 MW, 900 MW and 1100 MW respectively. As shown in Figure 3-4 and Table 3.4, the amount of PFR available in the system affects the frequency nadir and the quasi-steady-state frequency. An increase in the PFR reserve lifts both the frequency nadir and the quasi-steady-state frequency, i.e. increasing from 49.31 Hz and 49.38 Hz, respectively, for 700 MW PFR reserve to 49.41 Hz and 49.77 Hz, respectively, for the system with 1100 MW PFR reserve. The reason for the lift is because in order to stop the frequency drop, the insufficient PFR is compensated by the frequency-sensitive load which will lead to a larger frequency deviation.

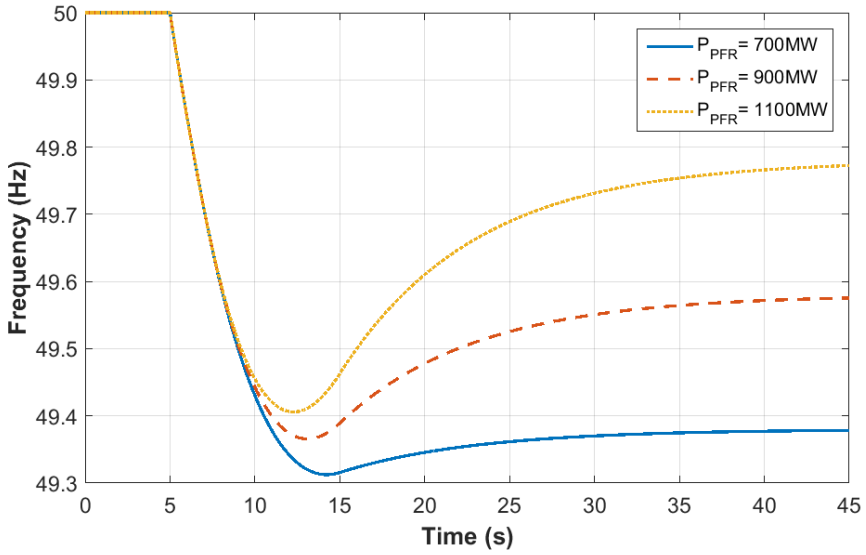

Figure 3-4: Frequency curves for different PFR availabilities

The available PFR reserve decides both the frequency nadir and the quasi-steady-state frequency. With more PFR reserve in the system, it is easier to meet the frequency

Table 3.4: Results of different PFR availabilities

PFR availability (MW)	700	900	1100
Frequency nadir (Hz)	49.31	49.37	49.41
Quasi-steady-state frequency (Hz)	49.38	49.58	49.77

requirements. When the frequency response can fully fill up the power imbalance the system frequency will return to the nominal value.

3.3.3 Primary Frequency Response Speed for Frequency Performance

Due to the governor deadband, the traditional PFR is unable to react to the frequency deviation instantly. Before PFR kicks in, the frequency is dropping mainly dependant on the system inertia. Increasing the response speed of PFR can prevent the frequency falling too much before any control mechanisms begin. The PFR response time varies for different generation technologies. The typical start time for PFR is 2 second after the frequency contingency. This is especially important in low inertia circumstances because the frequency might already drop to the line of automatic load shedding within the initial several seconds. The UK transmission network operator, National Grid, specifies the PFR to be delivered within 10 seconds after the contingency [20]; while in Ireland due to the size and robustness of the network, the PFR is required to deliver within 5 seconds [27].

To investigate the influence of PFR response speed to the frequency performance, three scenarios have been created, where the PFR is delivered within 15 seconds, 10 seconds and 5 seconds, respectively. A 1320 MW generation loss is applied to a 40 GW demand system at 5 seconds and the system has 1000 MW PFR reserve and 5 s system inertia constant in the total system demand base.

Figure 3-5 and Table 3.5 shows the frequency curves and results for the three scenarios. The PFR response speed affects the frequency nadir with 49.55 Hz for 5 seconds of delivery time and 49.28 Hz for 15 seconds of delivery time. Although the total amount of PFR reserves are the same, reducing the delivery time can increase the injected PFR per unit time to help arrest the frequency drop more effectively.

The PFR response speed is especially important in low inertia systems. Figure 3-6 demonstrates the simulation of the frequency behaviour with a reduced system inertia

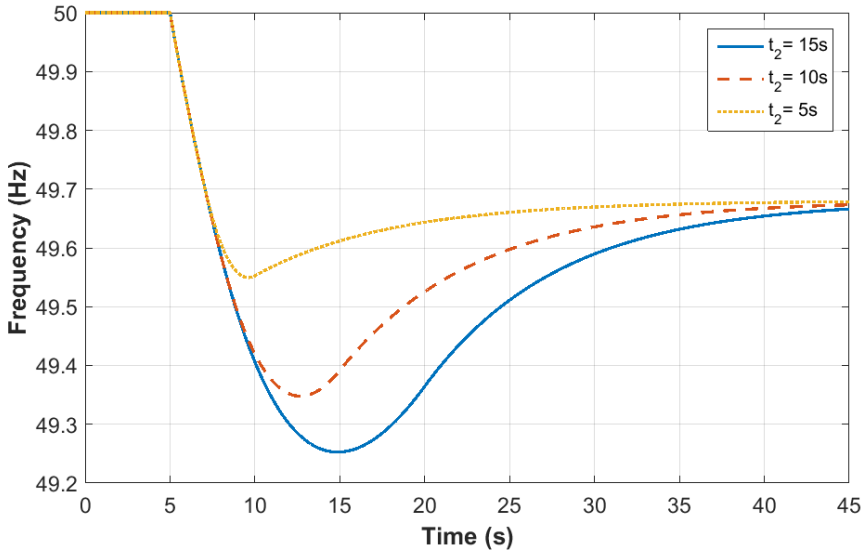

Figure 3-5: Frequency curves for different PFR response speeds

Table 3.5: Results of different PFR response speeds

PFR delivery time t_2 (seconds)	15	10	5
Frequency nadir (Hz)	49.28	49.39	49.55

Table 3.6: Results of different PFR response speeds with reduced system inertia

PFR delivery time t_2 (seconds)	15	10	5
Frequency nadir (Hz)	49.13	49.22	49.37

constant from 5 s to 3 s in the total system demand base. The system demand, generation loss, PFR reserve and PFR delivery times for all three scenarios remain the same. The frequency curves for all scenarios in Figure 3-6 already fall below 49.4 Hz before any PFR start to react to the frequency dip. The frequency nadir reduced to 49.13 Hz for 15 seconds PFR delivery time and 49.37 Hz for 5 seconds PFR delivery time as shown in Table 3.6.

The PFR response speed affects the lowest frequency in an event and boosts the response speed by means of injecting more PFR into the system to prevent excessive frequency drop especially for low inertia system. The research of fast frequency response

supplied by wind turbines and batteries has gained increasing attention because of the low inertia problem.

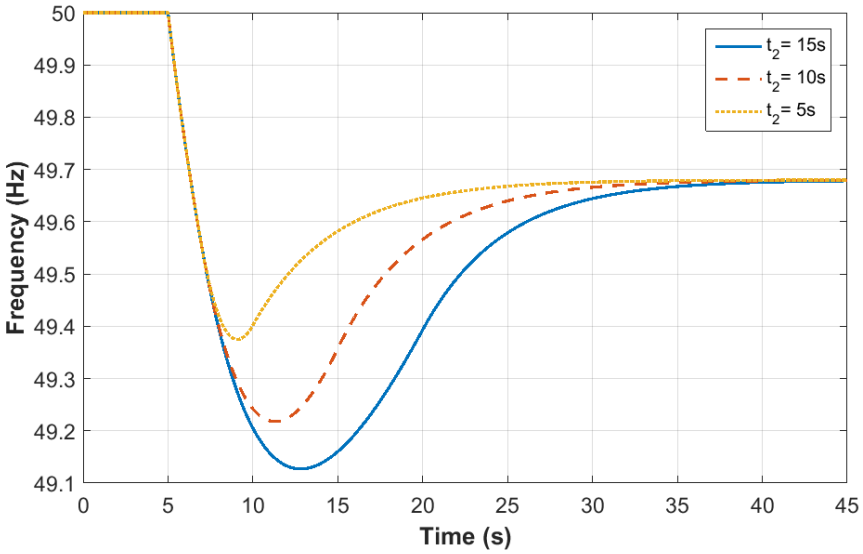

Figure 3-6: Frequency curves for different PFR response speeds with reduced system inertia

3.3.4 Load Frequency Sensitivity for Frequency Performance

The electricity demand damping to the frequency variations is fundamentally based on the frequency-sensitive loads whose power absorption are correlated with frequency deviations [98]. National Grid estimates the demand frequency ratio in the UK to be 2.5%, representing a 1 Hz change in frequency leads to a 2.5% change in demand. The response to the falling frequency from frequency-sensitive load helps to fill the power deficit and slows the frequency drop.

Table 3.7: Results of different PFR availabilities

Demand frequency ratio k_{DFR}	1.5%	2.5%	3.5%
Frequency nadir (Hz)	49.24	49.39	49.48
Quasi-steady-state frequency (Hz)	49.46	49.68	49.77

The influence of load frequency sensitivity is carried out with three demand frequency

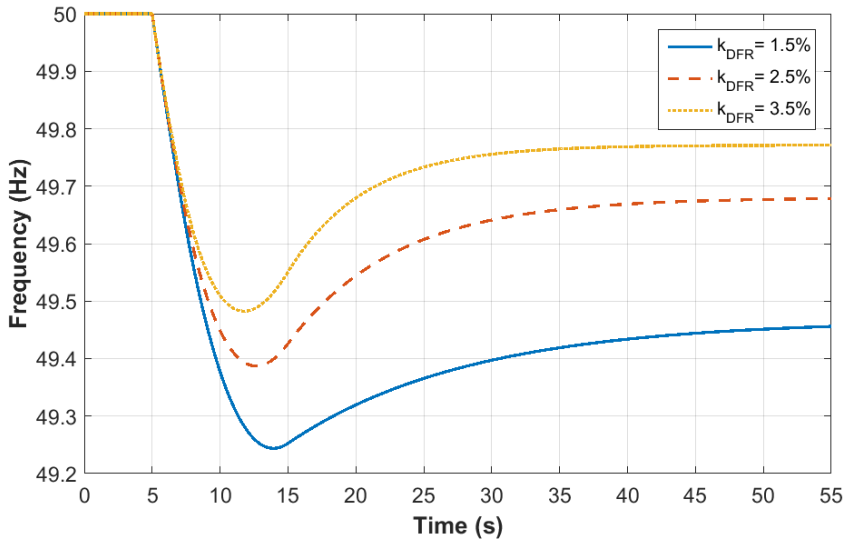

Figure 3-7: Frequency curves for different demand frequency ratios

ratio levels: 1.5%, 2.5% and 3.5% representing demand change per 1 Hz frequency change. A 40 GW demand system is subjected to a 1320 MW generation loss at 5 seconds, the PFR reserve is 1000 MW and the system inertia constant is 5 s in the base of total system demand. The frequency curves are shown in Figure 3-7 and the results are shown in Table 3.7. The demand frequency ratio has an influence on the frequency nadir and the quasi-steady-state frequency. The increased 3.5% demand frequency ratio is able to lift both the frequency nadir and quasi-steady state frequency from 49.24 Hz and 49.46 Hz to 49.48 Hz and 49.77 Hz respectively compared with 1.5% demand frequency ratio.

The response from frequency-sensitive load influences both the frequency nadir and the quasi-steady-state frequency. Increasing the demand frequency ratio can lift both the frequency nadir and quasi-steady-state frequency. However, the load frequency sensitivity can be affected by the power electronic controlled devices and the distributed renewable generations which alters the load frequency sensitivity seen by National Grid [98].

3.3.5 Key Findings

This section identifies the key elements that decide the frequency performance followed by a contingency based on the mathematical model introduced in the last section. The key findings regarding the frequency requirements in the event of a contingency are

listed below:

- The initial ROCOF is purely decided by the total system inertia.
- The frequency nadir is dependent on the total system inertia, the amount and response speed of PFR and the load frequency sensitivity.
- The quasi-steady-state frequency is influenced by the amount of PFR reserve and the load frequency sensitivity.

3.4 Chapter Summary

This chapter places the foundation for this research work. The studies in this chapter:

- Propose an aggregated mathematical model for frequency simulation
- Identify the key elements in maintaining the stability of system frequency under contingencies

The work in this chapter introduces a mathematical approach to simulate the system frequency behaviour after a sudden load/generation imbalance. The model is based on the synchronous generator swing equation and divides the frequency curve into three stages depending on the PFR availability. The impacts of total system inertia and PFR are investigated using the mathematical model representing the key system parameters regarding frequency stability.

The findings in this chapter inspire the works in Chapter 4 and 6.

Chapter 4

Inertia-Dependent Frequency-Related Constraints

THIS chapter proposes a novel method to stipulate the inertia-dependent constraints to meet the frequency regulations in the UK, ensuring the continuous system operation.

4.1 Introduction

The power system requires a stable system frequency to enable continued operation. Failure to do so would lead to several problems such as the increased network losses, decreased power equipment efficiency and unexpected LFDD. Hence, the contingency plan of a major frequency deviation event is essential to the power system frequency stability. In the UK, the frequency is regulated under the TSO, National Grid, through several ancillary services mechanisms. The regulations of the system frequency under contingencies are stated in the SQSS [20] which mainly considers three aspects: the ROCOF, the frequency nadir and the quasi-steady-state frequency.

Since all the interconnectors between the UK and mainland Europe are HVDC lines which are equivalent to DC generators, the UK power system operates as an isolated island system. The SQSS requires the UK power system to have sufficient frequency response to cover the maximum potential generation loss constantly. However, that regulation is focused solely on frequency response reserve. The learnings from Chapter 3 introduce other key elements regarding frequency stability, especially the total system inertia. With a reduced total system inertia, a relatively small disturbance could produce with large frequency deviations. Therefore, the current practice has the potential to violate the frequency requirements even if sufficient PFR reserves are in place for a future high renewable low inertia system.

The work in this chapter presents a solution to stipulate the constraints for both the total system inertia and frequency response to ensure the frequency requirements are satisfied for the UK power system. The initial ROCOF, quasi-steady-state frequency and frequency nadir are inertia only, PFR only and inertia plus PFR constraints, respectively. The relationship between total system inertia and PFR reserve is also investigated based on the frequency mathematical model presented in Chapter 3.

The rest of the chapter is organised as: Section 4.2 investigates the inertia requirements in the UK power system to ensure the constant operation. Section 4.3 provides a method to quantify the equivalent PFR to the inertia depending on the frequency nadir requirements in the UK. Section 4.4 presents a summary of the chapter.

4.2 Frequency Related Inertia Constraints

The current operation of the UK power system does not take into account the inertia reserve in the system which will introduce some new problems regarding the frequency stability. The work in this section investigates the inertia requirements in the UK power system to ensure the constant operation of the system. The case studies of inertia constraints are conducted for 4 cases representing different demand levels and ROCOF requirements.

4.2.1 Inertia Constraint for Initial Rate of Change of Frequency

The initial ROCOF is the largest ROCOF in a frequency excursions, which is purely decided by the total system inertia, described by the equation (3.13), for a certain generation loss. The ROCOF limit in the system is elaborated in the previous section, and the inertia constraint for initial ROCOF is expressed as:

$$\left.\frac{df}{dt}\right|_{t=0} = \left|\frac{P_{loss}}{2H_{sys}}\right| \leq \frac{ROCOF_{limit}}{f_N} \tag{4.1}$$

Hence,

$$\begin{aligned} H_{sys} &\geq \left|\frac{P_{loss}}{2ROCOF_{limit}}\right| \cdot f_N \\ E_{sys} &\geq \left|\frac{P_{loss} \cdot S_N}{2ROCOF_{limit}}\right| \cdot f_N \end{aligned} \tag{4.2}$$

where,

- P_{loss} is the generation loss in p.u.,
- $ROCOF_{limit}$ is the largest ROCOF allowed in the system which is 0.125 Hz/s before 2016 and 0.5 Hz/s nowadays,
- f_N is the system nominal frequency, i.e. 50 Hz.

Note that for a frequency contingency with generation loss the initial ROCOF is always negative value, however, sometimes the sign of ROCOF is neglected. To get rid of the misleading, the equation is adopted into the absolute value.

4.2.2 Inertia Constraint for Frequency Nadir

Conclusions from Section 3.3 indicate the frequency nadir during a contingency is determined by the combined effect of the total system inertia and PFR. Hence, the inertia constraint for frequency nadir is correlated with PFR. Assuming the system has sufficient PFR reserve to arrest the frequency drop, the frequency nadir can only appear in the Stage 2 of the mathematical model presented in Section 3.2. Otherwise, if the system has insufficient PFR, the frequency drop is countered by the extra response from the frequency-sensitive load and the frequency nadir is equal to the quasi-steady-state frequency.

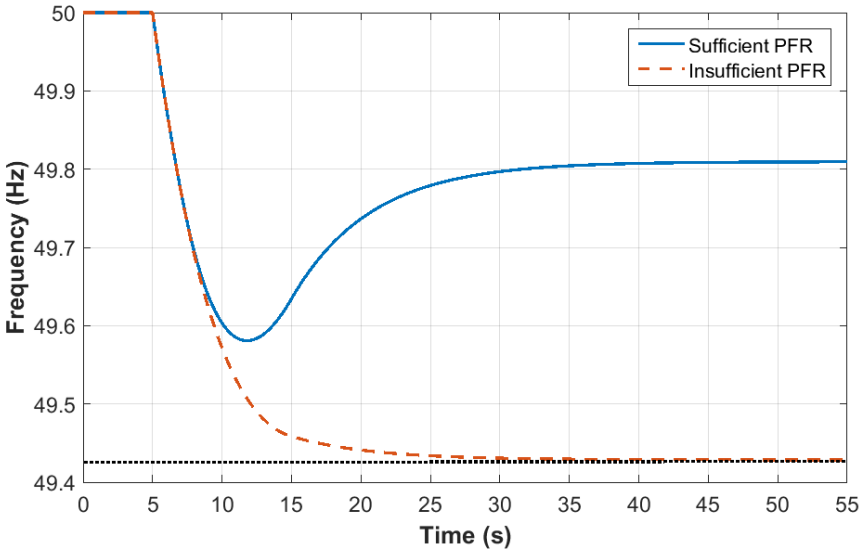

Figure 4-1: Frequency nadir with sufficient and insufficient PFR

Figure 4-1 demonstrates the frequency nadir with sufficient PFR and insufficient PFR for a 30 GW system subject to 800 MW loss. However, the inertia level affects the frequency nadir for the same PFR reserve in the system as shown in Figure 3-3. For any PFR reserve levels which are sufficient to arrest the frequency drop, there is an inertia limit to meet the frequency requirements for the UK system.

Assuming at time t_{min} the system frequency reaches the frequency nadir, f_{min}, and substituting t_{min} and f_{min} into the frequency expression for Stage 2 gives:

$$f_{min} = f_2(t_{min}) = a_1 + a_2 \cdot e^{-\frac{k_{dfr} t_{min}}{2H_{sys}}} + \frac{r t_{min}}{k_{dfr}} \tag{4.3}$$

When the frequency is at frequency nadir the derivative of frequency is zero, setting df_2/dt to zero provides:

$$\left.\frac{df_2}{dt}\right|_{t=t_{min}} = -\frac{k_{dfr}}{2H_{sys}} \cdot a_2 \cdot e^{-\frac{k_{dfr}t_{min}}{2H_{sys}}} + \frac{r}{k_{dfr}} \tag{4.4}$$

Hence, the time of frequency nadir is obtained as:

$$t_{min} = \frac{2H_{sys}}{k_{dfr}} \ln \frac{2H_{sys}r}{a_2{k_{dfr}}^2} \tag{4.5}$$

Substituting (4.5) into (4.3), the frequency nadir as a function of the total system inertia can be obtained:

$$f_{min} = a_1(H_{sys}) + a_5(H_{sys}) \cdot \left[1 + \ln \frac{a_2(H_{sys})}{a_5(H_{sys})}\right] \tag{4.6}$$

where a_1, a_2 and a_5 are three inertia related functions:

$$\begin{aligned} a_1 &= \left(f_n - \frac{P_{loss}}{k_{dfr}}\right) - \frac{r \cdot t_1}{k_{dfr}} - \frac{2r}{{k_{dfr}}^2} \cdot H_{sys} \\ a_2 &= \left(f_0 - f_n + \frac{P_{loss}}{k_{dfr}}\right) + \frac{2r}{{k_{dfr}}^2} \cdot e^{\frac{k_{dfr} \cdot t_1}{2H_{sys}}} \cdot H_{sys} \\ a_5 &= \frac{2r}{{k_{dfr}}^2} \cdot H_{sys} \end{aligned} \tag{4.7}$$

Let a new function of $G(H_{sys})$ be defined as:

$$G(H_{sys}) = a_1(H_{sys}) + a_5(H_{sys}) \cdot \left[1 + \ln \frac{a_2(H_{sys})}{a_5(H_{sys})}\right] - f_{min} \tag{4.8}$$

With the given frequency nadir, f_{min}, the inertia requirement for the system is expressed as the minima H_{sys} that makes the function $G(H_{sys}) \geq 0$. The Newton-Raphson method is adopted to find the optimised minima of H_{sys}. The derivative of the function $G(H_{sys})$ is $G'(H_{sys})$:

$$G'(H_{sys}) = \frac{a_5}{H_{sys}} \cdot \ln \frac{a_2}{a_5} + \left(\frac{1}{H_{sys}} - \frac{k_{dfr}t_1}{{H_{sys}}^2}\right) \cdot e^{\frac{k_{dfr}t_1}{H_{sys}}} \cdot \frac{{a_5}^2}{a_2} - \frac{a_5}{H_{sys}} \tag{4.9}$$

The minimal H_{sys} requirement can be updated as

$$H_{sys(n+1)} = H_{sys(n)} - \frac{G(H_{sys(n)})}{G'(H_{sys(n)})} \tag{4.10}$$

With an initial guess of $H_{sys(0)}$, the corresponding optimised minima of system inertia is obtained until the acceptable tolerance for $\Delta H_{sys(n)}$ is reached.

4.2.3 Primary Frequency Response Constraint for Quasi-steady-state Frequency

Results from Chapter 3 indicate the quasi-steady-state frequency is solely dependent on the available PFR. The requirements for quasi-steady-state frequency are stated in Section 3.2 with the Operation Limit, 49.8 Hz, for the contingencies smaller than 300 MW and the Statutory Limit, 49.5 Hz, for the contingencies greater than 300 MW.

The quasi-steady-state frequency is acquired by assuming no SFR is injected into the system and substituting $t = \infty$ for the frequency expression in Stage 3:

$$f_{qss} = \left(f_n + \frac{P_{PFR} - P_{loss}}{k_{dfr}} \right) \geq \frac{f_{SL}}{f_N} \tag{4.11}$$

where,

- f_{qss} is the quasi-steady-state frequency in p.u.,
- f_{SL} is the Statutory Limit of the system frequency, i.e. 49.5 Hz.

Therefore, the minimal amount of PFR reserve that the system should have can be obtained as:

$$P_{PFR} \geq P_{loss} - \left(f_n - \frac{f_{SL}}{f_N} \right) \cdot k_{dfr} \tag{4.12}$$

4.2.4 Case Study

The case study for inertia constraints is conducted for four scenarios depending on different demand levels and different ROCOF limits. The trough demand in the UK in 2017 happened on 11^{th} of June at 6:00 a.m. with 16.6GW, whilst the peak demand occurred on 26^{th} of January at 18:00 p.m. with 49.8 GW [102]. The ROCOF limit 0.125 Hz/s and 0.5 Hz/s are selected for the representation of the old and new ROCOF requirements in the UK [52, 53].

Hence, the demand levels of 49.9 GW and 16.6 GW are selected for the case studies. For each scenario, the range of possible generation loss is from 400 MW up to the largest infeed generator 1800 MW, with the same range of the frequency response. The

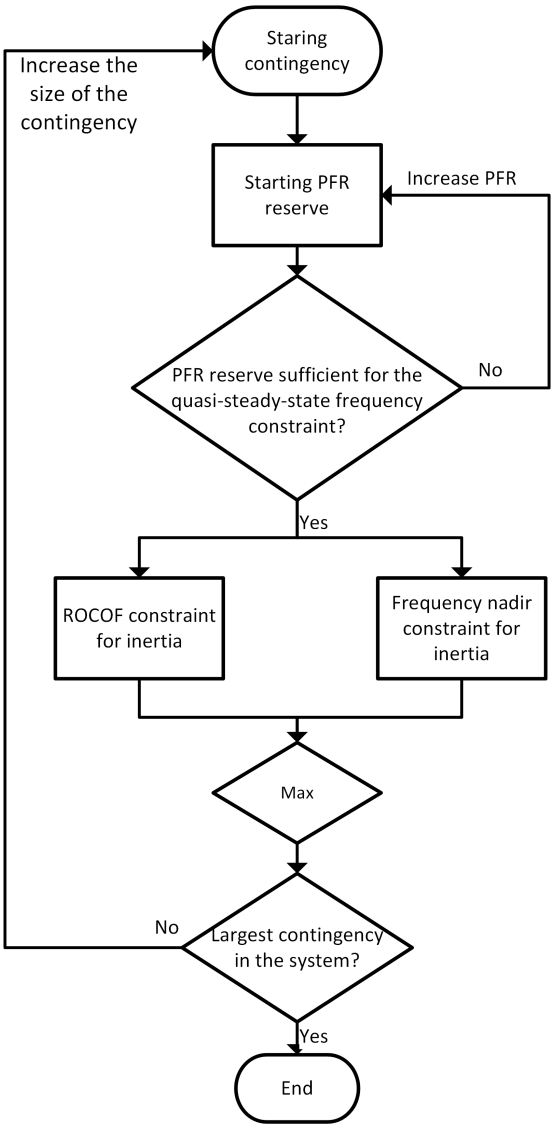

Figure 4-2: Flowchart for the inertia constraint

flowchart of the method is shown in Figure 4-2, starting with the minimum loss and calculates the inertia constraints for different PFR reserve levels up to the 1800 MW loss.

Case 1 (trough demand with 0.125 Hz/s ROCOF limit)

Case 1 represents the inertia constraints for trough demand period with the previous ROCOF limits, i.e. 0.125 Hz/s. As shown in Figure 4-3, the inertia constraints are

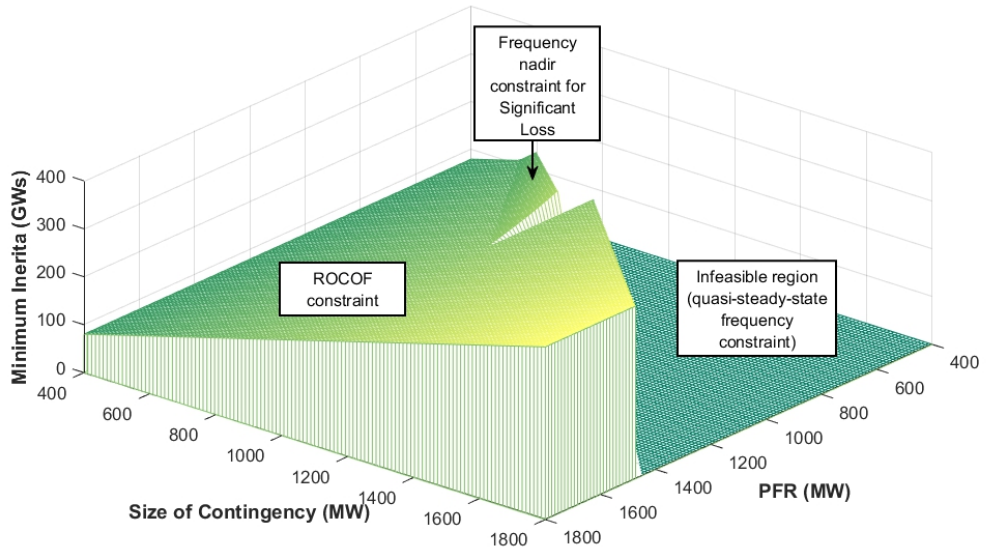

Figure 4-3: Inertia constraints for Case 1

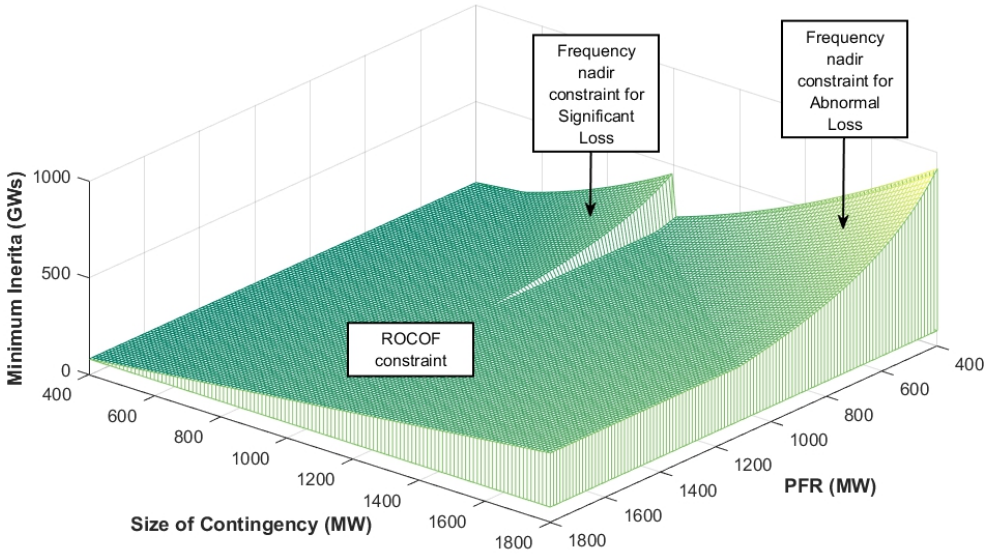

Figure 4-4: Inertia constraints for Case 1 with relaxed quasi-steady-state frequency requirement

largely dominated by the ROCOF requirements and there is a significant area of the infeasible region indicating that no matter how much inertia is available in the system,

the system still unable to meet the quasi-steady-state frequency requirements due to the lack of PFR. A small protrusion can be observed towards the maximum Significant Loss, due to the different frequency nadir requirements for the contingency below and above 1000 MW. Hence, there is a dip at the boundary between Significant Loss and Abnormal Loss.

Figure 4-4 shows the inertias constraint for Case 1 with the quasi-steady-state frequency requirements being relaxed. A triangle area towards both the maximum Significant and Abnormal Loss can be found depending on the frequency nadir constraint. Because of the lack of PFR, the inertia constraints climb to an unreasonable high level which indicates the necessity of sufficient PFR reserve.

Case 2 (peak demand with 0.125 Hz.s ROCOF limit)

Case 2 represents the peak demand situation with the previous ROCOF requirements, i.e. 0.125 Hz/s. The inertia constraints for Case 2 are shown in Figure 4-5, which purely dependent on the ROCOF requirements. However, the area of the infeasible region is reduced due to the increased response contribution from the frequency-sensitive load which has been stated in Section 3.3.4.

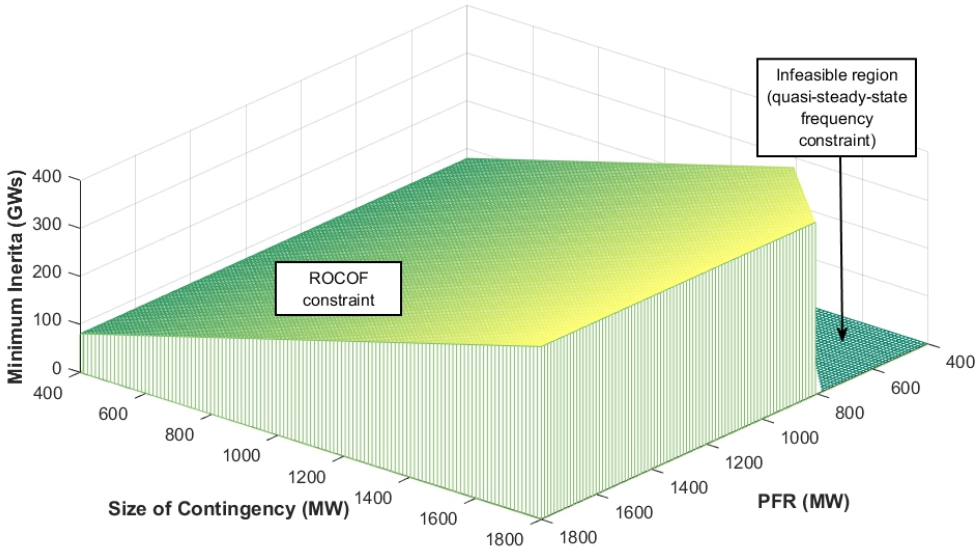

Figure 4-5: Inertia constraints for Case 2

The results shown in Figure 4-3 and 4-5 indicate that the frequency nadir requirements

are largely dependant on the ROCOF requirements regardless of the demand levels with a ROCOF limit of 0.125 Hz/s. This means that the ROCOF limit of 0.125 Hz/s is not applicable to the system, as the inertia constraints are primarily determined by the ROCOF requirements and can be relaxed if the ROCOF requirements are able to be designed more appropriate.

Case 3 (trough demand with 0.5 Hz/s ROCOF limit)

Case 3 represents the inertia constraints for trough demand period with the increased ROCOF limit, i.e. 0.5 Hz/s, and Figure 4-6 shows the inertia constraints for Case 3. As in Case 1, the infeasible region implies the PFR reserve is insufficient for the quasi-steady-state frequency requirements and is related to the demand level because the increased demand can provide more support to the falling frequency from the frequency-sensitive load. For Case 3, the inertia constraints are purely determined by the frequency nadir constraints.

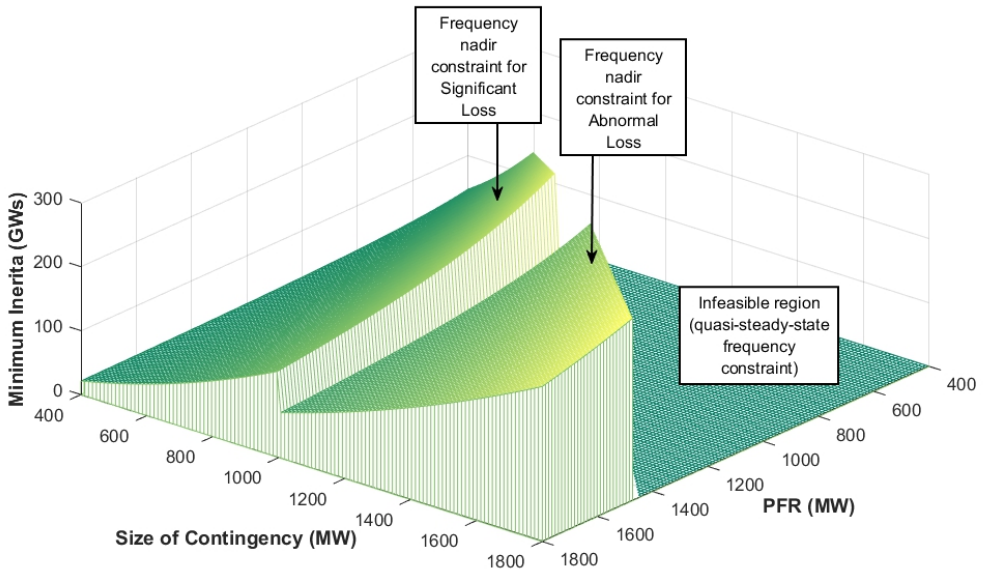

Figure 4-6: Inertia constraints for Case 3

Case 4 (peak demand with 0.5 Hz/s ROCOF limit)

Case 4 represents the inertia constraints with 0.5 Hz/s ROCOF requirements for the peak demand period. As shown in Figure 4-7, the inertia constraints are divided into 3 areas, determined by the ROCOF requirements, frequency nadir requirements for Significant Loss and frequency nadir requirements for Abnormal Loss respectively.

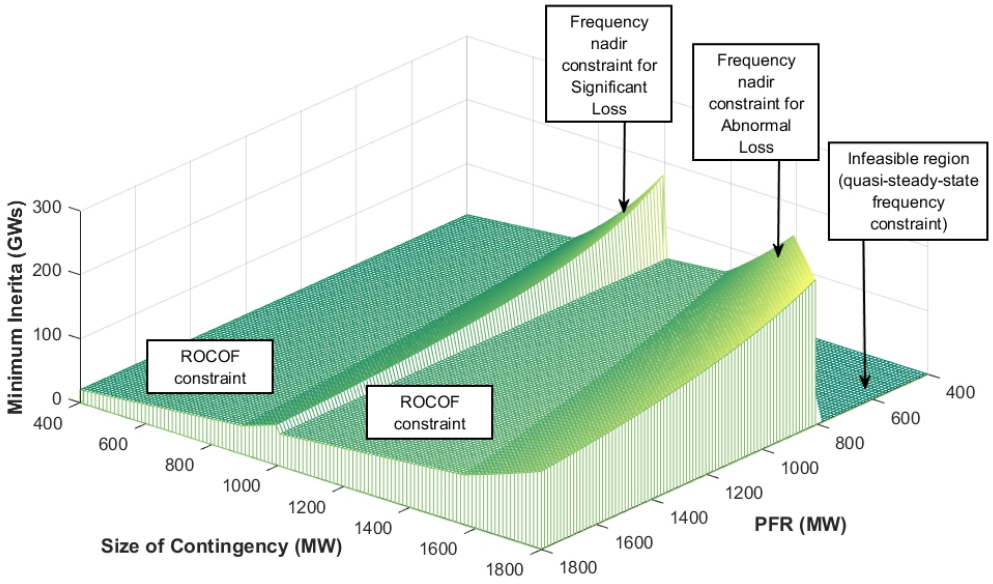

Figure 4-7: Inertia constraints for Case 4

4.2.5 Key Findings

The key findings from the four case studies are listed below:

- The infeasible region is determined by the demand level which indicates the minimum required PFR reserve in the system to satisfy the quasi-steady-state frequency requirements.
- The inertia constraints determined by ROCOF requirements are linear with the size of the contingency regardless of the PFR reserve and demand levels.
- The inertia constraints determined by frequency nadir requirements are non-linear and correlated with the size of the contingency and the PFR reserves. Due to the different frequency nadir requirements for the contingency above and below

1000 MW, a steep drop is obtained at the boundary of Significant and Abnormal Losses.

4.3 Equivalent Primary Frequency Response

The frequency nadir is determined by the collaboration of total system inertia and the PFR reserve. When the available inertia in the system increases, the requirements for PFR reserve will be relaxed accordingly; hence, the inertia can be considered as an alternative to PFR. For some cases, an increased inertia is more economical than increasing the PFR. This section provides a novel method to quantify the equivalent PFR to the inertia depending on the frequency nadir requirements in the UK.

4.3.1 Problem Formulation

Consider the expression for minimum frequency of Stage 2 in equation (4.6) as a function of both PFR reserve and the total system inertia instead of inertia only. If the PFR reserve is represented by the PFR ramping rate, r, the minimum frequency should be no smaller than the frequency nadir requirements. Hence, equation (4.6) can be rewritten as:

$$f_{min}(r, H_{sys}) = a_1(r, H_{sys}) + a_5(r, H_{sys}) \cdot \left[1 + \ln \frac{a_2(r, H_{sys})}{a_5(r, H_{sys})}\right] \geq \frac{f_{limit}}{f_N} \qquad (4.13)$$

where,

- f_{min} is a function of r, H_{sys} representing the minimum frequency in Stage 2.,
- a_1, a_2 and a_5 are three non-time related functions of r and H_{sys} to simply the expression provided in Chapter 3,
- f_{limit} is the frequency nadir requirements for the system in Hz, e.g. 49.2 Hz for the loss of 1800 MW,
- f_N is the nominal frequency in Hz.

The relationship of inertia and PFR can be deducted from the expression (4.13):

$$-\frac{rt_1}{k_{dfr}}+1-\frac{P_{loss}}{k_{dfr}}+\frac{r\cdot 2H_{sys}}{{k_{dfr}}^2}\cdot\left[\ln\frac{\left(f_0-1+\frac{P_{loss}}{k_{dfr}}\right)+\frac{r\cdot 2H_{sys}}{{k_{dfr}}^2}\cdot e^{\frac{k_{dfr}t_1}{2H_{sys}}}}{\frac{r\cdot 2H_{sys}}{{k_{dfr}}^2}}\right]\geq f_{limit}$$
$$\frac{\left(f_0-1+\frac{P_{loss}}{k_{dfr}}\right)+\frac{r\cdot 2H_{sys}}{{k_{dfr}}^2}\cdot e^{\frac{k_{dfr}t_1}{2H_{sys}}}}{\frac{r\cdot 2H_{sys}}{{k_{dfr}}^2}}\geq e^{\left(f_{limit}+\frac{rt_1}{k_{dfr}}-1+\frac{P_{loss}}{k_{dfr}}\right)\cdot\frac{{k_{dfr}}^2}{r\cdot 2H_{sys}}} \tag{4.14}$$

However, the relationship (4-14) is a transcendental equation with no analytical solution. Alternatively, the inertia and PFR relationship can be plotted point by point using the method described in Section 4.3.2. Figure 4-8 shows the relationship between the total system inertia and the PFR reserve to ensure the frequency nadir constraints when subjected to 1800 MW generation loss for 23 GW, 40 GW and 50 GW demand, respectively. The two ends of the curve are constrained by the ROCOF and quasi-steady-state frequency requirements for minimum system inertia and minimum PFR reserve, respectively. As the system demand increase, the relationship curve moves downward, which means less combined PFR and inertia are required.

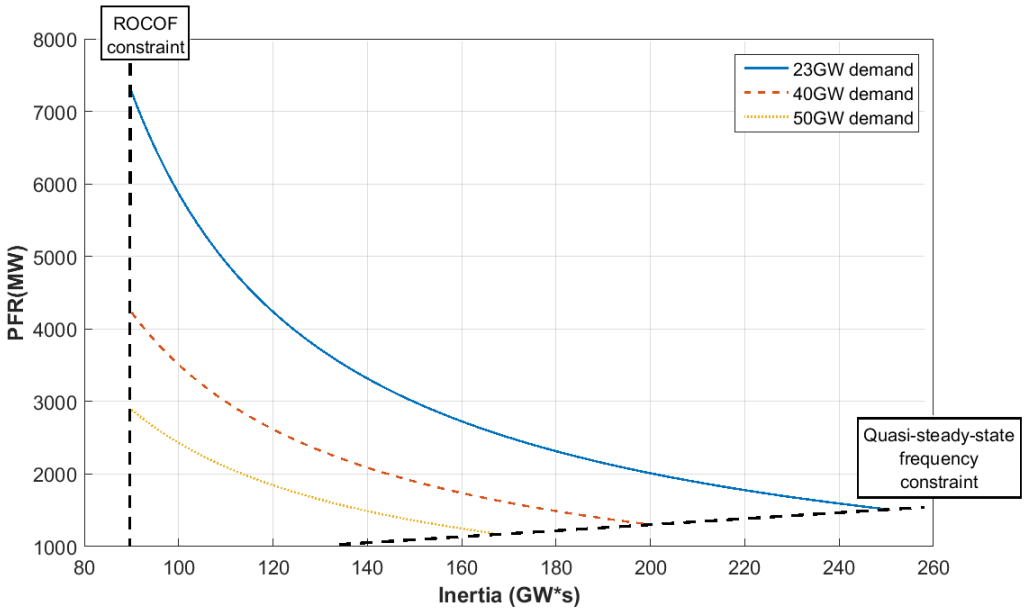

Figure 4-8: Inertia-PFR relationship

Figure 4-9 shows the amount of PFR that can be relaxed per 1 GWs inertia increase when subjected to 1800 MW generation loss for 23 GW, 40 GW and 50 GW demand,

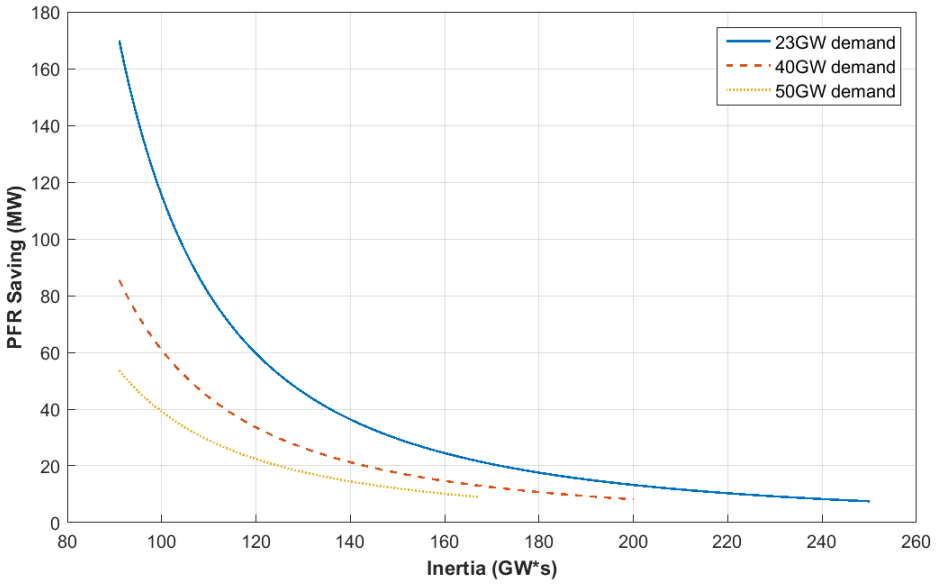

Figure 4-9: PFR saving per unit inertia increase

respectively. As can be seen from the figure, the less the inertia, the more PFR can be relaxed per unit inertia increase. This indicates that when the inertia is at a low level, an increase in inertia can help the system to meet frequency regulation more effectively than by increasing the PFR reserve.

4.3.2 Polynomial Fitting

The inertia-PFR relationship shown in Figure 4-8 is discrete and plotted point-by-point due to the transcendence of the function. For ease of use, a mathematical expression is necessary to analyse the relationship between inertia and PFR. A polynomial fitting is used to find the expression for the equivalent PFR.

It is assumed that the relationship between inertia and equivalent PFR has the following form:

$$P_{PFR} = Fit_a \cdot {H_{sys}}^2 + Fit_b \cdot H_{sys} + Fit_c + \frac{Fit_d}{H_{sys}} \tag{4.15}$$

where Fit_a, Fit_b, Fit_c and Fit_d are the coefficients of the polynomial fitting. The estimation of the coefficients can be implemented using MATLAB through a training process [103].

4.3.3 Case Study

Significant Loss

The system parameters for the Significant Loss case study are listed in Table 4.1. A 40 GW system subject to 900 MW generation loss with the frequency regulations for Significant Loss is considered.

Table 4.1: System parameters for the polynomial fitting case study for 900 MW loss

Generation Loss (MW)	Frequency nadir (Hz)	Quasi-steady-state frequency (Hz)	ROCOF (Hz/s)
900	49.5	49.5	0.5
Demand (GW)	**Response start time (Second)**	**Response fully applied time (second)**	**Demand frequency ratio (%)**
40	2	7	2.5

The polynomial fitting coefficients and results are shown in Table 4.2 and Figure 4-10, respectively. The degree of fitting indicates the quality of the fit, the R-square value is equal to 0.9976.

Table 4.2: Inertia-PFR relationship fitting coefficients for 900 MW loss

Fit_a	Fit_b	Fit_c	Fit_d
-0.3344	$1.0011 \cdot 10^2$	$-1.0038 \cdot 10^4$	$3.9631 \cdot 10^5$

Table 4.3: Inertia-PFR combinations for 900 MW loss

	Combination A	Combination B	Combination C	Combination D
Inertia (GWs)	90	100	110	120
PFR (MW)	666.5	591.9	530.5	462.4

Four inertia-PFR combinations, shown in Table 4.3, on the fitting curve are selected to

verify that the frequency nadir requirements are met. Figure 4-11 shows the frequency curves for the selected inertia-PFR combinations. The frequency nadir for all cases fall on the limit of 49.5 Hz which indicates all the inertia-PFR combinations above the curve in Figure 4-10 can meet the frequency nadir constraints.

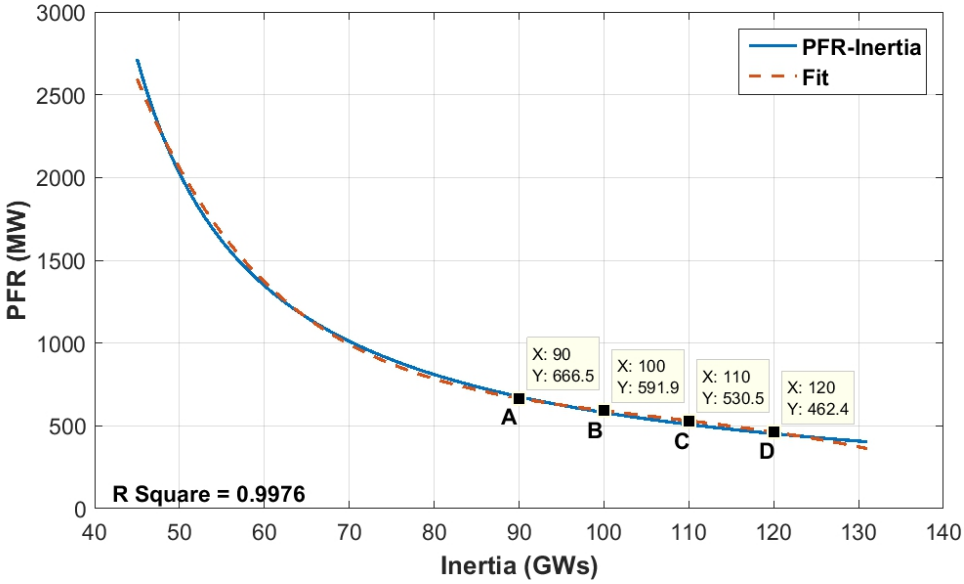

Figure 4-10: Polynomial fitting for the inertia-PFR relationship for 900 MW loss

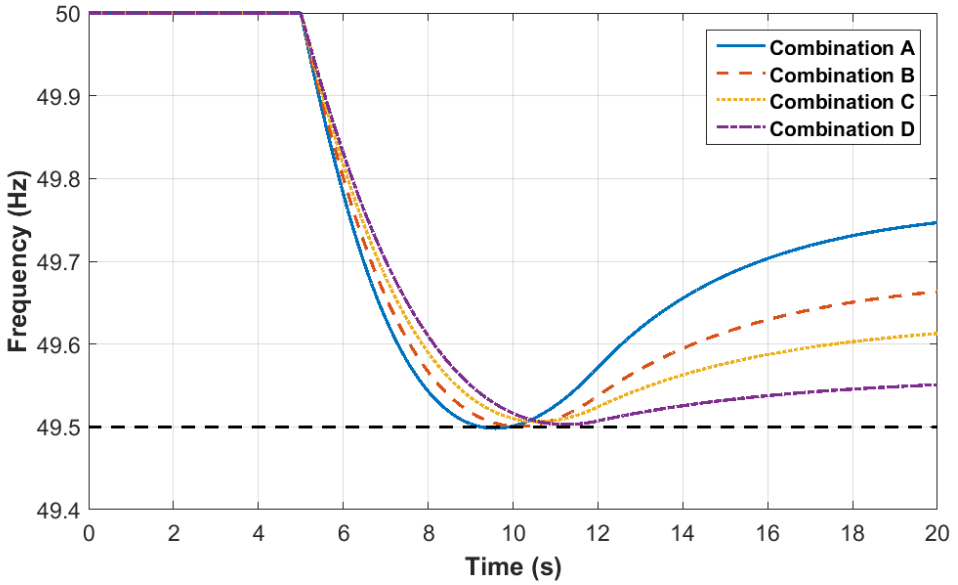

Figure 4-11: Inertia-PFR combination frequency curves for 900 MW loss

Abnormal Loss

The case study for Abnormal Loss is conducted for the system subject to the largest potential infeed loss in the UK, 1800 MW, with the demand at 40 GW. The frequency constraints are following the regulations for Abnormal Loss. The system parameters for the case study are listed in Table 4.4.

Table 4.4: System parameters for the polynomial fitting case study for 1800 MW loss

Generation Loss (MW)	Frequency nadir (Hz)	Quasi-steady-state frequency (Hz)	ROCOF (Hz/s)
1800	49.2	49.5	0.5
Demand (GW)	**Response start time (Second)**	**Response fully applied time (second)**	**Demand frequency ratio (%)**
40	2	10	2.5

Figure 4-12 shows the results of the inertia-PFR relationship polynomial fitting for 1800 MW generation loss. The degree of fitting R-square value is equal to 0.9991, and the fitting coefficients are listed in Table 4.5.

Table 4.5: Inertia-PFR relationship fitting coefficients for 1800 MW loss

Fit_a	Fit_b	Fit_c	Fit_d
-0.3344	$1.0011 \cdot 10^2$	$-1.0038 \cdot 10^4$	$3.9631 \cdot 10^5$

Table 4.6: Inertia-PFR combinations for 1800 MW loss

	Combination E	Combination F	Combination G	Combination H
Inertia (GWs)	160	170	180	190
PFR (MW)	1741	1610	1496	1390

Table 4.6 shows the four selected inertia-PFR combinations on the fitting curve for the validation of the frequency requirements. The results are shown in Figure 4-13,

the frequency nadir for all cases are at the limit of 49.2 Hz which indicates all the inertia-PFR combinations above the curve in Figure 4-12 can meet the frequency nadir constraints.

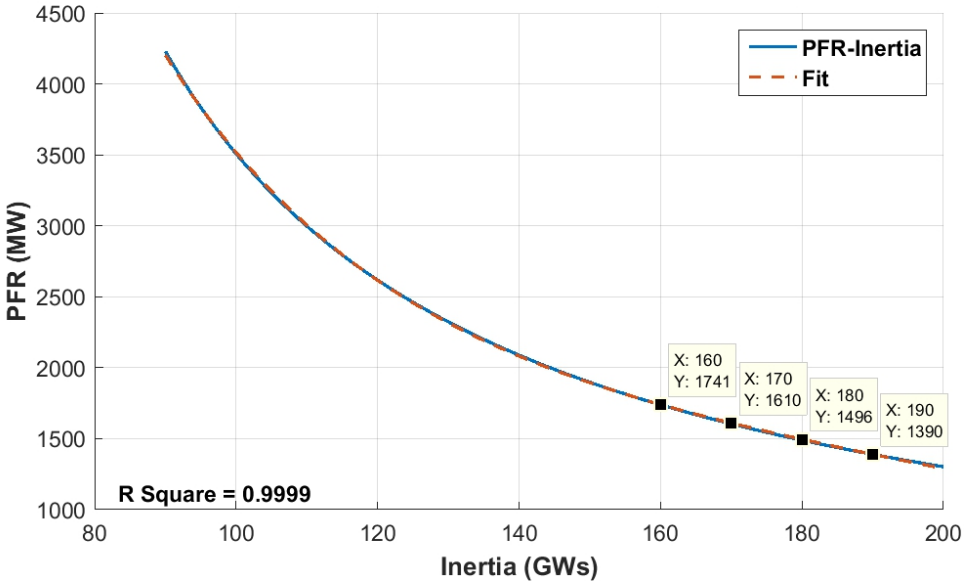

Figure 4-12: Polynomial fitting for the inertia-PFR relationship for 1800 MW loss

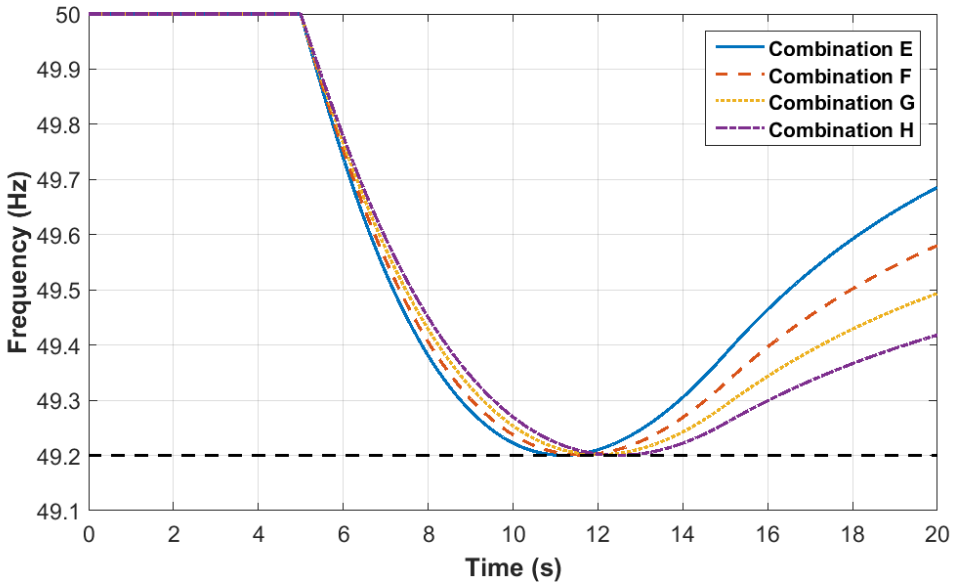

Figure 4-13: Inertia-PFR combination frequency curves for 1800 MW loss

4.3.4 Key Findings

The keying learnings from the case study are:

- Abnormal Loss is more challenging compared to Significant Loss regarding the frequency nadir constraints, as more combined inertia and PFR are needed to meet the requirements.
- When the inertia is at a low level, an increase in inertia can help the system to meet frequency regulation more effectively than increase the PFR reserve in the system.

4.4 Chapter Summary

The work in this chapter:

- Proposes a method to stipulate the inertia constraints of the system regarding different sizes of contingency and PFR reserves.
- Quantifies the equivalent PFR to the system inertia in terms of meeting the frequency nadir requirements.

The equivalent PFR to the system inertia is quantified by mathematical analysis of the frequency behaviour. The inertia-PFR relationship is transcendental; therefore, a polynomial fitting is applied to provide a high-quality estimation. The inertia-related frequency-dependent constraints are stipulated based on the frequency regulations during contingencies which are affected by the ROCOF and frequency nadir requirements. The inertia constraints also provide the basis for the unit commitment generation scheduling in Chapter 6.

Chapter 5

Demand Side Contributions for System Inertia

THIS chapter develops a novel method to quantify the inertia contributions from the demand side based on the historical data of frequency outage events in the UK power system.

5.1 Introduction

Existing inertia quantification methods can be divided into two categories: focusing on a single generator and the entire system respectively. Research on the single machine inertia constant is largely dependent on the specific generation technologies [21, 104], whilst the system inertia quantification methods rely on the analysis of the frequency outage events regarding the swing equation, also known as a post-mortem analysis [24, 73, 105, 74, 76].

Two aspects on the total system inertia estimation are often being overlooked in previous research:

- A single generator's inertia contribution is determined by its rated capacity regardless of the actual power output.
- The inertia contribution from demand side is often overlooked, which also contributes to the total system inertia.

Those two aspects lead to inaccurate estimations of the total system inertia that either generation side or demand side inertia contributions are underestimated.

For a potential low-inertia system in the future due to the increasing utilisation of inertia-less renewable generation, the inertia contribution from the demand side will become a significant inertia provider in terms of the frequency stability. Understanding the quantity of inertia that the demand side can provide is essential to the analysis of future low-inertia power system frequency control mechanisms.

This chapter proposes a novel method to estimate the inertia contribution from the demand side based on the limited publicly available information regarding the past frequency outage events. The estimation is applied by separating the generation inertia contribution from the total system inertia while bringing in a correction factor, linked with the power/frequency ratio, to convert the actual generation outputs into the connected rated capacity which required for the inertia calculation.

The inertia contributions from the demand side are provided by any load that is synchronous to the system, i.e. the synchronous motors, mainly embedded in the industrial demand. The utilisation of variable frequency drives (VFDs) decouples the machines from the main grid while having the following advantages: adjusting the motor speed, improving the efficiency of the machine and eventually reduce the overall electricity consumption [106]. However, motors connected through VFDs will limit the inertial

response to the system [107]. As the utilisation of VFDs is inevitable in the future due to their advantages, the total system inertia reduction will not only exist in the generation side because of the increasing penetration of inertia-less renewable generations, but also exist in the demand side due to the accumulating implementation of VFDs.

An overview of the proposed method to quantify the demand side inertia contribution is shown in a flowchart in Section 5.2. The methodology of the proposed method is explained in Section 5.3. A demonstration of the proposed method is presented in Section 5.4. Section 5.5 studies the influence of different VFDs penetration levels to the system frequency regulation. Section 5.6 summarises the chapter.

5.2 Flowchart of the Proposed Method

Figure 5-1 shows the flowchart of the proposed method. The quantification of the demand side inertia contribution is achieved by subtracting the generation side inertia contribution from the total system inertia using the data of past frequency deviation events. The whole process can be divided into three phases.

Phase 1 is about gathering and preparing the data required for the proposed method. This includes each frequency outage events including the power imbalance (generation loss), the generation mix when the event occurs, the initial ROCOF, the frequency prior to the event and the power/frequency ratio.

However, the generation mix data that is publicly available is the generation output by fuel type [57], which is the actual power outputs of each generation type instead of their rated capacity. This underestimates the generation contribution. The reason for the underestimation is because the inertia contributed by each generator is primarily determined by the connected capacity rather than its actual power output. Hence, Phase 2 brings a correction factor derived from the power/frequency ratio to reflect the connected generation rated capacity to calculate a more representative estimation of the generation side inertia contribution. In the meantime, the total system inertia of the event can be obtained using the initial ROCOF represented in the frequency behaviour mathematical approach in Section 3.2.4.

In Phase 3, the least squares estimation is applied to work out the inertia contribution based on the date of frequency outage events. The outputs of Phase 3 are the demand side inertia constant in the base of total system demand and a constant α which indicates the additional inertia contribution from the partial loaded generators.

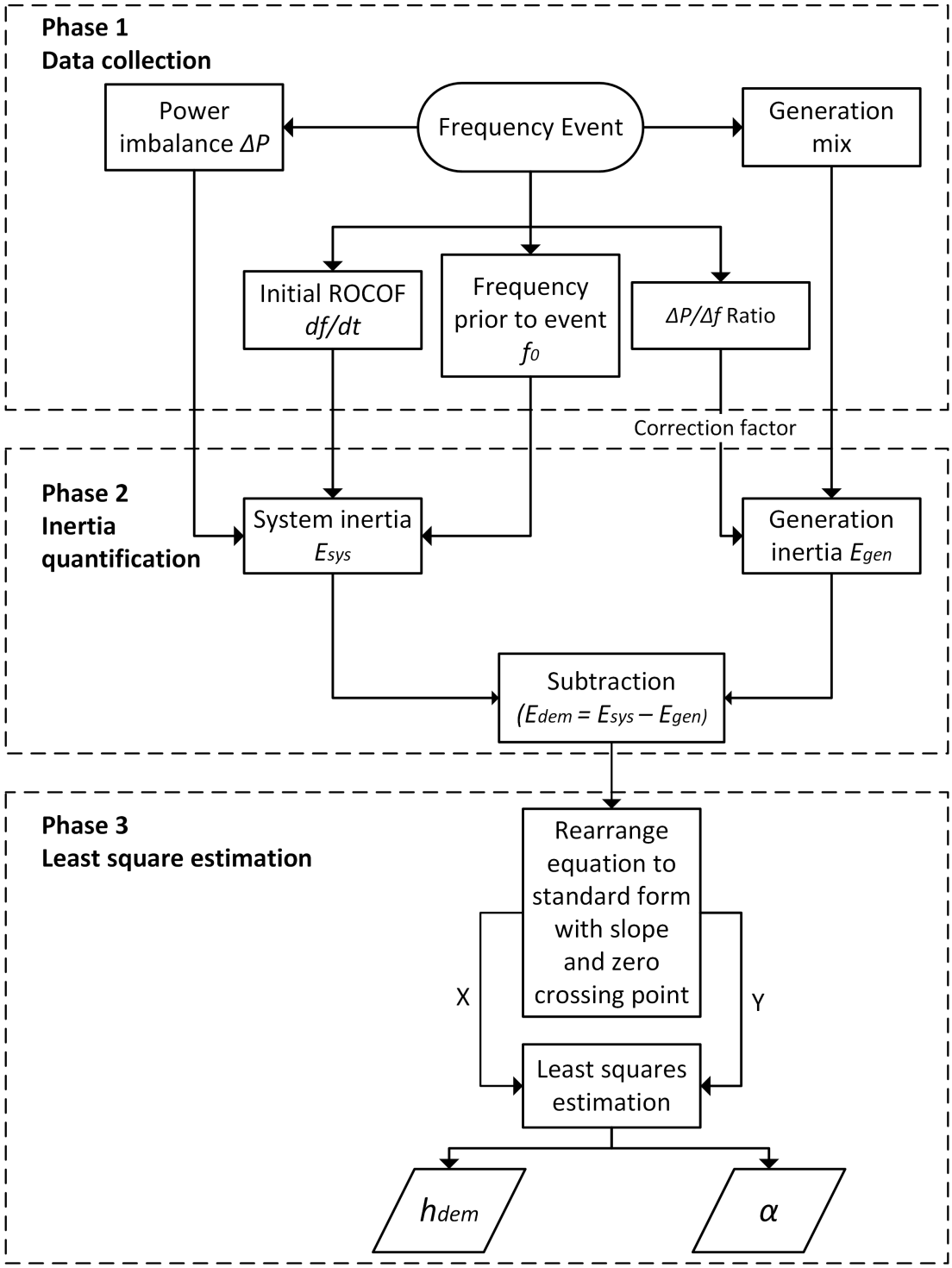

Figure 5-1: Flowchart of the proposed method to quantify the demand side inertia contribution

5.3 Principles of the Proposed Method

This section introduces the proposed method to quantify the demand side inertia contribution. The principle is to subtract the generation side inertia contribution from the total system inertia and considers the power/frequency ratio as an indicator to the additional inertia contribution in spinning reserve.

5.3.1 Total Power System Inertia

A single machine's stored kinetic energy is determined by the moment of inertia and the rotational velocity:

$$E_i = \frac{1}{2} J_i {\omega_{ni}}^2 \tag{5.1}$$

where,

- E_i is the inertia of the machine in terms of stored kinetic energy,
- J_i is the moment of inertia of the machine,
- ω_{ni} is the designed nominal angular velocity of the machine.

As shown in (5-1), when a machine is spinning at the designed rated rotational speed ω_{ni}, the inertia provided by the machine is fixed. If the machine is a generator, the rated angular velocity is the synchronous speed of the power system, and the inertia provided by the generator is fixed no matter if the generator is fully loaded or de-loaded.

The inertia constant of a single machine, representing the per-unit value of inertia, is the ratio between the stored kinetic energy and the base value of the rated apparent power. The physical meaning of inertia constant can be interpreted as the time in seconds that the machine is able to supply a load equal to the rated power purely dependent on the stored kinetic energy in all rotating elements of the machine [1]. The inertia constant is defined as:

$$H_i = \frac{\frac{1}{2} J_i {\omega_{ni}}^2}{S_{ni}} \tag{5.2}$$

where,

- H_i is the inertia constant of the machine in s,
- S_{ni} is the rated apparent power of the machine.

The total power system inertia is the summation of the stored kinetic energy of all synchronously rotating elements for both generators and machines in demand side. Which can be obtained in the form of either kinetic energy or inertia constants:

$$E_{sys} = \sum_{i \in Gen} \frac{1}{2} J_i {\omega_{ni}}^2 + \sum_{j \in Dem} \frac{1}{2} J_j {\omega_{nj}}^2 = \sum_{i \in Gen} H_i S_{ni} + \sum_{j \in Dem} H_j S_{nj} \tag{5.3}$$

where,

- i represents all the synchronous generating units in the generation side,
- j represents all the synchronous motors in the demand side.

Taking the system demand as base value, the system inertia constant can be expressed as:

$$H_{sys} = \frac{E_{sys}}{P_D} \tag{5.4}$$

where,

- H_{sys} is the system inertia constant,
- E_{sys} is the system inertia in the form of kinetic energy,
- P_D is the selected base value, (in this case, the system demand).

However, calculating the total system inertia using equation (5.3) is unrealistic because of the complexity of the demand and it is impossible to accurately count how many motors are connected to the system. Instead, the mathematical approach of the frequency behaviour after network contingencies suggests that the total system inertia is correlated with the initial ROCOF in a frequency deviation event.

The frequency behaviour after a large power imbalance, i.e. a trip of a production unit, is described by the swing equation. The stored kinetic energy is released in order to slow the frequency drop and the power frequency characteristic of the power system is represented by the power/frequency ratio K:

$$\Delta P = 2E_{sys} \frac{df}{dt} + K\Delta f \tag{5.5}$$

where,

- ΔP is the active power imbalance in MW,

- Δf is the frequency deviation in Hz,
- K is the system power/frequency ratio in MW/Hz, representing the system overall droop characteristics.

The power/frequency ratio is positively correlated with the spinning reserve in the system, which indicates the ratio will be larger when more generators are part-loaded [1, 24].

The initial ROCOF as explained in Chapter 3 is modified as equation (5-6) as the power system is not always operating at the nominal frequency. A slight deviation within the operational limit is acceptable. When the frequency deviation event occurs, the system frequency might not be the nominal; therefore, the base value for the equation (5.6) is the frequency prior to the event instead of the nominal frequency.

$$E_{sys} = \frac{\Delta P}{2\frac{df}{dt}} \cdot f_0 \tag{5.6}$$

where,

- E_{sys} is the total system inertia in the form of kinetic energy,
- f_0 is the system frequency prior to the frequency outage event in Hz.

For each recorded frequency outage events, the initial ROCOF, the frequency prior to the event and the power imbalance are required to determine the total system inertia, which is more practical than the use of equation (5.3).

5.3.2 Phase 1: Data Collection

The data collection process gathers all the required data for the demand side inertia contribution quantification. The initial ROCOF, the frequency prior to the event and the power deficit are the input for the calculation of total system inertia. The power/frequency ratio and the generation mix for the frequency outage event are required to determine the generation side inertia contributions. The initial ROCOF, the frequency prior to the event and the power/frequency ratio can be obtained through the analysis of the frequency curve of each frequency outage event. The generation mix for the UK power system can be found at ELEXON, which is the UK wholesale market operator [57]. However, the generation data available from ELEXON only provides the actual generation output of different generation types instead of the connected total capacity, which will underestimate the inertia contributions from the generation side.

To avoid miscalculations, a constant of α is introduced as a supplement to the additional inertia contribution from spinning reserves. The inertia constant used for the proposed method takes the typical value of each generation type based on their rated capacity, larger generators generally contribute more inertia to the system.

5.3.3 Phase 2: Inertia Quantification

The total system inertia consists of the inertia contributions from the generation side, demand side and the distributed generators. The inertia provided by distributed generators is neglected due to its minimal influence. Therefore, the demand side inertia contribution is quantified by subtracting the generation side inertia contribution from the total system inertia.

$$E_{dem} = E_{sys} - E_{gen} \tag{5.7}$$

where,

- E_{dem} is the inertia contribution from the demand in the form of kinetic energy,
- E_{gen} is the inertia contribution from the generation in the form of kinetic energy.

The total system inertia can be quantified by equation (5.6), while the generation side inertia contribution can be estimated using equation (5.3). However, the estimation requires the total capacity of each generator, which may not be available. Instead, the actual generation outputs of each type of generator are used together with the power/frequency ratio as a supplement to the inertia contribution from partially-loaded generators.

The preliminary system frequency drop following a system contingency is only dependent on the total system inertia for the initial few seconds, as known as the inertial response. After that, the PFR starts to react to the frequency decrease. The greater the number of the conventional generators that operate partially-loaded will increase the number of connected generators as well as the spinning reserve availability; thereby, increasing the overall system inertia and the governor reaction to counter the frequency deviations. Hence, the power/frequency ratio is positively correlated with the amount of spinning reserve. Assuming the relationship between the power/frequency ratio and the additional inertia contribution is correlated with a first-order function, and the

generation side inertia contribution can be estimated as:

$$E_{gen} = \sum_{i \in Gen} H_i P_{ni} + \alpha \cdot K = E_{gen,output} + \alpha \cdot K \tag{5.8}$$

where,

- H_i is the averaged inertia constant of a particular generation type,
- P_{ni} is the actual generation output of a particular generation type,
- $E_{gen,output}$ is the total generation side inertia estimation considering the generation outputs of different fuel types,
- α is the constant indicates the additional inertia contribution from partially-loaded spinning reserve.

The power/frequency ratio is estimated through the analysis of the frequency curve for each frequency outage event. Since the typical time window for PFR starts at 2 seconds and the full response fully applied within 10 seconds [108, 109], the frequency deviation for the initial 10 seconds is selected to estimate the value of power/frequency ratio K.

$$K = \frac{\Delta P}{\Delta f \mid_{t=10}} \tag{5.9}$$

Dividing the inertia contribution from demand side by the demand inertia constant in the base of total system demand:

$$E_{dem} = h_{dem} \cdot P_D \tag{5.10}$$

where,

- h_{dem} is the demand side inertia constant with the base of total demand,
- P_D is the total system demand.

Substituting (5.8) and (5.10) into (5.7) gives:

$$E_{sys} - E_{gen,output} = h_{dem} \cdot P_D + \alpha \cdot K \tag{5.11}$$

Thus, only h_{dem} and α are unknowns. The rest of the variables are directly available for each recorded frequency outage events or can be obtained through calculations.

5.3.4 Phase 3: Least Squares Estimation

Equation (5.11) can be rearranged by dividing both sides by the total system demand to transform the binary equation into a linear equation:

$$\frac{E_{sys} - E_{gen,output}}{P_D} = h_{dem} + \alpha \cdot \frac{K}{P_D} \tag{5.12}$$

Assuming:

$$\begin{aligned} X =& \frac{K}{P_D} \\ Y =& \frac{E_{sys} - E_{gen,output}}{P_D} \end{aligned} \tag{5.13}$$

The equation (5.12) becomes:

$$Y = h_{dem} + \alpha \cdot X \tag{5.14}$$

where α and h_{dem} represents the slope and intercept in a linear equation respectively. Appling the least squares estimation, the demand side inertia constant in total system demand base and the coefficient α can be obtained as:

$$\begin{aligned} \alpha &= \frac{\sum_{m=1}^{n} X_m Y_m - n\bar{X}\bar{Y}}{\sum_{m=1}^{n} {X_m}^2 - n\bar{X}^2} \\ h_{dem} &= \bar{Y} - \alpha \cdot \bar{X} \end{aligned} \tag{5.15}$$

where $\bar{X}$ and $\bar{Y}$ represent the average value of X and Y, respectively. This allows the demand side inertia contributions to be estimated.

5.4 Demonstration of the Proposed Method

The demonstration of the proposed method is carried out using the frequency outage events in the UK power system occurred in 2010.

5.4.1 Frequency Events in 2010

Fifteen frequency outage events caused by Significant Losses were recorded by the Electricity National Control Centre (ENCC) of National Grid with 100 milliseconds intervals between April 2010 and August 2010 [110]. The frequency curves are shown

in Figure 5-2, and for each event, the generation loss is equal to the pre-scheduled generation from the faulted BMU.

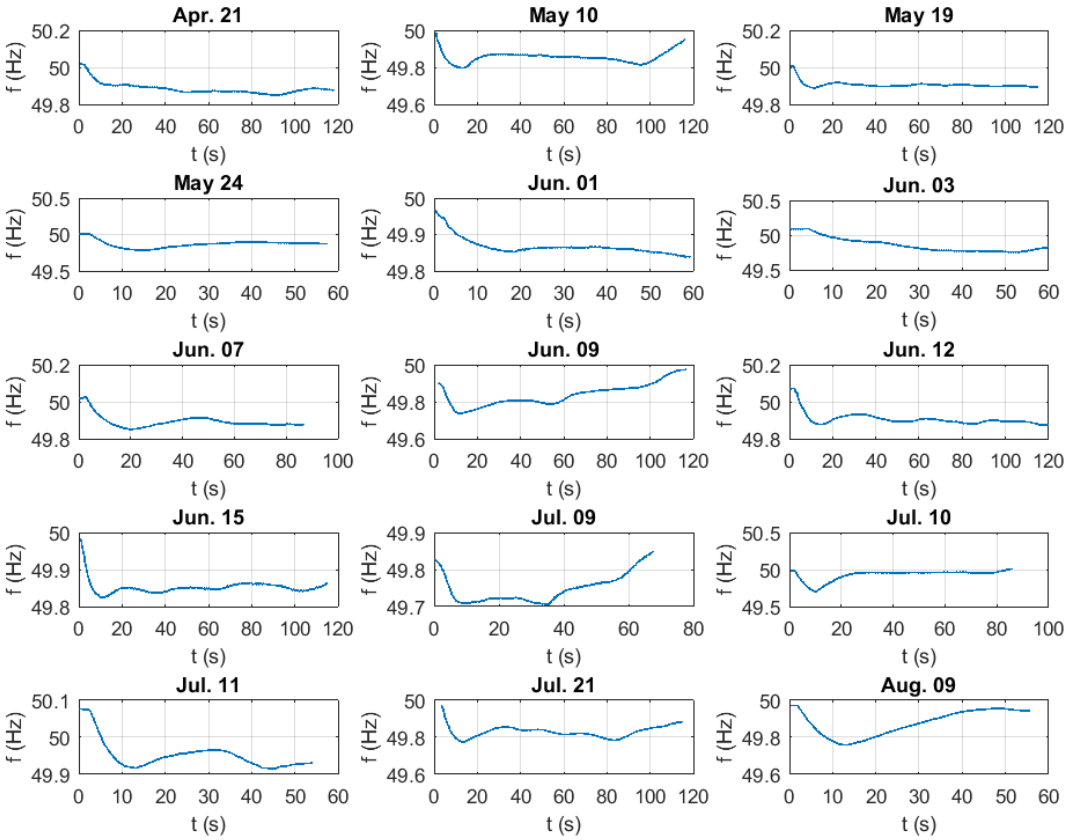

Figure 5-2: Frequency events in 2010 [110]

The key data regarding the fifteen events are listed in Table 5.1, including the time and date, the scheduled generation of the faulted BMU, the frequency before the event, the minimal frequency, the initial ROCOF and the total system demand. The generation losses range from 379 MW to 720 MW and total system demand levels range between 23.5 GW to 42 GW. All the generation losses belong to the Significant Loss and the frequency nadirs for all the events satisfy the frequency nadir constraints for Significant Loss with the frequency deviations smaller than 0.5 Hz. The initial ROCOF for all events also satisfies the maximum allowed ROCOF limit of 0.125 Hz/s for old distributed generators and 0.5 Hz/s for the distributed generators built after 2016.

Table 5.1: Frequency events in 2010 [110]

Date	Time	BMU	Loss	f_0	f_{min}	$\frac{df}{dt}$	Demand
			(MW)	(Hz)	(Hz)	(Hz/s)	(GW)
Apr. 21	10:14	SHOS-1	380	50.02	49.85	0.026	41.8
May 10	11:50	LOAN-2	570	49.94	49.79	0.038	42.0
May 19	00.36	SCCL-3	379	50.01	49.89	0.038	25.9
May 24	12:07	DRAX-5	645	50.01	49.78	0.050	40.8
Jun. 01	11:44	PEHE-1	400	49.97	49.83	0.028	40.6
Jun. 03	06:30	HEYM-11	440	50.09	49.74	0.038	31.7
Jun. 07	19:20	LOAN-1	540	50.01	49.79	0.045	36.6
Jun. 09	16:17	DIDCB-5	650	49.89	49.74	0.050	37.5
Jun. 12	14:10	BAGE-1	459	50.07	49.87	0.050	31.5
Jun. 15	02.52	BP-2	500	49.98	49.82	0.050	23.5
Jul. 09	22:33	LOAN-1	570	49.83	49.70	0.057	30.6
Jul. 10	09:13	PEHE-1	720	49.98	49.70	0.07	34.5
Jul. 11	16:26	KINO-1	485	50.06	49.90	0.049	32.1
Jul. 21	20.37	DRAX-2	600	49.97	49.77	0.050	34.8
Aug. 09	10:24	RHYPS-1	570	49.97	49.76	0.045	38.5

5.4.2 Results and Discussions

Results

Table 5.2 illustrates the results of the method to estimate the inertia contribution from the demand side. The process is summarised as follows:

- The total system inertia is calculated using (5.6) based on the generation loss, initial ROCOF and the system frequency prior to the event.
- The generation side inertia contribution contains two parts: the generation mix together with the averaged value for inertia constants for the inertia contribution estimated by the actual power generated, and the additional inertia contribution

Table 5.2: Results of the proposed methods

Date	Time	K MW/Hz	X	Y	Inertia (GW· s)				Loading level
					Total	Generation		Demand	
						output	$\alpha \cdot K$		
Apr. 21	10:14	138.34	101.70	3.83	365.1	205.05	81.17	78.88	0.716
May 10	11:50	141.05	99.54	3.81	374.5	214.54	79.8	80.16	0.729
May 19	00.36	98.35	133.10	4.92	249.4	121.97	65.83	61.6	0.649
May 24	12:07	107.19	79.71	3.32	322.4	186.90	62.11	73.39	0.751
Jun. 01	11:44	134.96	117.77	3.97	356.7	195.45	91.31	69.94	0.682
Jun. 03	06:30	117.37	139.71	4.51	290.0	146.92	84.59	58.49	0.635
Jun. 07	19:20	124.73	90.03	3.44	300.1	174.18	62.97	62.95	0.734
Jun. 09	16:17	100.48	107.59	3.92	324.3	177.24	77.07	69.99	0.697
Jun. 12	14:10	64.40	80.46	2.75	229.8	142.99	50.87	35.94	0.738
Jun. 15	02.52	105.38	220.85	5.74	249.9	114.81	85.72	49.37	0.573
Jul. 09	22:33	87.36	111.13	3.54	249.1	140.51	65.29	43.3	0.683
Jul. 10	09:13	85.58	86.96	3.04	257.0	152.12	57.23	47.65	0.727
Jul. 11	16:26	91.46	99.38	3.51	247.8	135.16	60.94	51.7	0.689
Jul. 21	20.37	115.29	106.33	4.03	300.0	159.89	70.67	69.44	0.693
Aug. 09	10:24	115.74	79.11	3.60	316.5	177.96	58.19	80.35	0.754

from partially-loaded spinning reserves.

- The power/frequency ratio K is obtained from the frequency curve for the initial 10 seconds after the generation loss when no SFR is deployed.
- Variables X and Y derived in Phase 3 are used to allocate the inertia contribution for the demand side and spinning reserves from the inertia deficit between the total system inertia and the generation side inertia without considering spinning reserves.

The result of the least squares estimation is shown in Figure 5-3. The coefficient of additional inertia contribution from the spinning reserves of the partially-loaded generators, α, is equal to 0.192 and the demand side inertia constant in the total system demand base, h_{dem}, is 1.75 s. As shown in Table 5.2, the demand-based inertia

weights from 17% to 25% of the total system inertia with the highest percentage on 19th of May at 0:36 a.m. when demand was only 25.9 GW and the lowest share on the Friday evening at 22:33 p.m. 9th of July. The averaged demand side inertia contribution for the fifteen events is 20%.

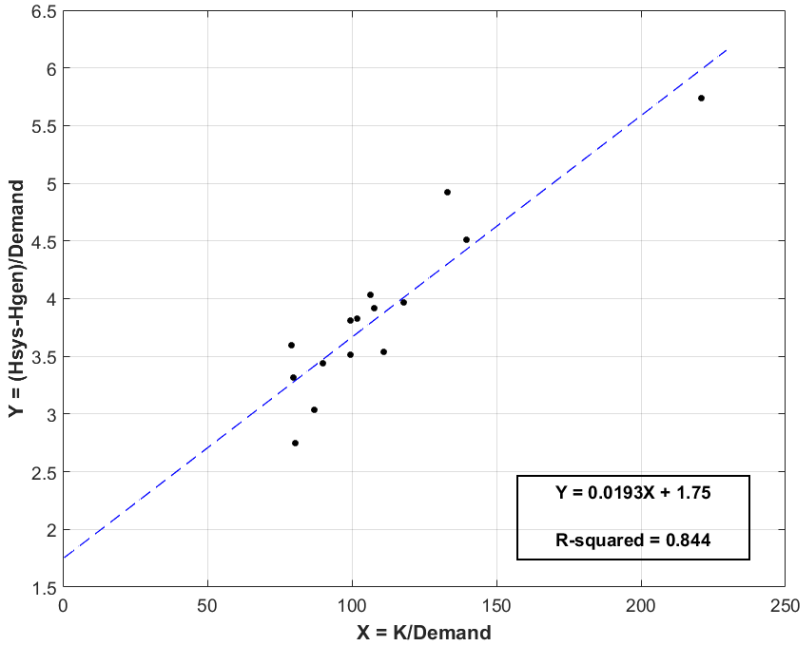

Figure 5-3: Least squares estimation

The coefficient of determination, the R-squared value, is the proportion of the variance of dependent variables predicted by the independent variables which indicates the accuracy of the interpretation of the proposed model [111]. The R-squared value lies between 0 and 1. The closer it is to 1 suggests more of the variation in the data can be explained by the regression model. For the proposed method, the R-squared value equals 0.844, as calculated by:

$$\begin{aligned} R^2 = 1 - \frac{SSE}{SST} = \frac{SSR}{SST} = 0.844 \\ \text{where, } SST = \sum \left(Y_i - \bar{Y}\right)^2 \\ SSE = \sum \left(Y_i - \widehat{Y}_i\right)^2 \\ SSR = \sum \left(\widehat{Y}_i - \bar{Y}\right)^2 \end{aligned} \tag{5.16}$$

where,

- SST is the total sum of squares,
- SSE is the error sum of squares,
- SSR is the regression sum of squares,
- $\bar{Y}$ is the mean value of Y_i,
- $\widehat{Y}_i$ is the predicted value of Y_i.

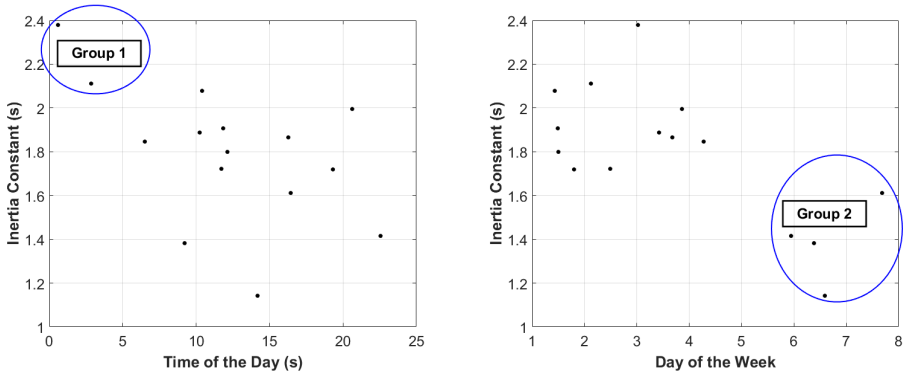

Figure 5-4: Variations of the demand side inertia constants

Figure 5-4 illustrates the variations in the demand side inertia constants for the fifteen frequency outage events. The variations are caused by various factors such as the weather, the temperature, the demand mix, time of the day, day of the week. Among all those factors, some patterns can be found by the results:

- Group 1 represents the events which happened overnight. The demand side inertia constant tends to be higher than the inertia constant at daytime. The reason for that is because for the overnight period the industrial load takes up a greater percentage of the total demand. However, although the inertia constant is high for the overnight period, the inertia contribution from demand is still low due to the low electricity needs.
- Group 2 represents the events occurring over the weekend, and the demand side inertia constant tend to be lower. This might be due to the higher percentage of total system demand taken by domestic consumption.

The average loading level of the generators can also be inferred from Table 5.2. The loading level can be estimated using the ratio between the inertia contributions from

generation output and the total generation inertia contribution:

$$\text{Loading Level} = \frac{E_{gen,output}}{E_{gen}} = \frac{E_{gen,output}}{E_{gen,output} + E_{gen,\alpha \cdot K}} \tag{5.17}$$

Figure 5-5 illustrates the system loading levels plotted against the time of the day for the fifteen events. The averaged system loading level for all events is 70%. The system loading level is correlated with the demand level with the lower generator loading levels when at trough demand period while the higher generator loading levels for peak demand period.

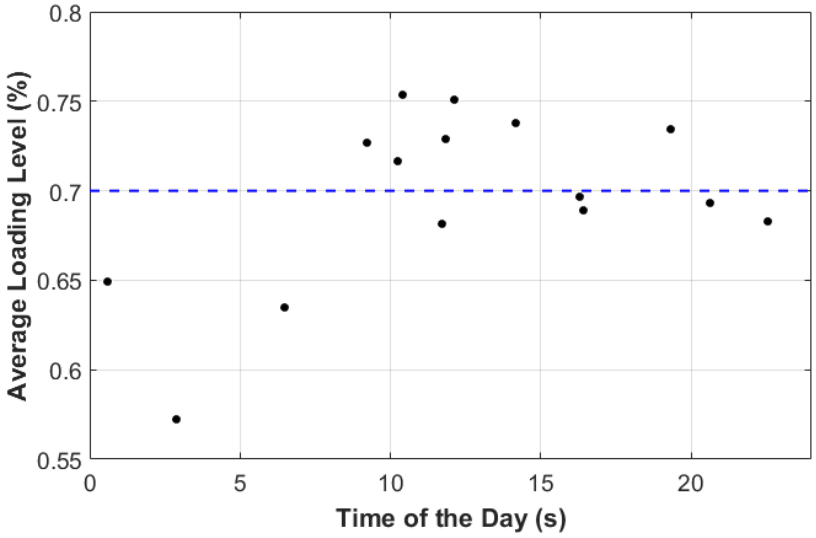

Figure 5-5: Averaged system loading levels for the fifteen events

Discussion

The results from the fifteen events indicate the demand could affect the total system inertia, which in turn affects the system frequency performance during contingencies. Assuming the demand side inertia constant is 1.75 s in the total demand base and the averaged generator loading level is 70%, the inertia profile can be plotted out according to the demand profile and the generation mix throughout a day. Figure 5-6 shows the variations of the total system inertia and the system demand in 48 settlements (half hour interval) for a typical weekday in January (20/01/2015). As can be seen from the figure, the inertia profile generally follows the same pattern as the demand profile throughout a day with the same nadir period between 4 and 6 a.m. and the same peak

period between 5 and 7 p.m.

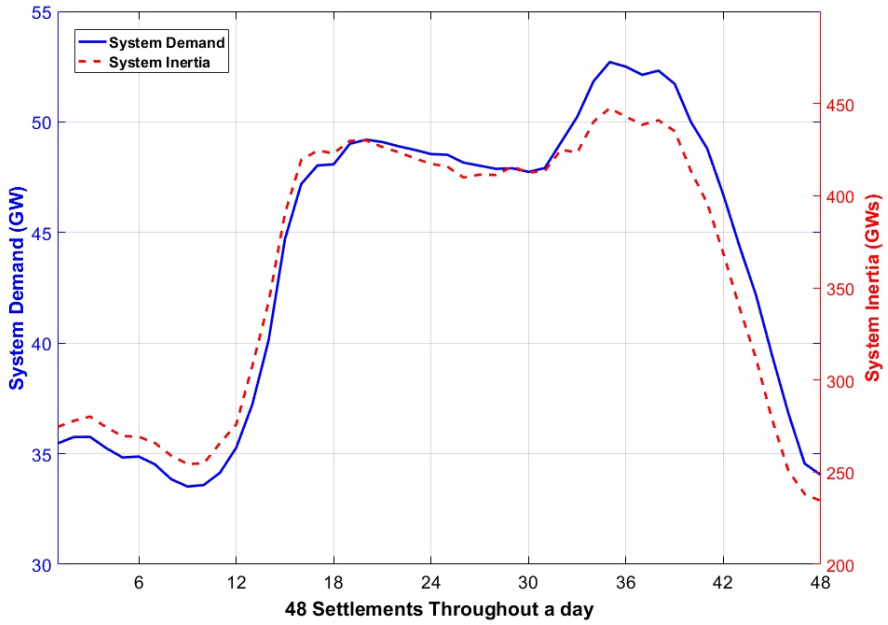

Figure 5-6: Demand and inertia profiles

The reasons for the profile similarity between the system demand and system inertia can be explained as follows:

- The demand variations are largely compensated by the traditional fossil-fired power stations, especially gas-fired power station for the case of UK power system, due to the intermittency of renewable generation and the slow response of nuclear generators. Most of the traditional fossil-fired power stations are synchronously connected to the power grid and are the main contributors to the system inertia. Hence, the inertia contribution from the generation side follows the same shape as the demand profile.

- On average 20% of the inertia is contributed by the demand side. The inertia contributions from the demand side are the synchronous motors connected to the system, which can be found in all demand types but most prevalently in the industrial load. Hence, the demand inertia contribution is related to the demand levels and follows the demand profile, meaning that as demand increases more synchronous motors are connected to provide inertia.

The demand levels primarily decide the total system inertia under the current cir-

cumstances of balancing the demand variation depending on traditional generators. Therefore, the demand levels, in turn, affect the system frequency stability in terms of the total system inertia. Assuming the generation mix remains the same, the influences of demand levels to the initial ROCOF can be plotted out.

$$\left.\frac{df}{dt}\right|_{t=0} = \frac{\Delta P}{2E_{sys}(P_D)} \cdot f_0 \tag{5.18}$$

where $E_{sys}(P_D)$ represents the function of demand to determine the total system inertia.

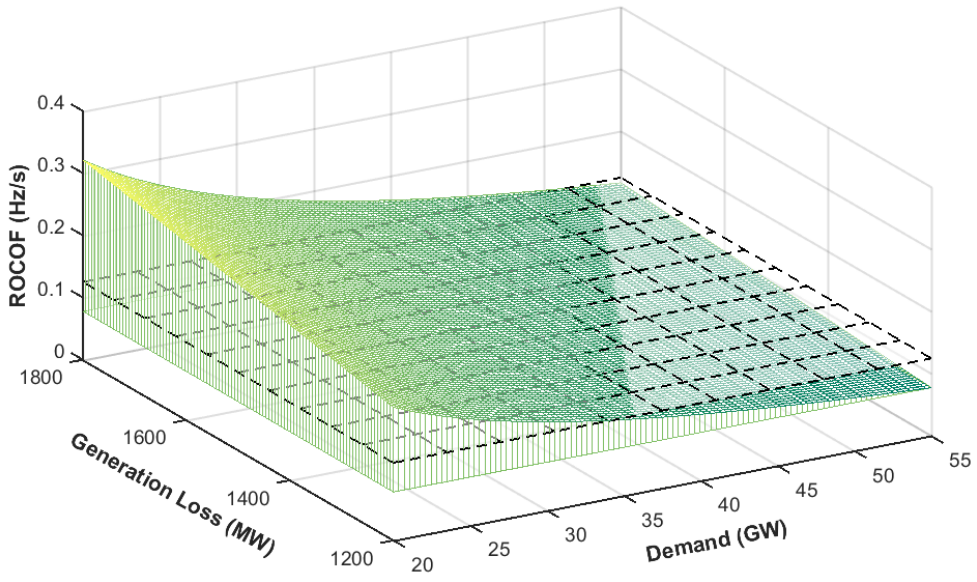

Figure 5-7: Initial ROCOF for abnormal losses regarding different demand levels

Figure 5-7 illustrates the initial ROCOF for the demand level ranging from 20 GW to 55 GW when the system subject to Abnormal Losses. As it can be seen from the figure, if the demand at trough period, i.e. 20 GW, any Abnormal Loss could potentially trip the ROCOF relay for embedded generators built before 2016 [52, 53] due to the 0.125 Hz/s relay settings. For the different demand levels, the system can be divided into a weak period and a safe period in relation to the trough demand period and peak demand period respectively in the aspect of inertia.

The minimum PFR requirements for different demand levels regarding the Abnormal Losses can be investigated as well based on the frequency behaviour mathematical

approach presented in Chapter 3. Assuming the frequency nadir occurs in *Stage 2* and the total system inertia is a function of total system demand, the frequency nadir can be expressed as:

$$
\begin{aligned}
f_{min} &= a_1(r, P_D) + a_5(r, P_D) \cdot \left[1 + \ln \frac{a_2(r, P_D)}{a_5(r, P_D)}\right] \\
a_1 &= \left(f_n - \frac{P_{loss}}{k_{dfr}}\right) - \frac{r \cdot t_1}{k_{dfr}} - \frac{2r}{{k_{dfr}}^2} \cdot H_{sys}(P_D) \\
a_2 &= \left(f_0 - f_n + \frac{P_{loss}}{k_{dfr}}\right) + \frac{2r}{{k_{dfr}}^2} \cdot e^{-\frac{k_{dfr} \cdot t_1}{2H_{sys}(P_D)}} \cdot H_{sys}(P_D) \\
a_5 &= \frac{2r}{{k_{dfr}}^2} \cdot H_{sys}(P_D)
\end{aligned}
\tag{5.19}
$$

where,

- r is the PFR ramping rate,
- P_D is the total system demand,
- $H_{sys}(P_D)$ is the system inertia constant as a function of total demand.

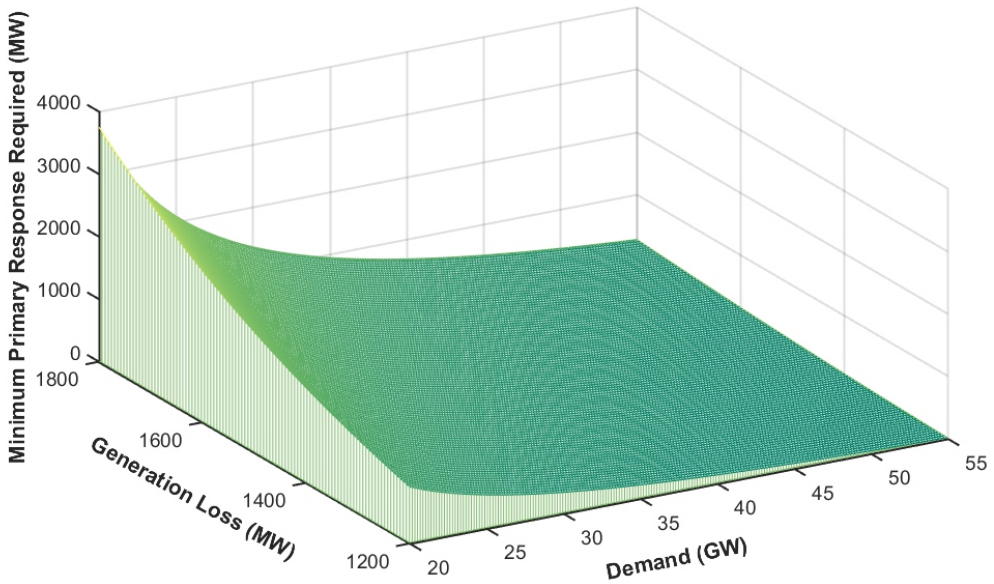

Figure 5-8: Initial minimum PFR for abnormal losses regarding different demand levels

For Abnormal Loss, the allowed frequency nadir is 49.2 Hz. A new function $R(r)$ is

defined to find the minimum required ramp rate:

$$R(r) = a_1(r, P_D) + a_5(r, P_D) \cdot \left[1 + \ln \frac{a_2(r, P_D)}{a_5(r, P_D)}\right] - \frac{49.2}{f_N} \tag{5.20}$$

The optimal ramp rate can be obtained using the Newton-Raphson method as:

$$r_{n+1} = r_n - \frac{R(r_n)}{R'(r_n)} \tag{5.21}$$

The minimum PFR required is:

$$P_{PFR,min} = r_{opt} \cdot (t_2 - t_1) \tag{5.22}$$

Figure 5-8 shows the resultant minimum PFR requirement for different demand levels when the system is subjected to Abnormal Losses. When the system is at the weak period, i.e. 20 GW, the required PFR is extremely high due to the lack of inertia.

5.5 Assessments of the Variable Frequency Drive Penetration

The use of VFDs is predicted to increase as the development of power electronic devices and its control mechanism. The benefits of connecting the motors via VFDs includes enabling the speed change, improving the machine efficiency and reducing the electricity consumptions. Studies show that with the help of VFDs, motors can reduce the electricity needed by up to 70% [112]. However, the utilisations of VFDs will block the inertial response by the motors, which in turn decrease the overall system inertia.

The potential of the VFDs regarding energy and cost saving are far from being fully realised [112]. The VFD penetrations as a proportion of the total installed motors for the United States, Europe, China and the UK for the year 2010 are shown in Table 5.3. The VFD penetration for the UK back in 2010 was less than 10%, and this value is predicted to increase to 50% within 30 years [113].

Table 5.3: VFD penetration levels (2010) [113]

	US	Europe	China	UK
Penetration of VFDs (as a proportion of installed motors)	$< 20\%$	$< 15\%$	$< 10\%$	$< 10\%$

Table 5.4: VFD Penetration Projections

	VFD Penetration	Renewable Penetration
2010	10%	15%
Projection 1	50%	15%
Projection 2	100%	15%
Projection 3	50%	40%

The inertia reduction in the future will not only exist in the generation side due to the increasing penetrations of renewable generation but also exist in the demand side due to the utilisation of VFDs. Three future projections, shown in Table 5.4, are created to assess the VFD penetrations: projection 1 represents the future 50% of VFD penetrations, projection 2 assumes an extreme case where all the motors are equipped with VFDs, and the last but not the least, projection 3 considers the inertia reduction in both generation and demand side which is a possible assumption for the future [112, 113].

Figure 5-9 shows the frequency performances curves regarding the future projections for 900 MW, 1320 MW and 1800 MW respectively. The dotted line in the left represents the reference ROCOF limit of 0.125 Hz/s, and the dotted line in the right indicates the PFR requirements depending on the quasi-steady-state frequency. Due to the decrease of the demand side inertia contribution, the system encounters higher initial ROCOFs and at the same time requires more PFR to satisfy the frequency nadir requirements. The system becomes even weaker in terms of inertia when considering the penetrations of inertia-less renewables. The worst-case scenario, as shown in Figure 5-9, suggests when a 25 GW system experiences an 1800 MW generation loss, the system needs 5000 MW PFR to make sure the frequency nadir above the allowed limits for the projection 3.

Figure 5-10 further demonstrates the visualisation of the VFD and renewable penetration for demand and generation up to 100% and 60%, respectively, in terms of the initial ROCOF and PFR requirements. The demonstration is carried out for a system with 35 GW demand which is the averaged demand level for the UK power system in the year 2017 [57]. The generation losses being tested are 1320 MW, which is the largest infeed generator currently, and 1800 MW, the future largest infeed generator after the completion of the new nuclear power plant at Hinkley Point C. The results in-

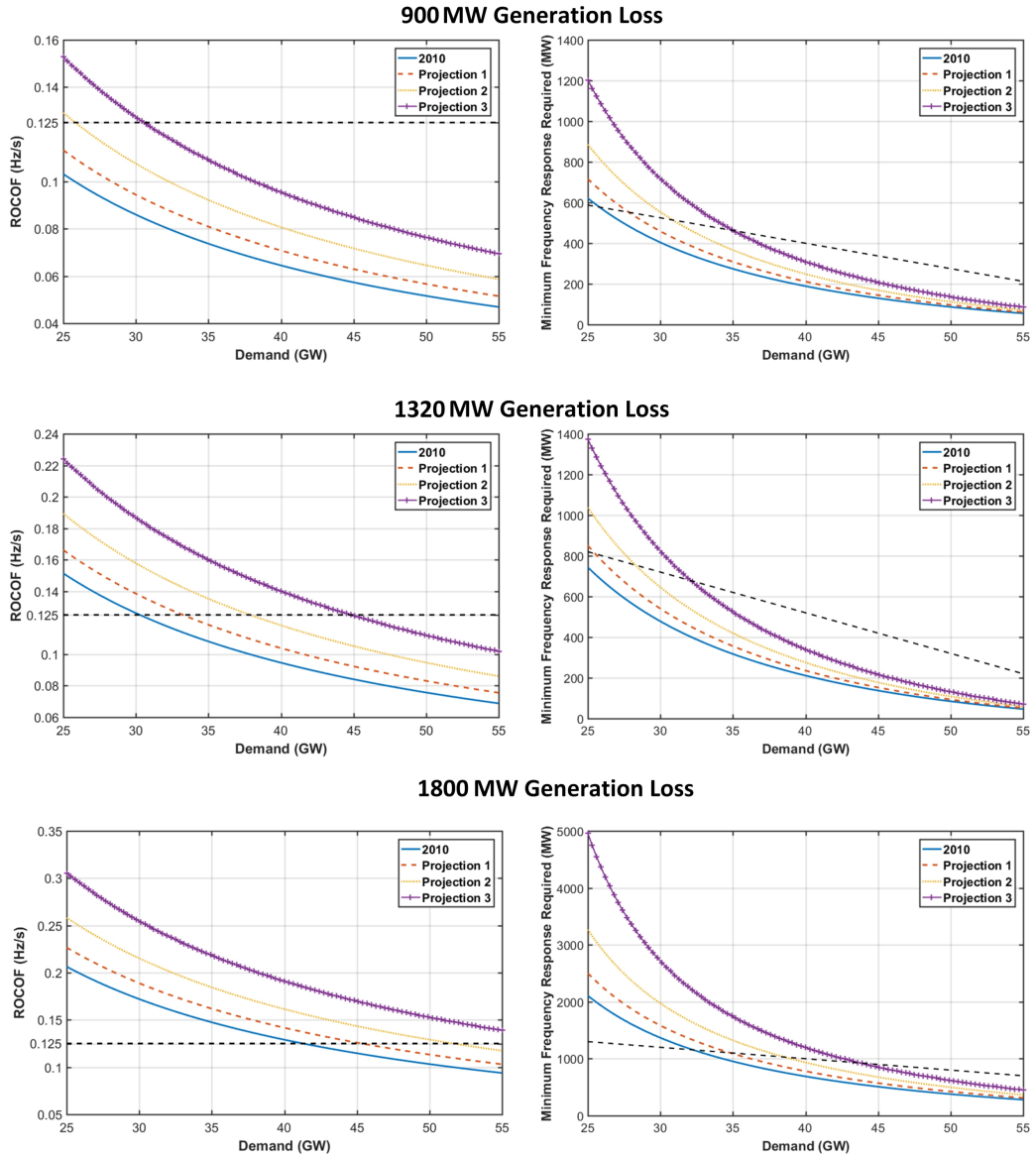

Figure 5-9: Future projections regarding 900/1320/1800 MW loss

dicate that when the penetration of VFD and renewable reach a certain level, i.e. 62% VFD penetration and 28% renewable penetration, the system can no longer meet the ROCOF requirements of 0.125 Hz/s for the embedded generators constructed before 2016 for the 1320 MW loss. As for 1800 MW loss, even the current system without the inertia reduction cannot withstand the 1800 MW loss without violating the ROCOF limit. Besides, an exponential increase in the PFR requirements as the combined inertia reduction from the penetrations of VFD and renewable progress.

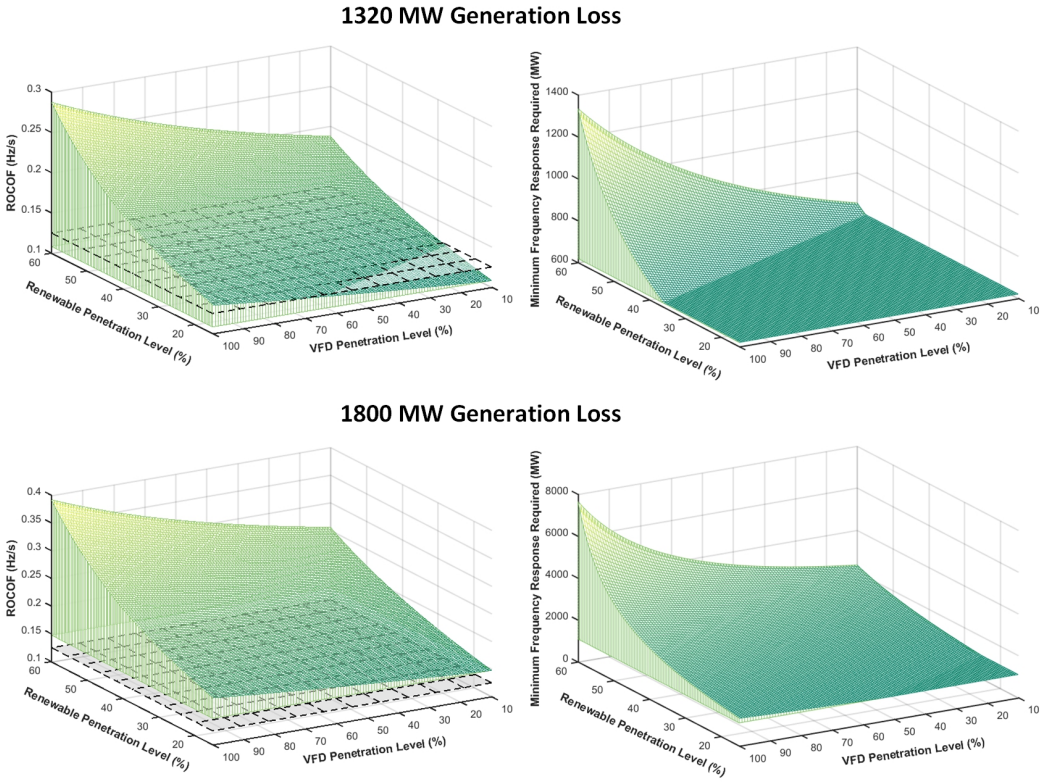

Figure 5-10: Future projections regarding 900/1320/1800 MW loss

5.6 Chapter Summary

The total system inertia is decreasing due to the increasing penetration of inertia-less low carbon generation and VFDs, and the reduced system inertia poses a major threat to the system frequency stability. The insufficient total system inertia leads to higher initial ROCOF, which may end up with the trapping of ROCOF-based relays for the distributed generators when the system is encountered with a large disturbance.

The majority of the research regarding the inertia problems is focused on the generation side. This chapter provides a new perspective of inspecting the inertia problem from the demand side. The work in this chapter presents a novel method to quantify the inertia contributions from demand side based on the past frequency outage events. The results of the quantification indicate the demand could contribute 20% of the total system inertia with an averaged inertia constant of 1.75 s in the system demand base. The results also show that the averaged generation loading level for the traditional fossil-fired generators in the UK is 70%. Those values can be further used to analyse

the inertia profiles in relation to the demand profile. The resultant inertia profile suggests demand levels primarily decide the amount of inertia in the system under the current renewable and VFD penetrations. A hidden benefit of shifting the demand from peak to trough is to shift the redundant inertia in the safe period to the weak period, thus improving the system frequency stability.

This chapter also assesses the influence of VFD penetration to the frequency performances. The results suggest that the system can no longer meet the ROCOF requirements for the ROCOF-based relay limit when the VFD penetration reaches 64% or the renewable penetration reaches 28%. To satisfy the frequency nadir requirements for the potential largest infeed generation loss, the requested PFR reserves climbs to 7800 MW which is unrealistic. To solve the inertia problem, either introducing new technologies such as synthetic inertia, fast frequency response into the system urgently or bringing a market for inertia to provide incentives for the inertia provider and improve the competitiveness of inertia-rich traditional generators.

The results of this chapter provide the input parameters for the implementation of the frequency-constrained UC generation scheduling optimisation problem in the next chapter.

Chapter 6

Frequency Constrained Unit Commitment and Pricing for Inertia

THIS chapter presents the approach to implement the frequency-related constraints in the UC problem, as well as the pricing method for system inertia based on the marginal price in UC.

6.1 Introduction

In 2017, the share of the renewable energy in the total generation mix increased from 7% in 2010 to 29.3%, while the share of the conventional generators fell from 75% in 2010 to 47.1% for the UK power system [12, 13]. Since the conventional generators are the main inertia providers, the increasing popularity of renewable generation has led to a continuous decline of the total power system inertia. The problem of the reduced inertia is a threat to frequency stability. However, the only frequency-related service in the ancillary market currently is the frequency response service. The benefits of incorporating the inertia service into the ancillary services market are threefold: (i) incentivising inertia providers, (ii) improving the competitiveness of the conventional generators, and (iii) opening the window for non-BMUs participants in the frequency services, such as the inertia contributed from the synchronous compensator and demand motor clusters.

The work in this chapter firstly proposes a method to incorporate the frequency-related constraints into the generation scheduling UC problem to assess the influences of the frequency constraints on the system operational cost. Secondly, the pricing for inertia is analysed using Lagrange multipliers in the Lagrange relaxation UC optimisations, since the Lagrange multiplier represents the marginal price for satisfying an associated constraint.

The rest of the chapter as organised as follows Section 6.2 presents the UC optimisation with the frequency-related constraints; Section 6.3 further investigates the marginal price for proving inertia based on the frequency-constrained UC for the reduced UK system model; Section 6.4 concludes the chapter.

6.2 Frequency-Constrained Unit Commitment

The UC algorithm solves problems of the power system operation planning, and decides the optimal operation schedule for the generating units to meet the given load profiles under different technical and environmental constraints [89]. The UC has the potential to manage the challenges caused by the utilisation of renewable generation from the perspective of system planning. The system reliability requires the UC decision to be robust. In terms of frequency stability, robustness means an adequate PFR and inertia in place to counter the largest potential system contingency.

The UC optimisation is a mixed-integer nonlinear problem, and the optimal UC decisions can be acquired through enumerations methods such as dynamic programming. However, the NP-hard nature of the UC problem brings excessive computational burden to the problem-solving process [114]. A variety of methods have been proposed to solve the UC problem. Since the Lagrange multiplier reflects the marginal price to satisfy the associated constraint, Lagrange relaxation is selected for this research [27, 96, 97].

The work in this section provides a solution to incorporate the frequency-related constraints into the UC consideration, thus improving the frequency stability. The innovations regarding the better representation of system dynamics are listed below:

- The inertia and PFR constraints are introduced to cope with the frequency requirements for the largest potential infeed generation loss to improve the frequency robustness.
- The demand side inertia contribution and demand droop to frequency deviations are considered in the UC decision-making, thus transforming the demand from a simple generation target to a key player to ensure frequency stability.
- Renewable generation is not a negative demand, allowing it to be curtailed when necessary.

The innovations regarding the UC algorithms are listed below:

- Polynomial fitting is applied to deal with the transcendence of inertia and PFR relationship for the frequency nadir requirements.
- The update criteria of the Lagrange multipliers is modified to a two-layer structure. The first layer represents the multipliers associated with traditional constraints and the second layer focuses on the update of inertia and PFR constraints.

6.2.1 Flowchart of the Proposed Method

The flowchart of the proposed inertia-dependent frequency-constrained UC is shown in Figure 6-1. The whole process can be divided into three subtasks: initialisation, the Lagrange relaxation UC, and the heuristic Lagrange multiplier update.

The ***initialisation*** process firstly reads the system data, e.g. the generational constraints, demand profile, renewable generation capacity. Then based on the system parameters, the following system characteristics can be obtained: the initial Lagrange

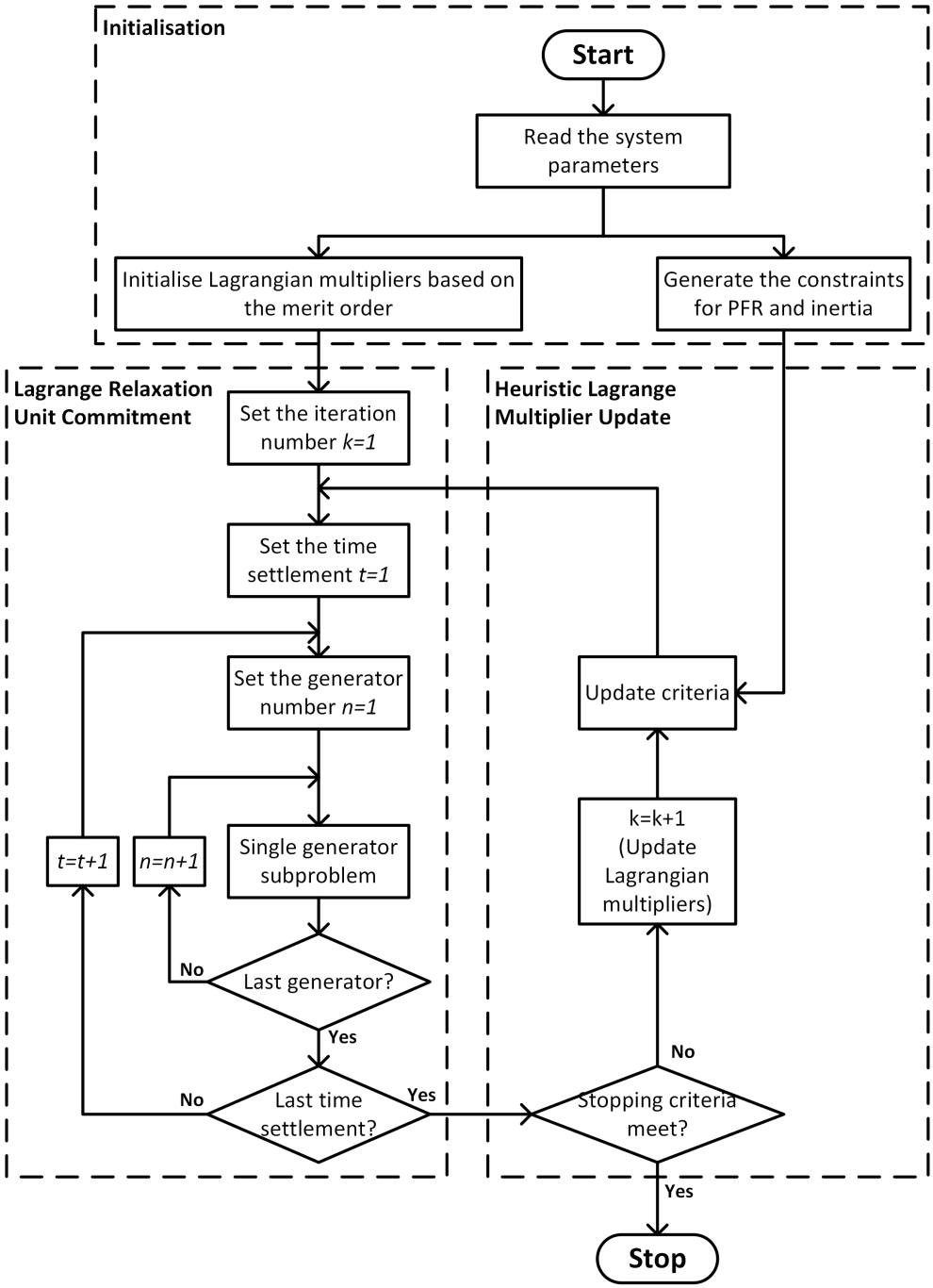

Figure 6-1: Flowchart of the frequency constrained unit commitment

multipliers are calculated based on the merit order of the full-load averaged cost; the inertia and PFR constraints are stipulated according to the demand level and the largest generator in the system; the wind generation output are modelled based on the

historical data.

Lagrange relaxation UC represents the conventional method to solve the UC problems. In this process, the global constraints are being relaxed and the single-generator sub-problems are optimised associated with the Lagrange multipliers. Physical constraints of the generation are all being considered such as: the ramp up, minimum up/down time *etc.*

Heuristic Lagrange multiplier update is a two-layer process to update the Lagrange multipliers and assessing the stopping criteria. The two layers represent the conventional UC constraints and the frequency constraints, respectively. The stopping criteria are based on the duality gap between the original objective function and the Lagrange function.

6.2.2 Problem Formulation

The proposed formulation of the frequency-constrained UC (FCUC) optimisation is to determine the optimal generation schedules, with the lowest operation cost, that the adequate inertia and PFR reserve have to meet the frequency requirements when the system subjected to the largest infeed generation loss. The operation cost in the FCUC includes the generation fuel cost and the cost of frequency response, as the two costs currently exist in the UK power system. The objective function to be minimised is:

$$\begin{aligned} &F\ (P_{i,t},PFR_{i,t},E_{i,t},U_{i,t},B_{i,t},X_{i,t}) \\ &\qquad = \sum_{t=1}^{T}\sum_{i=1}^{N}[FC_i(P_{i,t})U_{i,t} + RC_i(PFR_{i,t}) + ST_iB_{i,t} + SD_iX_{i,t}] \end{aligned} \tag{6.1}$$

where,

- T is the total number of hours in the set $\mathscr{T} = \{1, 2, \cdots, T\}$, t is the time index, and $t \in \mathscr{T}$;
- N is the total number of generators in the set $\mathscr{N} = \{1, 2, \cdots, N\}$, i is the generator index, and $i \in \mathscr{N}$;
- $P_{i,t}$, $PFR_{i,t}$ and $E_{i,t}$ are the generation power, PFR contribution and inertia contribution of the generator i at time t, respectively, and $P_{i,t}$, $PFR_{i,t}$ and $E_{i,t}$ are continuous variables;
- $U_{i,t}$, $B_{i,t}$ and $X_{i,t}$ are three integers (0 or 1) representing the on-off states, the

start-up signal and the shut-down signal of the generator i at time t;

- FC_i, RC_i are the fuel cost and PFR providing cost of generator i;
- ST_i, SD_i are the start-up cost and shut down cost of generator i.

In equation (6.1) the fuel cost is modelled by a quadratic function. The fuel cost of the generator i at time t is expressed as [96]:

$$FC_i(P_{i,t}) = a_i {P_{i,t}}^2 + b_i P_{i,t} + c_i \tag{6.2}$$

where a_i, b_i and c_i are the quadratic fuel cost function coefficients of the generator i.

The cost for the generator i at time t to provide PFR is modelled linearly by the bid price, d_i, in the mandatory frequency response services depending on the generation technology.

$$RC_i(PFR_{i,t}) = d_i PFR_{i,t} \tag{6.3}$$

The constraints for the objective function (6.1) can be categorised into the system coupling constraints and individual generator constraints, constraining the system requirements and the generator operation respectively. The constraints are summarised as follows.

Generator operational constraints (for $\forall\ i \in \mathscr{N}, \forall\ t \in \mathscr{T}$):

(a) Start-up and shut-down signals

$$\begin{aligned} B_{i,t} &= \begin{cases} 1, & \text{when } U_{i,t} = 1 \text{ and } U_{i,t-1} = 0 \\ 0, & \text{otherwise} \end{cases} \\ X_{i,t} &= \begin{cases} 1, & \text{when } U_{i,t} = 0 \text{ and } U_{i,t-1} = 1 \\ 0, & \text{otherwise} \end{cases} \end{aligned} \tag{6.4}$$

(b) Generator capacity

$$P_i^{min} U_{i,t} \leq P_{i,t} \leq P_i^{max} U_{i,t} \tag{6.5}$$

where,

- P_i^{min} is the minimum generation output of generator i,

- P_i^{max} is the maximum generation output of generator i.

(c) Minimum up/down time

$$U_{i,t} = \begin{cases} 1, & if\ T_{i,on} < {t_i}^u \\ 0, & if\ T_{i,on} < {t_i}^d \\ 0 \text{ or } 1, & \text{otherwise} \end{cases} \tag{6.6}$$

where,

- $T_{i,on}$ and $T_{i,off}$ represents the consecutive time that generator i is at on-state and off-state, respectively;
- ${t_i}^u$ and ${t_i}^d$ represents the minimum up time and minimum downtime of the generator i.

Represented by the start-up and shut-down signal, the minimum up/down time can be interpreted as $U_{i,t} = 0$ when the start-up signals in previous $(t^{'} - 1)$ time periods should all be 0; and $U_{i,t} = 1$ when the shut-down signals in previous $(t^{'} - 1)$ time periods should all be 0.

$$\begin{aligned} \sum_{t'=t-{t_i}^u+1}^{t} B_{i,t'} &\leq U_{i,t} \\ \sum_{t'=t-{t_i}^d+1}^{t} x_{i,t'} &\leq 1 - U_{i,t} \end{aligned} \tag{6.7}$$

(d) Ramp up/down

$$\begin{aligned} P_{i,t} - P_{i,t-1} &\leq U_{i,t-1}{r_i}^u + B_{i,t}{r_i}^{su} \\ P_{i,t-1} - P_{i,t} &\leq U_{i,t-1}{r_i}^d + X_{i,t}{r_i}^{sd} \end{aligned} \tag{6.8}$$

where,

- ${r_i}^u$ and ${r_i}^d$ represents the ramp up and ramp down rate of the generator i,
- ${r_i}^{su}$ and ${r_i}^{sd}$ represents the start-up and shut-down rate of the generator i.

(e) PFR contribution from the generator

$$PFR_{i,t} = DP_iP_{i,t} \tag{6.9}$$

where DP_i is the governor droop of the generator i.

(f) Inertia contribution from the generator

$$E_{i,t} = H_i {P_i}^{max} U_{i,t} \tag{6.10}$$

where H_i is the inertia constant of the generator i. The inertia contribution from the generators is determined by its rate capacity.

In conclusion, the start-up and shut-down signals are determined by the generators states; the generator capacity, minimum up/down time and ramp up/down constraints are inequality constraints; the PFR and inertia contribution of the generator.

System Coupling constraints (for $\forall\ i \in \mathscr{N}, \forall\ t \in \mathscr{T}$):

(a) Power balance

$$P_{D,t} = \sum_{i=1}^{N} P_{i,t} U_{i,t} \tag{6.11}$$

where $P_{D,t}$ represents the system demand that needs to be met at time t.

(b) Spinning reserve

$$P_{D,t} + R_t \leq \sum_{i=1}^{N} {P_i}^{max} U_{i,t} \tag{6.12}$$

where R_t represents the system reserve requirement at time t.

(c) PFR requirement

$$PFR_{Req,t} \leq \sum_{i=1}^{N} PFR_{i,t} \tag{6.13}$$

where $PFR_{Req,t}$ represents the system PFR requirement at time t.

(d) Inertia requirement

$$E_{Req,t} \leq \sum_{i=1}^{N} E_{i,t} + H_{Dem} P_{D,t} \tag{6.14}$$

where $E_{Req,t}$ represents the system inertia requirement at time t.

In conclusion, the power balance is the only equality constraint for the system operation and the rest of the constraints, i.e. spinning reserve, PFR and inertia requirements, are all inequalities. The spinning reserve, in this case, refers to the secondary response or tertiary response that does not affect the frequency transient. Therefore, the spinning reserve is not considered in the frequency dynamic simulations, and the frequency transient dynamics are regulated by the amount of inertia and PFR in the system. The inertia contribution of each generator is determined by the on-off state of the generator while the PFR contribution of each generator is determined by the governor droop. National Grid specifies the generators should have a 3% to 5% governor droop setting to participate in the MFR in the UK power system [49].

6.2.3 Modified Lagrange Relaxation for Unit Commitment

The Lagrange relaxation solves the UC problem by temporarily relaxing the system coupling constraints and solving the single-generator sub-problem without the coupled system coupling constraints. This is done by forming the Lagrange function that brings the system coupling constraints into the objective function by the introduction of Lagrange multipliers.

Lagrange Function

The Lagrange function L can be formed as:

$$\begin{aligned} L\ (P_{i,t}, PFR_{i,t}, E_{i,t}, U_{i,t}, B_{i,t}, X_{i,t}, {\lambda_t}^D, {\lambda_t}^R, {\lambda_t}^{PFR}, {\lambda_t}^E) \\ =&F\ (P_{i,t}, PFR_{i,t}, E_{i,t}, U_{i,t}, B_{i,t}, X_{i,t}) \\ &+\sum_{t=1}^{T} {\lambda_t}^D \left(P_{D,t} - \sum_{i=1}^{N} P_{i,t} U_{i,t} \right) \\ &+\sum_{t=1}^{T} {\lambda_t}^R \left(P_{D,t} + R_t - \sum_{i=1}^{N} {P_i}^{max} U_{i,t} \right) \\ &+\sum_{t=1}^{T} {\lambda_t}^{PFR} \left(PFR_{Req,t} - \sum_{i=1}^{N} PFR_{i,t} \right) \\ &+\sum_{t=1}^{T} {\lambda_t}^E \left(E_{Req,t} - \left[\sum_{i=1}^{N} E_{i,t} + H_{Dem} P_{D,t} \right] \right) \end{aligned} \tag{6.15}$$

where ${\lambda_t}^D$, ${\lambda_t}^R$, ${\lambda_t}^{PFR}$ and ${\lambda_t}^E$ are the non-negative Lagrange multipliers for power

balance, spinning reserve, PFR requirement and inertia requirement constraints, respectively. Note that the Lagrange multipliers perform as the penalty factor in violation of the associated constraint, reflecting the extent of the impact of the system coupling constraints on the total operational cost. In practice, the Lagrange multipliers can be the marginal prices that satisfy the associated constraints. A higher inertia-based Lagrange multiplier will rise the penalty in terms of the total cost for violating the inertia constraints and, therefore, more conventional generators will be dispatched to fulfil the inertia requirement. For each time settlement t, the Lagrange multiplier for each system coupling constraint is unified and applied to all units.

The optimisation of the original objective function F is done by the dual optimisation process by firstly maximising the Lagrange function with respect to the Lagrange multipliers, and then minimising the Lagrange function with respect to the rest of the variables:

$$\begin{aligned} &\text{Step 1 : Max } L\ ({\lambda_t}^D, {\lambda_t}^R, {\lambda_t}^{PFR}, {\lambda_t}^E)) \\ &\text{Step 2 : Min } L\ (P_{i,t}, PFR_{i,t}, E_{i,t}, U_{i,t}, B_{i,t}, X_{i,t}) \end{aligned} \tag{6.16}$$

Step 1 maximising the Lagrange function with respect to Lagrange multipliers is done through the update process which will be explained in the next section. Step 2 minimises the Lagrange function by considering the Lagrange multipliers as constants; therefore, reorganises the Lagrange function (6-15) by taking out the system coupling constraints as:

$$\begin{aligned} L = &\sum_{i=1}^{N}\sum_{t=1}^{T}\{[FC_i(P_{i,t}) + RC_i(PFR_{i,t}) + ST_iB_{i,t} + SD_iX_{i,t}] \\ &- {\lambda_t}^D P_{i,t} - {\lambda_t}^R P_i^{max} U_{i,t} - {\lambda_t}^{PFR} PFR_{i,t} - {\lambda_t}^E E_{i,t}\} \\ &+ \sum_{t=1}^{T}[{\lambda_t}^D P_{D,t} + {\lambda_t}^R(P_{D,t} + R_t) + {\lambda_t}^{PFR} PFR_{Req,t} + {\lambda_t}^E(E_{Req.t} - H_{Dem}P_{D,t})] \end{aligned} \tag{6.17}$$

where,

- The second part, $\sum_{t=1}^{T}[{\lambda_t}^D P_{D,t} + {\lambda_t}^R(P_{D,t} + R_t) + {\lambda_t}^{PFR} PFR_{Req,t} + {\lambda_t}^E(E_{Req.t} - H_{Dem}P_{D,t})]$, representing the system coupling constraints, has no influence on the optimisation as it can be considered as a constant. Hence, the second part can be temporary ignored.
- The first part, $\sum_{i=1}^{N}\sum_{t=1}^{T}\{[FC_i(P_{i,t}) + RC_i(PFR_{i,t}) + ST_iB_{i,t} + SD_iX_{i,t}]{\lambda_t}^D P_{i,t} - {\lambda_t}^R P_i^{max} U_{i,t} - {\lambda_t}^{PFR} PFR_{i,t} - {\lambda_t}^E E_{i,t}\}$, is the summation of the N single-generator

sub-problems over the time horizon T, and the single-generator sub-problem can be optimised separately.

Thus, the Lagrange function can be solved by minimising the single-generator sub-problems. The Lagrange function is rewritten as:

$$\begin{aligned} L = \sum_{i=1}^{N} \Big\{ \text{Min} \sum_{t=1}^{T} \big([FC_i(P_{i,t}) + RC_i(PFR_{i,t}) + ST_i B_{i,t} + SD_i X_{i,t}] \\ - \lambda_t{}^{D} P_{i,t} - \lambda_t{}^{R} P_i{}^{max} U_{i,t} - \lambda_t{}^{PFR} PFR_{i,t} - \lambda_t{}^{E} E_{i,t} \big) \Big\} \end{aligned} \tag{6.18}$$

Single-generator Sub-Problem

The traditional approach to solve the single-generator sub-problem is through dynamic programming, which attempts each possible routes and traces back for the optimal generator on-off state tree. At each time, the generator has two states, i.e. on and off, for the time horizon T, the total possible routes are $2T$. Therefore, by using Lagrange Relaxation, the problem dimension is reduced from $2^N \cdot T$ to $2T \cdot N$ for each iteration. As the system size expands, the problem dimension increases linearly rather than exponentially, which reduces the computational burden of the UC.

The single-generator sub-problem belongs to the optimisation model called the mixed-integer quadratic programming (MIQP) whose objective function contains quadratic terms with linear or quadratic equality and inequality constraints. In this thesis, CPLEX is the solver selected for the MIQP sub-problem [115]. The single-generator sub-problem is summarised as follows:

$$\begin{aligned} \text{Min} \sum_{t=1}^{T} \Big\{ [a_i P_{i,t}{}^2 + b_i P_{i,t} + C_i + d_i PFR_{i,t} + ST_i B_{i,t} + SD_i X_{i,t}] \\ - \lambda_t{}^{D} P_{i,t} - \lambda_t{}^{R} P_i{}^{max} U_{i,t} - \lambda_t{}^{PFR} PFR_{i,t} - \lambda_t{}^{E} E_{i,t} \Big\} \end{aligned} \tag{6.19}$$

$$\text{s.t.} \quad B_{i,t} \geq U_{i,t} - U_{i,t-1} \tag{6.19a}$$

$$X_{i,t} \geq U_{i,t-1} - U_{i,t} \tag{6.19b}$$

$$P_i{}^{min} U_{i,t} \geq P_{i,t} \geq P_i{}^{max} U_{i,t} \tag{6.19c}$$

$$\textstyle\sum_{t'=t-t_i{}^{u}+1}^{t} B_{i,t'} \leq U_{i,t} \tag{6.19d}$$

$$\textstyle\sum_{t'=t-t_i{}^{d}+1}^{t} x_{i,t'} \leq 1 - U_{i,t} \tag{6.19e}$$

$$P_{i,t} - P_{i,t-1} \leq U_{i,t-1} r_i{}^{u} + B_{i,t} r_i{}^{su} \tag{6.19f}$$

$$P_{i,t-1} - P_{i,t} \leq U_{i,t} r_i{}^{d} + X_{i,t} r_i{}^{sd} \tag{6.19g}$$

where,

- (6.19a) and (6.19b) are the constraints for start-up and shut-down signal. Since the start-up signal $B_{i,t}$ is either 0 or 1, $B_{i,t}$ will be 1 only if $U_{i,t} = 1$ and $U_{i,t-1} = 0$; similarly, the shut-down signal $X_{i,t}$ will be 1 only if $U_{i,t} = 0$ and $U_{i,t-1} = 1$;

- (6.19c) is the constraint for the minimum and maximum generation when the generator is scheduled, the generator's output $P_{i,t}$ is bonded with the on-off status $U_{i,t}$;

- (6.19d) and (6.19e) are the minimum up and down time constraints for generator respectively. When $U_{i,t} = 0$, the start-up signals in previous $(t - {t_i}^u)$ time settlements should all be 0; when $U_{i,t} = 1$, the shunt-down signals in settlements $(t - {t_i}^d)$ time periods should all be 0;

- (6.19f) and (6.19g) are the constraints for ramp up and ramp down respectively. It also ensures the start-up and shut-down rates follow the designed values of the generator.

Stopping Criteria

The duality gap is used to stop the Lagrange Relaxation optimisation iteration. The duality gap is measured by the difference between the original objective function and the Lagrange function. When the duality gap is less than the pre-defined value the Lagrange relaxation iteration stops. The duality gap is calculated as:

$$G^{(k)} = \frac{g^{(k)}}{L^{(k)}} = \frac{F^{(k)} - L^{(k)}}{L^{(k)}} \leq \varepsilon \tag{6.20}$$

where,

- k is the optimisation iteration index,

- $F^{(k)}$ is the value of the original objection function at iteration k,

- $L^{(k)}$ is the value of the Lagrange function at iteration k,

- $g^{(k)}$ is the duality gap difference indicating the difference between the original objection function and the Lagrange function,

- ε is the pre-defined gap.

Note that due to the involvement of the inequality constraints the duality gap cannot be fully eliminated. The differences between the original objection function and Lagrange function is due to the system coupling constraints, which is shown below:

$$\begin{aligned} g^{(k)} = & \sum_{t=1}^{T} {\lambda_t}^{D,(k)} \left(\sum_{i=1}^{N} {P_{i,t}}^{(k)} - P_{D,t} \right) \\ & + \sum_{t=1}^{T} {\lambda_t}^{R,(k)} \left(\sum_{i=1}^{N} {P_i}^{max} {U_{i,t}}^{(k)} - (P_{D,t} + R_t) \right) \\ & + \sum_{t=1}^{T} {\lambda_t}^{PFR,(k)} \left(\sum_{i=1}^{N} {PFR_{i,t}}^{(k)} - PFR_{Req,t}) \right) \\ & + \sum_{t=1}^{T} {\lambda_t}^{E,(k)} \left(\sum_{i=1}^{N} {E_{i,t}}^{(k)} - E_{Req,t}) \right) \end{aligned} \tag{6.21}$$

Since the generation/demand balance is the equality constraint, $\left(\sum_{i=1}^{N} {P_{i,t}}^{(k)} - P_{D,t} \right)$ can be as close to zero as possible. However, the rest of the constraints are all inequalities, meaning that the system must have sufficient scheduled spinning reserves, PFR and inertia rather than exactly the same as required. Therefore, the duality gap difference, $g^{(k)}$, should be non-negative. If the duality gap difference is negative indicates at least one of the system coupling constraint is not satisfied.

6.2.4 Lagrange Multiplier Update Criteria

The economic meaning of the Lagrange multiplier reflects the marginal price [116, 26, 27, 97], or shadow price in some literature [117, 118], of the associated constraint. The value of the Lagrange multiplier indicates the direction of change of the optimal solution when changing the associated constraint. In power systems, the marginal cost is often being selected as the cost for providing/delivering services. The ancillary services market tends to bond with the energy market with uniformed clearing prices based on the marginal prices of the services. By definition, the marginal price is the additional cost for producing one more unit. In the frequency-constraint UC problem, the marginal prices can be treated as the cost for providing the services such as spinning reserve, PFR and Inertia.

The Lagrange multipliers are the key in the Lagrange relaxation UC, which affect the accuracy of the optimisation; while the initial value selection and the update criteria are the key aspects for the Lagrange multipliers in terms of the convergence speed.

Initialisation

The random start of the Lagrange multipliers may lead to the local optimal instead of global optimal or requires a longer time to the reach the global optimal [119]. The selection of the initial values of the Lagrange multipliers should close to the optimal values with the less computational burden.

The initialisation process firstly calculate the full-load averaged cost of each generator:

$$FL_i = \frac{FC_i(P_i^{max})}{P_i^{max}} = \frac{a_i {P_i^{max}}^2 + b_i P_i^{max} + c_i}{P_i^{max}} \tag{6.22}$$

Then the generation units are sorted in ascending order based on the full-load averaged cost. For each time settlement, the generation units with the least full-load averaged costs will be committed until total generation capacity is larger than the demand settlement. Thus the generator on-off statuses are determined, and the ED is conducted for the committed generators. The initial value of the Lagrange multiplier associated with the power balance is then selected by the largest marginal price of the committed generators. The ED ignores the spinning reserve, PFR and inertia constraints because the ED optimisation is done with respect to the generation amount of each unit. Assuming ${P_{i,t}}^{ED}$ represents the optimised generation in ED, the initial Lagrange multiplier for power balance constraints is obtained through:

$$\text{Min } \left[FC_i({P_{i,t}}^{ED}) - {\lambda_t}^{D,(0)} {P_{i,t}}^{ED}\right] \tag{6.23}$$

Taking the first derivative with respect to ${P_{i,t}}^{ED}$ and making it equal to zero, the initial value for the power balance Lagrange multiplier is obtained:

$$\begin{aligned} \frac{d}{d{P_{i,t}}^{ED}} \left[FC_i({P_{i,t}}^{ED}) - {\lambda_t}^{D,(0)} {P_{i,t}}^{ED}\right] = 2a_i {P_{i,t}}^{ED^2} + b_i - {\lambda_t}^{D,(0)} = 0 \\ {\lambda_t}^{D,(0)} = 2a_i {P_{i,t}}^{ED^2} + b_i \end{aligned} \tag{6.24}$$

The initial value for the Lagrange multiplier associated with spinning reserve can be obtained by ignoring the PFR and inertia constraints. The single-generator sub-problem (6.19) is modified and set to zero:

$$\sum_{i=1}^{N} \left[FC_i({P_{i,t}}^{ED}) - {\lambda_t}^{D,(0)} {P_{i,t}}^{ED} - {\lambda_t}^{R,(0)} P_i^{max}\right] = 0 \tag{6.25}$$

The Lagrange multipliers are non-negative; hence, the initial value for the Lagrange

multiplier associated with spinning reserve at time t is found by:

$$\lambda_t{}^{R,(0)} = \text{Max}\left[\frac{\sum_{i=1}^{N}(FC_i(P_{i,t}{}^{ED}) - \lambda_t{}^{D,(0)}P_{i,t}{}^{ED})}{\sum_{i=1}^{N}P_i^{max}},\ 0\right] \tag{6.26}$$

Similarly, the initial Lagrange multipliers for PFR and inertia can be obtained following the same process:

$$\begin{aligned}\lambda_t{}^{PFR,(0)} &= \text{Max}\left[\frac{\sum_{i=1}^{N}(FC_i(P_{i,t}{}^{ED}) - \lambda_t{}^{D,(0)}P_{i,t}{}^{ED})}{\sum_{i=1}^{N}PFR_{i,t}},\ 0\right] \\ \lambda_t{}^{R,(0)} &= \text{Max}\left[\frac{\sum_{i=1}^{N}(FC_i(P_{i,t}{}^{ED}) - \lambda_t{}^{D,(0)}P_{i,t}{}^{ED})}{\sum_{i=1}^{N}E_{i,t}},\ 0\right]\end{aligned} \tag{6.27}$$

Update Criteria

Studies show that the performance of Lagrange relaxation, in terms of the convergence speed and optimisation accuracy, is heavily relied on the update criteria for the Lagrange multipliers. The update criteria are this work is proposed to have the following characteristics:

- The step size is decreasing as the iteration number increase to minimise the generation on-off oscillations. To do so, the iteration counter k is involved in the update rules.
- The Lagrange multipliers associated with PFR and inertia constraints are updated in a coupled manner to move toward the inertia-PFR equivalent curve derived in Chapter 4.
- The update criteria are determined by the deficits of the system coupling constraints to avoid redundant updates.

Since the Lagrange multipliers are non-negative, the minimum value of the Lagrange multiplier is zero. The update rule for the Lagrange multipliers associated with power balance and spinning reserve constraints for time settlement t are updated according to:

$$\begin{aligned}\lambda_t{}^{D,(k)} &= \text{Max}\left[\lambda_t{}^{D,(k-1)} + \frac{\Delta P_{D,t}}{(\alpha+\beta\cdot k)\cdot\text{norm}(\Delta P_D)}\right] \\ \lambda_t{}^{R,(k)} &= \text{Max}\left[\lambda_t{}^{R,(k-1)} + \frac{\Delta R_t}{(\alpha+\beta\cdot k)\cdot\text{norm}(\Delta R)}\right]\end{aligned} \tag{6.28}$$

where,

- α and β are two constants associated with the step size, which are determined heuristically [95].
- $\Delta P_{D,t}$ is the deficit of the power balance constraint.

$$\Delta P_{D,t} = P_{D,t} - \sum_{i=1}^{N} P_{i,t} \tag{6.29}$$

- ΔR_t is the deficit of the spinning reserve constraint.

$$\Delta R_t = P_{D,t} + R_t - \sum_{i=1}^{N} {P_i}^{max} U_{i,t} \tag{6.30}$$

- $\text{norm}(\Delta P_D)$ is the Euclidean distance between the current state and the feasible region for the power balance constraint.

$$\text{norm}(\Delta P_D) = \sqrt{(\Delta P_{D,1})^2 + (\Delta P_{D,2})^2 + \cdots + (\Delta P_{D,T})^2} \tag{6.31}$$

- $\text{norm}(\Delta R)$ is the Euclidean distance between the current state and feasible region for the spinning reserve constraint.

$$\text{norm}(\Delta R) = \sqrt{(\Delta R_1)^2 + (\Delta R_2)^2 + \cdots + (\Delta R_T)^2} \tag{6.32}$$

The update cases for the Lagrange multipliers of ${\lambda_t}^D$ and ${\lambda_t}^R$ are summarised as:

(1) If $\Delta P_{D,t} < 0$ and $\Delta R_t < 0$: indicating the generations are over committed and the reserve constraint is satisfied. Update the Lagrange multiplier for both ${\lambda_t}^D$ and ${\lambda_t}^R$ to reduce the generation committed.

(2) If $\Delta P_{D,t} \geq 0$ and $\Delta R_t \geq 0$: indicating demand and reserve are both insufficient. Update the Lagrange multiplier for both ${\lambda_t}^D$ and ${\lambda_t}^R$ to turn on more generators.

(3) If $\Delta P_{D,t} < 0$ and $\Delta R_t > 0$: indicating the generation is enough but the reserve constraint is not satisfied, more generator should be turned on to increase the total generation capacity. Update the Lagrange multiplier for ${\lambda_t}^R$.

(4) If $\Delta P_{D,t} > 0$ and $\Delta R_t < 0$: this situation is theoretically impossible to occur in the optimisation process, because it indicates the total capacity is able to cover

the demand and the reserve target but the total generation is unable to meet the demand. This situation is only possible when the initial values of the Lagrange multipliers are generated incorrectly.

The PFR and inertia constraints are regulated based on the system frequency dynamic behaviours, i.e. the initial ROCOF, the quasi-steady-state frequency and the frequency nadir. The initial ROCOF is the inertia-only constraint which sets the minimum value of the inertia that should be available in the system to prevent the miss-trip of the protection relay of the distributed generators; the quasi-steady-state frequency is the PFR-only constraint which determines the minimum amount of PFR reserve to prevent the quasi-steady-state frequency below the limit stated in the Grid Code; the frequency nadir is affected by both PFR and inertia. Therefore, the PFR and inertia are coupled together to satisfy the frequency nadir requirements.

The updates for the Lagrange multipliers associated with PFR and inertia are dependent on the combination of PFR and inertia at the current iteration. There are five possible scenarios of the PFR and inertia combinations, summarised as follows:

(1) If $\sum_{i=1}^{N} E_{i,t} < E_{ROCOF}$ and $\sum_{i=1}^{N} PFR_{i,t} < PFR_{qst}$, update the Lagrange multiplier for both PFR, ${\lambda_t}^{PFR}$, and inertia, ${\lambda_t}^{E}$.

(2) If $\sum_{i=1}^{N} E_{i,t} < E_{ROCOF}$ and $\sum_{i=1}^{N} PFR_{i,t} \geq PFR_{qst}$, update the Lagrange multiplier for inertia, ${\lambda_t}^{E}$, only.

(3) If $\sum_{i=1}^{N} E_{i,t} \geq E_{ROCOF}$ and $\sum_{i=1}^{N} PFR_{i,t} < PFR_{qst}$, update the Lagrange multiplier for PFR, ${\lambda_t}^{PFR}$, only.

(4) If $\sum_{i=1}^{N} E_{i,t} \geq E_{ROCOF}$ and $\sum_{i=1}^{N} PFR_{i,t} \geq PFR_{qst}$, test whether the frequency nadir requirement is satisfied, if not update the Lagrange multiplier for both PFR, ${\lambda_t}^{PFR}$, and inertia, ${\lambda_t}^{E}$.

(5) If $\sum_{i=1}^{N} E_{i,t} \geq E_{ROCOF}$ and $\sum_{i=1}^{N} PFR_{i,t} \geq PFR_{qst}$, test whether the frequency nadir requirement is satisfied, if yes no updates required unless the on-off status changed.

where,

- E_{ROCOF} is the minimum inertia required to satisfy the ROCOF requirement.
- PFR_{qst} is the minimum PFR required to satisfy the quasi-steady-state frequency requirement.

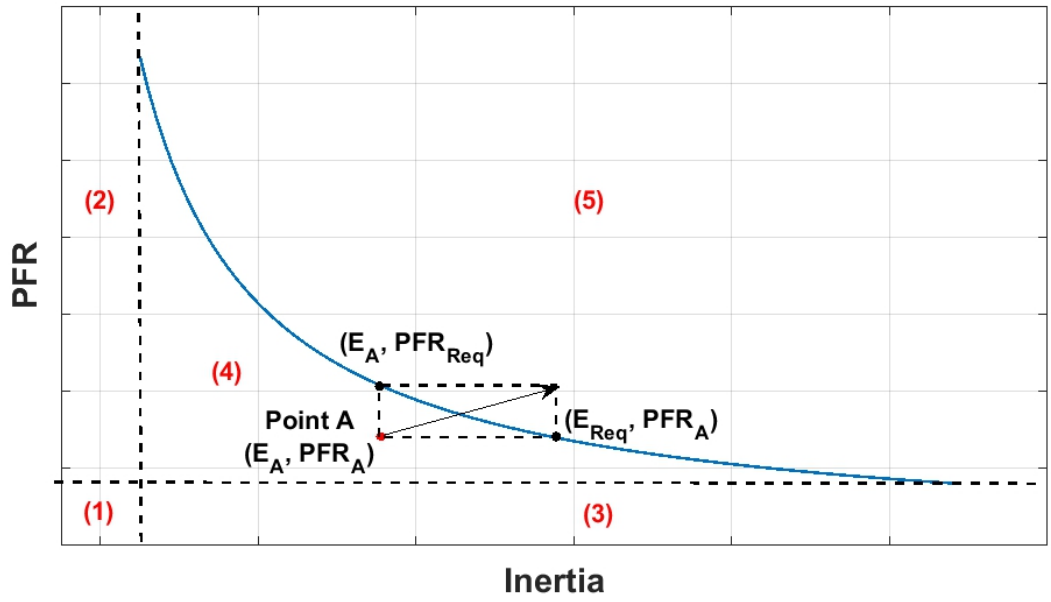

Figure 6-2: Update rules for PFR and inertia constraints

The position of the five possible scenarios are shown in Figure 6-2. The curve represents the relationship between PFR and inertia that the frequency nadir equals to the lowest allowed limit. Any point, in terms of PFR and inertia combinations, on or above the curve ensures the frequency nadir requirement is met. The possible scenarios are summarised as follows:

- Scenario (1) refers to a system heavily dominated by renewables and the curtailment of renewable generation is necessary in this case to commit more conventional generators with PFR and inertia contributions.
- Scenario (2) refers to a system with only ROCOF issues, i.e. UK power system. However, changing the setting of the protection relays of the distributed generators largely release the ROCOF pressure in the UK.
- Scenario (3) can be avoided by ensuring that the PFR reserve could cover the largest infeed generation loss. In the current system, the first three scenarios are very rare, but with the growing penetration of inertia-less renewables, the possibilities are increasing.
- For scenario (4) the ROCOF and quasi-steady-state frequency requirements are met. However, the PFR and inertia as a whole are unable to meet the frequency nadir requirement which may end up with unintentional LFDD. This potential

risks of LFDD are more likely to happen in the current power system.

- Scenario (5) refers to the situation that sufficient PFR and inertia are in place and all three frequency-related requirements are satisfied.

The update rules for that five scenarios are performed accordingly. Taking scenario (4) as an example, it is assumed that the PFR and inertia reserves are PFR_A and E_A respectively at the current iteration shown as by Point A in Figure 6-2. The PFR-inertia relationship derived in Chapter 4 is implemented by introducing two functions, f_{PFR} and f_E:

- f_{PFR} is the function to find the minimum PFR required for a given inertia, which is the projection of the current inertia reserve, E_A, on the PFR-inertia curve:

$$PFR_{Req} = f_{PFR}(E_A) \tag{6.33}$$

- f_E is the function to find the minimum inertia required for a given PFR, which represents the projection of the current PFR reserve, PFR_A, on the PFR-inertia curve:

$$E_{Req} = f_E(PFR_A) \tag{6.34}$$

The update of the Lagrange multipliers associated with PFR and inertia for time settlement t then can be obtained as:

$$\begin{aligned} {\lambda_t}^{PFR,(k)} &= \text{Max}\left[{\lambda_t}^{PFR,(k-1)} + \frac{\Delta PFR_t}{(\alpha+\beta\cdot k)\cdot \text{norm}(\Delta PFR)}\right] \\ {\lambda_t}^{E,(k)} &= \text{Max}\left[{\lambda_t}^{E,(k-1)} + \frac{\Delta E_t}{(\alpha+\beta\cdot k)\cdot \text{norm}(\Delta E)}\right] \end{aligned} \tag{6.35}$$

where,

- ΔPFR_t is the deficit between the current PFR reserve and the required PFR.

$$\Delta PFR_t = PFR_{Req,t} - \sum_{i=1}^{N} PFR_{i,t} \tag{6.36}$$

- ΔE_t is the deficit between the current total system inertia and the required

inertia.

$$\Delta E_t = (E_{Req,t} - h_{dem} P_{D,t}) - \sum_{i=1}^{N} E_{i,t} \tag{6.37}$$

- norm(ΔPFR) represents the Euclidean distance between the current PFR reserves and the feasible region of PFR reserves.

$$\text{norm}(\Delta PFR) = \sqrt{(\Delta PFR_1)^2 + (\Delta PFR_2)^2 + \cdots + (\Delta PFR_T)^2} \tag{6.38}$$

- norm(ΔE) represents the Euclidean distance between the current total system inertia and the feasible region of the inertia reserves.

$$\text{norm}(\Delta E) = \sqrt{(\Delta E_1)^2 + (\Delta E_2)^2 + \cdots + (\Delta E_T)^2} \tag{6.39}$$

In conclusion, the update rules for the Lagrange multipliers are implemented by a two-layer update action. The Lagrange multipliers associated with power balance and reserve constraints are grouped together while the PFR and inertia are grouped together. The update of Lagrange multipliers move the results towards the optimal solution by adjusting the gradient in each iteration. There are some intrinsic links between the Lagrange multipliers: the Lagrange multiplier for power balance and PFR constraints affect the power generated for each unit; while the on-off statuses of generators are primarily affected by the Lagrange multipliers for reserve and inertia.

6.3 Case Study of the Proposed Method

This section provides the demonstration and the results analysis of the proposed Lagrange relaxation UC optimisation. The demonstration is carried out based on the simplified UK power system. The Lagrange multipliers are used to obtain the marginal prices for the associated constraints.

6.3.1 Test System

When taking the largest infeed generation as the target for the robustness, the system size determines the difficulty of ensuring the frequency transient stability. For example, the minimum demand in the UK in 2017 was 16.6 GW [102]. Following the

SQSS standard, the 1800 MW loss accounts for 10.8% of the total demand, and the frequency transient stability can hardly meet the requirements. Hence, the size of the demonstration system should be relatively large to allow the SQSS requirements to be fulfilled.

The test system of the proposed method represents the simplified UK power system, which has 38 generators with a total generation capacity of 14.5 GW. These include seven coal-fired power stations, two of which are converted to biomass; ten combined cycle gas turbines (CCGT), with one operating as a combined heat and power (CHP); six hydro power stations, four are pumped storage stations whilst the other two are non-pumped hydro stations; four nuclear power stations, one pressurised water reactor (PWR) and three advanced gas reactor (AGR); and eleven wind farms, five onshore and six offshore. The total capacity and the share of each type of generation are shown in Figure 6-3 and Table 6.1. The complete data of the case studies are presented in the Appendix.

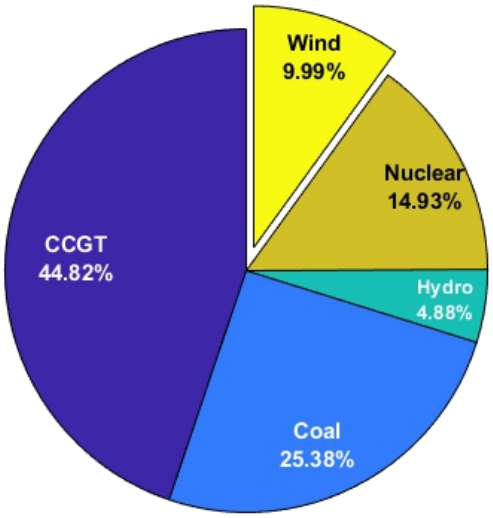

Figure 6-3: Capacity shares of the demonstration system

Table 6.1: Generation of the demonstration system

	CCGT	Coal	Hydro	Nuclear	Wind
Number of Generators	10	7	4	4	11
Total Capacity (MW)	6499	3680	707	2164	1449
Inertia Constant (s)	6.5	5	4.5	5	0

6.3.2 Proposed Method Implementation

Scaling Factor

The largest generator in the demonstration system is 885 MW (CCGT), and the total available inertia on the generation side is 75 GWs. Figure 6-4 shows the system inertia and PFR requirements for the largest generation loss when the demand equals to 8 GW. It can be seen in the figure that the required inertia exceeds the maximum inertia of the system, thus the PFR requirements will be amplified and the system frequency dynamic is not well reflected. To fit the system available range of PFR and inertia into the UC consideration, a scaling factor is introduced to scale down the largest infeed loss that the system is required to withstand.

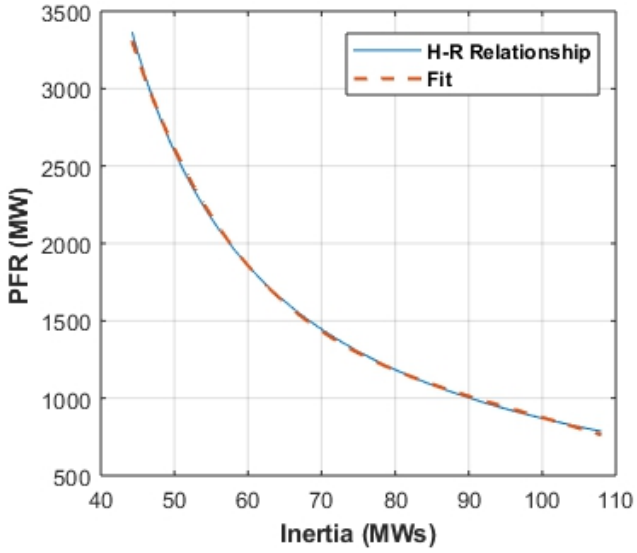

Figure 6-4: Frequency nadir requirements implementation

Frequency Constraints

The frequency-related constraints are the initial ROCOF, quasi-steady-state frequency and frequency nadir; which are the inertia-only, PFR-only and inertia plus PFR constraints respectively. Therefore, the minimum amount of the inertia and PFR can be represented as:

$$E_{min} \geq |\frac{P_{loss}/C_{SD}}{2ROCOF_{limit}}| \cdot f_N$$

$$PFR_{min} \geq \frac{P_{loss}}{C_{SD}} - (f_N - F_{SL}) \cdot k_{DFR}$$

where,

- P_{loss} is the largest infeed generation, 885 MW;
- C_{SD} is the scaling factor to reduce the impact of the largest infeed loss;
- $ROCOF_{limit}$ is the ROCOF limit for the protection of the distributed generation, 0.5 Hz/s;
- f_{SL} is the quasi-steady-state frequency limit, 49.5 Hz;
- k_{DFR} is demand frequency ratio, 2.5%.

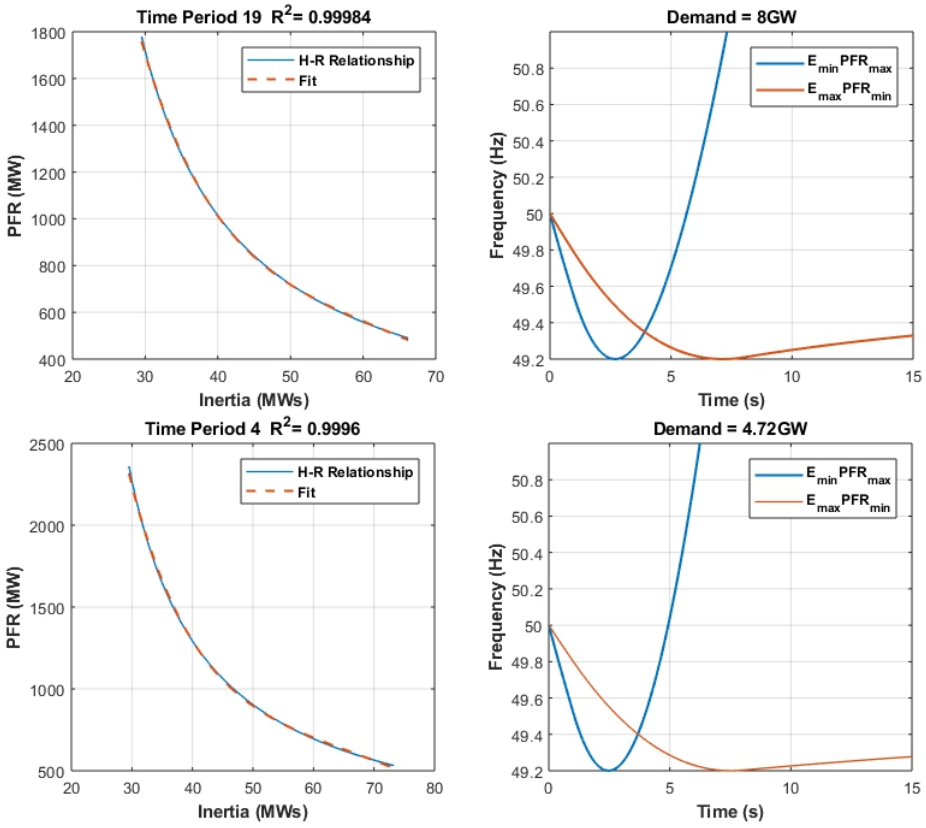

Figure 6-5: Implementation of the frequency-related constraints

The PFR and inertia combinations that satisfy the frequency nadir requirements can be found after the ROCOF and quasi-steady-state frequency requirements are met. Figure 6-5 shows the feasible region of the inertia and PFR combinations for the though and peak demand respectively. The graphs on the right side are the two extreme situations, i.e. maximum PFR and maximum inertia, which satisfy the frequency

nadir requirement.

Wind Generation Modelling

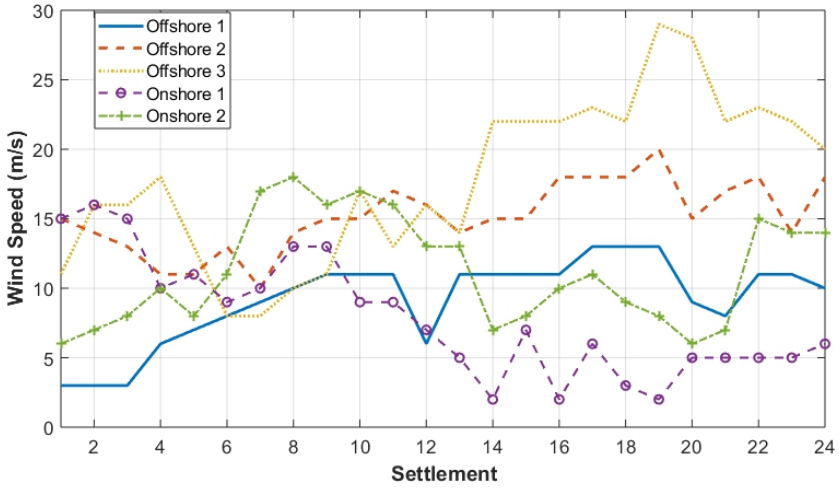

Figure 6-6: Wind speeds used in the case study

The wind generation can be described by the equation below [120, 121]:

$$P_w = \begin{cases} \frac{v_w - v_{ci}}{v_r - v_{ci}} P_r, & \text{for } v_{ci} < v_w < v_r \\ P_r, & \text{for } v_r \leq v_w \leq v_{co} \\ 0, & \text{for } v_w < v_{ci} \text{ or } v_w > v_{co} \end{cases} \tag{6.40}$$

where,

- P_w and P_r are the output power and the rated power of the wind turbine,
- v_w, v_{ci} and v_{co} are the wind speed, cut-in speed and cut-out speed respectively.

The methods of the wind speed simulations are focused on the probability distributions such as the Monte Carlo method [120] and Weibull distribution [121]. The problem with the wind speed generated by the previous methods is that wind speeds are all random. The situation of max-zero-max is possible when using the probability distribution methods. To avoid max-zero-max situations, the wind speed is the case study using the real wind speeds recorded in the UK [122], shown in Figure 6-6. The eleven wind generators are divided into five wind farms, three off-shore and two on-shore. All the wind generators in one farm have the same input wind speed data.

6.3.3 Results and Discussion

The demonstration of the results is conducted for four cases in terms of the different size of frequency contingencies. The four cases are listed as follows:

- **Case 0** is the traditional UC optimisation with no frequency-related constraints.
- **Case 1**: scaling factor, $C_{SD} = 1.7$, and the largest potential generation loss considered in the optimisation, $P_{loss} = 520$ MW.
- **Case 2**: scaling factor, $C_{SD} = 1.5$, and the largest potential generation loss considered in the optimisation, $P_{loss} = 590$ MW.
- **Case 3**: scaling factor, $C_{SD} = 1.3$, and the largest potential generation loss considered in the optimisation, $P_{loss} = 680$ MW.

Table 6.2: Summary of the test cases

Case	**0**	**1**	**2**	**3**
Scaling factor	-	1.7	1.5	1.3
Largest generation loss to be covered (MW)	-	520	590	680
Total Generation cost (£)	1,726,229	1,756,644	1,765,560	1,789,637
Increase (£)	-	1.76%	2.28%	3.67%

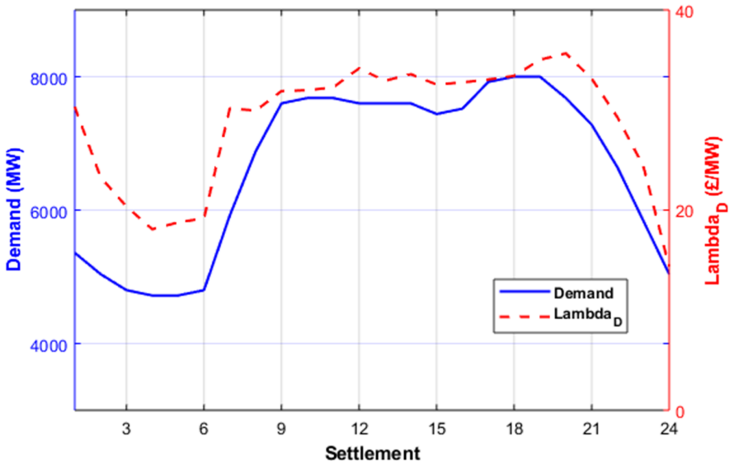

Figure 6-7: Demand profile and marginal energy price for Case 0

Case 0 is the base scenario used to compare the results with frequency-related requirements, and Case 1 to 3 represent the frequency contingencies as these become more and more severe. Table 6.2 shows the summary of the four cases and the total generation costs. The results indicate the system frequency stability can be guaranteed through the system planning with the slight operational cost increase. The demand profile and the marginal energy cost for case 0 are shown in Figure 6-7 as a base comparison to the cases with frequency-related requirements.

The marginal costs for energy, inertia and PFR are shown in Figure 6-8 (a), (b) and (c) respectively. The key findings are summarised as follows:

- The marginal cost for energy generally follows the same shape as the demand profile. However, with the increase of the generation loss, the marginal costs for energy reduces, especially during the low demand period (settlement 4-6). The low demand period is the weak period in terms of the inertia availability in the system which has been identified in Chapter 4. Additional conventional generators are needed to provide inertia and the provision of energy is not the primary goal of the new generators; hence the marginal cost of energy will decrease accordingly.

- The marginal cost for inertia follows the opposite shape of the demand profile. When demand falls the marginal cost for inertia increases and vice versa. The highest marginal cost for inertia occurs at the minimum demand period (settlement 4-6), and the lowest marginal cost for inertia is at the peak demand period (settlement 19-21). Since more generators are connected to meet the peak demand, this results in more inertia in the system, and eliminates the need for additional inertia. Hence, the marginal cost is zero for settlement 19-21. The largest generator considered in the UC increases linearly for each case, i.e. 70 MW, the marginal costs for inertia to withstand the loss of the largest generator increase exponentially, reflecting the severity of the inertia problems in the weak period.

- In addition to the peak demand period, the marginal costs for PFR do not have a strong implication on the demand profile. Due to the same reason, for the marginal cost of inertia in the peak demand period (settlement 19-21), the cost for additional PFR is zero. In case 1-3, the marginal cost for PFR increases linearly.

The number of the conventional generators connected, the system inertia and PFR reserves are shown in Figure 6-8 (d), (e) and (f) respectively. For different loss levels,

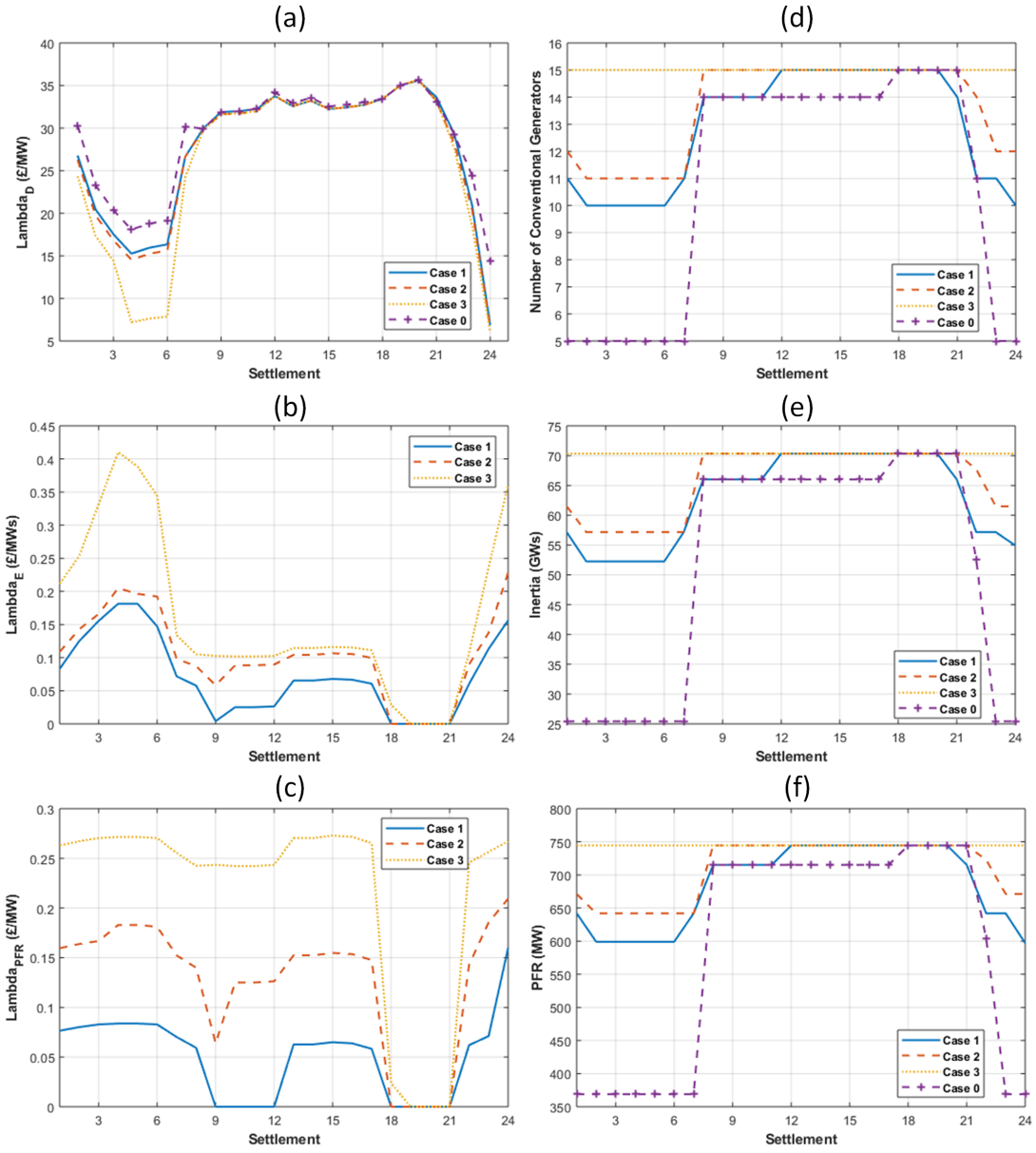

Figure 6-8: Results of the frequency-constrained UC
(a) marginal price for energy λ^D, (b) marginal price for inertia λ^E, (c) marginal price for PFR λ^{PFR}, (d) number of conventional generators, (e) inertia reserve, (f) PFR reserve

the total number of connected generators reflects the importance of the conventional generators in the provision of inertia and PFR. The inertia and PFR reserves for Case 1-3 all ensure the frequency transient stability in terms of the ROCOF, quasi-steady-state frequency and frequency nadir.

In conclusion, the marginal cost of inertia in different settlement reflects the need and availability of providing inertia which is a proper way to set the price for inertia. The involvement of provision cost for inertia can give the incentive for generators to implement the technology such as synthetic inertia, and improve the competitiveness of conventional generators in renewable-led energy transformations. The results also indicate the system frequency stability can be guaranteed through system planning, to withstand the loss of 680 MW the total generation increase by only 3.67%.

6.4 Chapter Summary

This chapter proposes a method to solve the frequency-constrained UC optimisation problems in order to examine the feasibility of ensuring the frequency transient stability through system planning. The frequency requirements in the UC optimisation considers the initial ROCOF, the quasi-steady-state frequency and the frequency nadir. The frequency-constrained UC is solved through the modified Lagrange relaxation to further investigate the marginal price of inertia. The key innovations regarding the Lagrange relaxation are the initialisation process and the two-layer heuristic Lagrange multiplier update structure.

The case studies of the frequency-constrained UC optimisation are carried out on a 38-generator system in MATLAB environment through CPLEX solver. The marginal price of inertia is obtained in terms of the Lagrange multiplier associated with inertia requirements which are constrained by the ROCOF and frequency nadir. The results from the case studies indicate the marginal price for inertia reflects the need and availability of the inertia provision; and by the implementation of smart system planning, the frequency transient stability can be enhanced to withstand the largest generation loss with minimum generation cost increase.

Chapter 7

Conclusions and Future Work

THIS chapter concludes the thesis by outlining the major contributions, the key findings and the potential future improvements of the research work.

7.1 Conclusions

This thesis addresses the inertia problems introduced by the utilisation of renewable generation in the perspective of system operation planning and market incentives to achieve a balance between efficiency and frequency stability. To investigate the frequency stability, a simulation tool is required to study the frequency dynamics after a sudden generation/load imbalance. Instead of the closed-loop transfer functions in the Laplace domain, an aggregated mathematical approach is proposed to describe the frequency dynamics by assuming the PFR is injected to the system linearly. The PFR response mechanism is simplified only focus on the maximum amount and response time; however, it does not affect the values of initial ROCOF, frequency nadir and quasi-steady-state frequency. Thus, the analysis of those three frequency-related parameters is simplified only focus on PFR and inertia reserves.

The SQSS requires the current system is able to withstand the largest potential generation loss, i.e. 1800MW. This value is used to stipulate the inertia and PFR requirements in Chapter 4 to ensure the frequency-related requirements are satisfied. However, the size of the contingency decides the infeasible region in Section 4.2.4, which refers to the situation that regardless of how much inertia is in place, the quasi-steady-state frequency requirements cannot be met. The initial ROCOF and quasi-steady-state frequency are inertia-only and PFR-only constraints, while the frequency nadir is determined by both inertia and PFR reserve. The method proposed in Chapter 4 can find the optimal inertia reserve with given PFR by an iteration process. However, the result can be verified only if the system parameters are in the realistic range, i.e. system size, the generation loss, PFR availability. Otherwise, it is an impractical value. These situations can be avoid by calculating the time when frequency reaches minimum, i.e. t_{min}, which should between the PFR starting time and PFR fully deployed time. That time can be used as the indicator for the authenticity of the result.

Total system inertia is declining due to the increasing popularity of renewable generation and VFD motors. Since inertia becomes a scarce property all the potential inertia providers should be taken into consideration. The results in Chapter 5 suggest demand could contribute 20% of the total system inertia with an averaged inertia constant of 1.75s in the system demand base for the fifteen frequency outage events in 2010. The inertia profile generally follows the shape of the demand profile under the current renewable and VFD penetrations. The benefit of shifting the demand from peak to trough can move the redundant inertia in safe period to the weak period, thus improving the system frequency stability.

Without the storage capacity for demand shifting, the reduced inertia lifts the difficulty of maintaining the system frequency transient stability for the daily operation. Chapter 6 proposes a method to incorporate frequency-dependent constraints into the power generation scheduling UC problem to assess the impact of frequency constraints on system operating costs. The marginal price for inertia is obtained based on the economic meaning of the Lagrange multiplier in Lagrange relaxation UC optimisation. The necessities of involving inertia into ancillary services market are threefold: (i) bringing incentives to the existing inertia providers and encouraging the future potential inertia providers to participate; (ii) improving the competitiveness of the conventional generators against renewable generation and provide a transformation solution for conventional generators; (iii) allowing the non-BMUs to contribute inertia such as demand motor groups and synchronous compensators. The innovations regrinding the better representation of system frequency dynamics are listed below:

- The inertia and PFR constraints are introduced to cope with the frequency requirements for the largest potential infeed generation loss to improve the frequency robustness. The inertia and PFR constraints are set to meet the requirements of the ROCOF, the quasi-steady-state frequency and frequency nadir.
- The demand side inertia contribution and demand droop to frequency deviations are considered in the UC decision-making, thus transforming the demand from a simple generation target to a key player to ensure frequency stability.
- Renewable generations are not negative demand which allows the renewable generation to be curtailed when necessary.

The innovations regarding the Lagrange Relaxation UC algorithms are listed below:

- Initialisation process generates the initial Lagrange multipliers based on the full-load averaged cost; the inertia and PFR constraints depending on the frequency nadir. Polynomial fit is applied to deal with the transcendence of inertia and PFR relationship for the frequency nadir requirements.
- The update criteria of the Lagrange multipliers is modified to a two-layer structure, the first layer represents the multipliers associated with traditional constraints and the second layer focuses on the update of inertia and PFR constraints.

The future trend of the frequency control method in a low-inertia future is the fast frequency response. The case studies and results in Chapter 6 only consider the conventional frequency response. Based on the response speed in the event of a generation

loss, the conventional frequency response refers to the inertial response starts instantly, the primary response starts within 10 seconds and the secondary response starts within 30 seconds. However, the fast frequency response refers to the additional active power injections provided by any generation technologies that are not based on swing equations such as DFIG and batteries. The fast frequency response allows the frequency drop to be arrested before the excessive decrease of frequency and transform the renewable generation from a problem-maker into a problem-solver for the frequency stability challenge reduced inertia. Hence, one of the future works of this research is to incorporate the low-inertia technologies into the scope.

7.2 Future Work

7.2.1 Improve the frequency Dynamics Model with Low-Inertia Technologies

The comprehensiveness of the representation for the frequency dynamic mathematical model proposed in Chapter 3 can be improved by considering the new technologies associated with the low-inertia risk for the future power system. The new technologies include, but are not limited to, the fast frequency response, synthetic inertia, dynamic inertia. Since the frequency indicates the dynamic balance between total generation and demand, the frequency dynamics follow a contingency are determined by the response and inertia. The improvements for the model can be further extended in following directions:

- The fast frequency response is able to provide the additional active power injection before the conventional PFR, which is more helpful in arresting the frequency drop. However, by doing so, the expression of the additional power injection into the system will be non-linear, making the frequency differential equation more complicated. The potential solution to solve the non-linear differential equation is piecewise linearisation for the response expression.

- For the current system, the inertia is assumed constant before and after the contingency, except for the inertia loss from the faulted generator. The new technologies such as the synthetic inertia from wind turbines can support the system inertia temporarily by releasing the kinetic energy in turbine blades. Since the inertia resists all frequency changes, the inertia also slows the frequency increase during the frequency recovery process. Hence, one of the benefits of synthetic

inertia is the inertial response only appears in the frequency arresting period and disappears in the frequency recovery process. Those technologies make the expression for inertia time-dependent, and the differential equation should change accordingly.

7.2.2 Optimal Largest Infeed Generator

To ensure frequency stability, the system should be able to withstand the loss of the largest infeed generator without violating the requirements for the frequency transient dynamics. The PFR and inertia constraints for the reliable system operation are primarily determined by the capacity of the largest infeed generator in the perspective of frequency stability. Regarding the optimisation of the largest infeed generator selection, the following aspects can be analysed:

- For different renewable penetration levels and frequency services upgrades, the maximum generation loss that can be tolerant in the system without violating the requirements transient dynamics can be investigated for future projections. That could potentially provide a guideline for the optimal size of the newly constructed generators.
- For the current system, de-loading the largest infeed generator can reduce the burden for maintaining the frequency stability, thereby reducing the need for PFR and inertia. However, de-loading the generator, especially a nuclear power plant, is against the practical and economical purposes of building the power plant. Hence, the optimal de-loading level for the largest infeed generator could be conducted with a co-optimisation of the energy market including capital cost and the ancillary services market.

7.2.3 Inertia Market Design with Agent Based Modelling

The marginal price of inertia proposed in Chapter 6 is based on the economic meaning of the Lagrange multipliers in the UC optimisation. The price is obtained from the perspective of the system operators, as the system operator is aware of the need for inertia and the availability of each plant to provide inertia, which is a proper way to set the price. The modelling of the inertia market operation is able to investigate the interactions between the power plant and system operators and the influences on the energy market. However, such a system is complicated to simulate as it contains many

components.

The agent-based modelling is a powerful mathematical tool for stochastic analysis in socio-technical systems, such as the energy market and the ancillary services market. The agent-based modelling is able to bring the details of the simulation process into consideration to find out the social actions by defining individual agent interactions and the updating rules [123, 124]. For the operation of the inertia market using agent-based modelling, the agents represent such as the generators, demand side response (DSR) suppliers, the system operator, each agent has a different purpose of the interactions with another agent. The system operator delivers the electricity and ensures the system reliability in an economical manner; the generators and DSR suppliers want to maximise their profits. The decision-making criteria of each agent can be updated to better fit the market needs which will provide a prediction of the operation of the future power system markets.

7.2.4 Inertia Forecasting

By increasing the frequency response reserve, the effect of the reduced inertia can be mitigated to achieve a satisfactory level of frequency stability, which is a major solution to the low-inertia issue in some power systems [118]. Therefore, the inertia forecasting is of great importance which indicates not only the requirements of the frequency response reserve but also the operation of the inertia markets.

The main task of the inertia forecasting is to find the key factors that affect the inertia. The key factors identified within this work are:

- **The system demand**: the demand variations are largely compensated by the traditional fossil-fired power stations, especially gas-fired power station for the case of UK power system. Most of the traditional fossil-fired power stations are synchronously connected to the power grid and are the main contributors to the system inertia. Hence, the inertia profile follows the same pattern as the demand profile.

- **The marginal price of electricity**: due to the cost difference between the renewable generations and the conventional generators, the marginal price for electricity is correlated with the penetration level of the renewable generation. When the renewable generations are being curtailed, the marginal price of electricity will increase which suggests the total system inertia will increase as well.

The accuracy of inertia forecasting is largely determined by the selection of the key factors rather than the prediction method. The inertia forecasting can be implemented through either traditional statistical methods or artificial intelligence based methods. However, due to the indirect and complicated relationship between the system inertia and the influencing factors, artificial intelligence is more advantageous. Classic artificial intelligence based methods, such as artificial neural networks, support vector machine, and fuzzy logic, perform particularly well in many fields like load forecasting and price forecasting. It would be meaningful to explore their application in inertia forecasting.

Appendix

A.1 Three-area Test System in Chapter 2

The three-area test is carried out for the demonstration of the centre of inertia frequency. The system configuration in each area is shown in Figure A-1. The frequency control in all areas is conducted through the ACE, which refers to the combined effect of the frequency response within the area and the tie-line power exchange. Based on the definition, the ACE in each area can be expressed as:

$$ACE_i = \Delta P_{tie,i} + \beta_i \Delta f_i \tag{A.1}$$

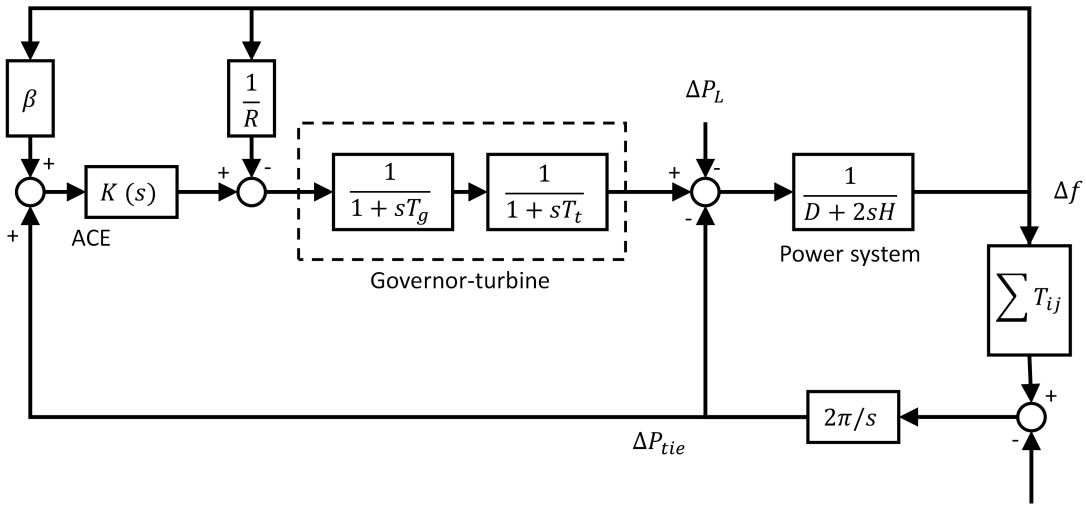

Figure A-1: System configuration for the three-area test [29]

A 0.02 p.u. disturbance of generation loss is applied to Area 1 and 3 at 2 seconds. The system parameters for the test are given in Table A.1 [29]. The results of the frequency

dynamics are shown in Chapter 2 Section 2.2.1.

Table A.1: Parameters for the three-area test system [29]

Area	K (s)	D (p.u./Hz)	H (s)	R (Hz/p.u.)	T_g (s)	T_t (s)	B (p.u./Hz)	T_{ij} (p.u./Hz)
Area 1	-0.3	0.015	0.1667	3	0.08	0.4	0.3483	T_{12}=0.2 T_{13}=0.25
Area 2	-0.2	0.016	0.2017	2.73	0.06	0.44	0.3827	T_{21}=0.20 T_{23}=0.12
Area 3	-0.4	0.015	0.1247	2.82	0.07	0.3	0.3692	T_{31}=0.25 T_{32}=0.12

A2 Solutions to the Differential Equation Set in Chapter 3

Solution to Stage 1

The differential equation for **Stage 1** is shown in equation (A.2):

$$\frac{df_1(t)}{dt} = \frac{-P_{loss} + k_{dfr}[f_n - f_1(t)]}{2H_{sys}} \quad \text{with } f_1(0) = f_0, \text{ for } 0 \leq t < t_1 \tag{A.2}$$

where f_0 is the system frequency prior to the event in p.u., and $f_1(0) = f_0$ is the initial condition of the frequency curve in **Stage 1**.

Since the power loss P_{loss} and the demand frequency ratio k_{dfr} are both non-time related variables, hence, a new function of $g_1(t)$ is formed to simplify the differential equation for **Stage 1**:

$$g_1(t) = f_1(t) - f_n + \frac{P_{loss}}{k_{dfr}} \tag{A.3}$$

Differentiating both sides of equation (A.3) with respect to t yields:

$$\frac{dg_1(t)}{dt} = \frac{df_1(t)}{dt} \tag{A.4}$$

Substituting equation (A.3, A.4) into (A.2) yields:

$$\frac{dg_1(t)}{dt} = \frac{k_{dfr}}{2H_{sys}} g_1(t) \tag{A.5}$$

The solution for function $g_1(t)$ can be obtained through the basic differential equation solutions which is:

$$g_1(t) = c_1 \cdot e^{-\frac{k_{dfr}}{2H_{sys}}t} \tag{A.6}$$

where c_1 is a non-time related constant or polynomial. Applying the initial condition of $f_1(0) = f_0$ to equation (A.6) provides:

$$g_1(0) = f_0 - f_n + \frac{P_{loss}}{k_{dfr}} = c_1 \tag{A.7}$$

The solution to function g_1 is shown as:

$$g_1(t) = (f_0 - f_n + \frac{P_{loss}}{k_{dfr}}) \cdot e^{-\frac{k_{dfr}}{2H_{sys}}t} \tag{A.8}$$

Substituting equation (A.8) into (A.3) can get the frequency expression for **Stage 1**:

$$f_1(t) = \left(f_n - \frac{P_{loss}}{k_{dfr}}\right) + \left(f_0 - f_n + \frac{P_{loss}}{k_{dfr}}\right) \cdot e^{-\frac{k_{dfr}}{2H_{sys}}t} \tag{A.9}$$

Solution to Stage 2

The differential equation for **Stage 2** considers the increase of the frequency response and is shown as:

$$\frac{df_2(t)}{dt} = \frac{-P_{loss} + k_{dfr}[f_n - f_2(t)] + r(t - t_1)}{2H_{sys}}, \text{ for } t_1 \leq t < t_2 \tag{A.10}$$

Differentiating both sides of the equation with respect to t yields:

$$\frac{d^2 f_2(t)}{dt^2} = -\frac{k_{dfr}}{2H_{sys}} \cdot \frac{df_2(t)}{dt} + \frac{r}{2H_{sys}} \tag{A.11}$$

Reorganising equation (A.11) provides a standard form of a second-order ordinary differential equation (ODE):

$$\frac{d^2 f_2(t)}{dt^2} + \frac{k_{dfr}}{2H_{sys}} \cdot \frac{df_2(t)}{dt} = \frac{r}{2H_{sys}} \tag{A.12}$$

Equation (A.12) is an non-homogeneous ODE which indicates the solution consists of a complementary function $f_{2CF}(t)$ and a particular integral $f_{2PI}(t)$ [125, 126].

$$f_2(t) = f_{2CF}(t) + f_{2PI}(t) \tag{A.13}$$

The complementary function is obtained by solving the characteristic equation of the corresponding homogeneous equation, which can be obtained by neglecting $\frac{r}{2H_{sys}}$. Replacing $\frac{d^2 f_2(t)}{dt^2}$ and $\frac{df_2(t)}{dt}$ by ${r_{cs}}^2$ and r_{cs}, respectively, to get the characteristic equation:

$${r_{cs}}^2 + \frac{k_{dfr}}{2H_{sys}} \cdot r_{cs} = 0 \tag{A.14}$$

The two roots of the characteristic equation are:

$$\begin{aligned} r_{cs1} &= 0 \\ r_{cs2} &= -\frac{k_{dfr}}{2H_{sys}} \end{aligned} \tag{A.15}$$

Hence, the complementary function of the second order ODE (3-24) can be written as:

$$\begin{aligned} f_{2CF}(t) =& a_1 e^{r_{cs1}t} + a_2 e^{r_{cs2}t} \\ =& a_1 + a_2 e^{-\frac{k_{dfr}}{2H_{sys}}} \end{aligned} \tag{A.16}$$

where a_1 and a_2 are two random non-time related functions which can be quantified depending on the boundary condition of the second order ODE.

Assuming the particular integral of the second order ODE (A.12) is of the form:

$$f_{2PI}(t) = C_{PI1}t + C_{PI2} \tag{A.17}$$

where C_{PI1} and C_{PI2} are two non-time related coefficients which need to be find.

Substituting the assumed particular integral (A.17) into the second order ODE (A.12) and yields:

$$\begin{aligned} \frac{d^2 f_{2PI}(t)}{dt^2} + \frac{k_{dfr}}{2H_{sys}} \cdot \frac{df_{2PI}(t)}{dt} &= \frac{r}{2H_{sys}} \\ C_{PI1} =& \frac{r}{k_{dfr}} \\ C_{PI2} =& 0 \end{aligned} \tag{A.18}$$

Hence, the particular integral of the second order ODE (3-24) is:

$$f_{2PI}(t) = \frac{r}{k_{dfr}} \cdot t \tag{A.19}$$

And the frequency expression for **Stage 2** is:

$$f_2(t) = a_1 + a_2 e^{-\frac{k_{dfr}}{2H_{sys}}t} + \frac{r}{k_{dfr}} \cdot t \tag{A.20}$$

Considering the continuity of frequency and the ROCOF, the frequency expression boundaries for the second order ODE for **Stage 2** are:

$$\begin{aligned} f_1(t_1) =& f_2(t_2) \\ \frac{df_1(t_1)}{dt_1} =& \frac{df_2(t_2)}{dt_2} \end{aligned} \tag{A.21}$$

Hence,

$$\begin{aligned}\left(f_n - \frac{P_{loss}}{k_{dfr}}\right) + \left(f_0 - f_n + \frac{P_{loss}}{k_{dfr}}\right) \cdot e^{-\frac{k_{dfr}}{2H_{sys}}t_1} =& a_1 + a_2 \cdot e^{-\frac{k_{dfr}}{2H_{sys}}t_1} + \frac{r}{k_{dfr}} \cdot t_1 \\ -\left(f_0 - f_n + \frac{P_{loss}}{k_{dfr}}\right) \cdot \frac{k_{dfr}}{2H_{sys}} \cdot e^{-\frac{k_{dfr}}{2H_{sys}}t_1} =& -a_2 \cdot \frac{k_{dfr}}{2H_{sys}} \cdot e^{-\frac{k_{dfr}}{2H_{sys}}t_1} + \frac{r}{k_{dfr}}\end{aligned} \tag{A.22}$$

To conclude, the second order ODE frequency expression in **Stage 2** is solved with the solution listed below:

$$f_2(t) = a_1 + a_2 \cdot e^{-\frac{k_{dfr}}{2H_{sys}} \cdot t} + \frac{r}{k_{dfr}} \cdot t$$

where,

$$\begin{aligned}&\bullet\ a_1 = (f_n - \frac{P_{loss}}{k_{dfr}}) - \frac{2H_{sys} \cdot r}{{k_{dfr}}^2} - \frac{r \cdot t_1}{k_{dfr}} \\ &\bullet\ a_2 = (f_0 - f_n + \frac{P_{loss}}{k_{dfr}}) + \frac{2H_{sys} \cdot r}{{k_{dfr}}^2} \cdot e^{-\frac{k_{dfr}}{2H_{sys}}t_1}\end{aligned} \tag{A.23}$$

Solution to Stage 3

The PFR is fully applied in *Stage 3*, the differential equation for the frequency expression is listed below:

$$\frac{df_3(t)}{dt} = \frac{-P_{loss} + k_{dfr}[f_n - f_3(t)] + P_{PFR}}{2H_{sys}} \tag{A.24}$$

Reorganise the equation to the standard form:

$$\frac{df_3(t)}{dt} + \frac{k_{dfr}}{2H_{sys}} \cdot f_3(t) = \frac{-P_{loss} + k_{dfr} \cdot f_n + P_{PFR}}{2H_{sys}} \tag{A.25}$$

The corresponding homogeneous equation is obtained by neglecting the right-hand side:

$$\frac{df_3(t)}{dt} + \frac{k_{dfr}}{2H_{sys}} \cdot f_3(t) = 0 \tag{A.26}$$

The solution to the homogeneous equation is:

$$f_3(t) = a_3 \cdot \exp\left(-\int_{t_2}^{t_2+t} \frac{k_{dfr}}{2H_{sys}} dt\right) = a_3 \cdot e^{-\frac{k_{dfr}}{2H_{sys}}t} \tag{A.27}$$

where a_3 is a non-time related function. To find the solution to the non-homogeneous equation, adding another non-time related function a_4 to the solution of the homoge-

neous equation:

$$f_3(t) = a_3 \cdot \exp\left(-\int_{t_2}^{t_2+t} \frac{k_{dfr}}{2H_{sys}} dt\right) = a_3 \cdot e^{-\frac{k_{dfr}}{2H_{sys}}t} + a_4 \tag{A.28}$$

Replacing $f_3(t)$ in the differential equation (A.25) by (A.28) yields:

$$-a_3 \cdot \frac{k_{dfr}}{2H_{sys}} \cdot e^{-\frac{k_{dfr}}{2H_{sys}}t} + \frac{k_{dfr}}{2H_{sys}} \cdot (a_3 \cdot e^{-\frac{k_{dfr}}{2H_{sys}}t} + a_4) = \frac{-P_{loss} + k_{dfr} \cdot f_n + P_{PFR}}{2H_{sys}} \tag{A.29}$$

The polynomial of a_3 can be obtained based on the boundaries between **Stage 2** and **Stage 3**. The boundaries are:

$$\begin{aligned} f_2(t_2) &= f_3(t_2) \\ \frac{df_2(t_2)}{dt_2} &= \frac{df_3(t_2)}{dt_2} \end{aligned} \tag{A.30}$$

Translate the boundary constraints into the frequency expressions get:

$$\begin{aligned} a_1 + a_2 \cdot e^{-\frac{k_{dfr}}{2H_{sys}}t_2} + \frac{r}{k_{dfr}} \cdot t_2 &= a_3 \cdot e^{-\frac{k_{dfr}}{2H_{sys}}t_2} + a_4 \\ -a_2 \cdot \frac{k_{dfr}}{2H_{sys}} \cdot e^{-\frac{k_{dfr}}{2H_{sys}}t_2} + \frac{r}{k_{dfr}} &= -\frac{k_{dfr}}{2H_{sys}} \cdot a_3 \cdot e^{-\frac{k_{dfr}}{2H_{sys}}t_2} \end{aligned} \tag{A.31}$$

Hence, the polynomial of a_3 can be found as:

$$a_3 = \frac{2H_{sys} \cdot r}{{k_{dfr}}^2} \cdot \left(e^{-\frac{k_{dfr}}{2H_{sys}}t_1} - e^{-\frac{k_{dfr}}{2H_{sys}}t_2}\right) + \left(f_0 - f_n + \frac{P_{loss}}{k_{dfr}}\right) \tag{A.32}$$

To conclude, the frequency expression for **Stage 3** is solved and listed below:

$$f_3(t) = a_3 \cdot e^{-\frac{k_{dfr}}{2H_{sys}}t} + a_4$$

where,

- $a_3 = \frac{2H_{sys} \cdot r}{{k_{dfr}}^2} \cdot \left(e^{\frac{k_{dfr} \cdot t_1}{2H_{sys}}} - e^{\frac{k_{dfr} \cdot t_2}{2H_{sys}}}\right) + \left(f_0 - f_n + \frac{P_{loss}}{k_{dfr}}\right)$
- $a_4 = f_n + \frac{P_{PFR} - P_{loss}}{k_{dfr}}$

(A.33)

A3 Results of the Case Study in Chapter 6

Lagrange Multipliers

λ_D				λ_E			λ_{PFR}		
Case 0	Case 1	Case 2	Case 3	Case 1	Case 2	Case 3	Case 1	Case 2	Case 3
30.32	26.78	26.26	24.39	0.083	0.109	0.211	0.077	0.16	0.263
23.28	20.46	19.75	17.35	0.125	0.143	0.253	0.08	0.164	0.267
20.36	17.53	16.82	14.43	0.155	0.166	0.332	0.083	0.167	0.27
18.09	15.26	14.55	7.2	0.181	0.205	0.41	0.084	0.183	0.272
18.77	15.95	15.24	7.63	0.181	0.196	0.388	0.084	0.183	0.272
19.17	16.35	15.63	7.87	0.147	0.192	0.344	0.083	0.181	0.27
30.17	26.63	26.63	24.24	0.072	0.098	0.134	0.07	0.152	0.255
29.94	29.94	29.78	29.79	0.058	0.087	0.105	0.059	0.14	0.243
31.89	31.89	31.62	31.63	0.004	0.058	0.103	0	0.064	0.243
31.98	31.98	31.7	31.72	0.025	0.088	0.102	0	0.125	0.242
32.26	32.26	31.97	31.99	0.025	0.088	0.102	0	0.125	0.242
34.17	33.76	33.77	33.8	0.026	0.09	0.103	0	0.126	0.243
32.92	32.57	32.59	32.62	0.065	0.104	0.114	0.063	0.152	0.27
33.58	33.22	33.22	33.25	0.065	0.104	0.114	0.063	0.152	0.27
32.55	32.23	32.24	32.26	0.068	0.107	0.116	0.065	0.155	0.273
32.76	32.44	32.44	32.47	0.067	0.105	0.115	0.064	0.154	0.272
33.05	32.74	32.71	32.74	0.061	0.1	0.111	0.058	0.148	0.265
33.41	33.42	33.47	33.47	0	0	0.029	0	0	0.024
35.03	35.03	35.03	35.02	0	0	0	0	0	0
35.66	35.6	35.66	35.66	0	0	0	0	0	0
33.13	33.63	33.18	33.26	0	0	0	0	0	0
29.26	29.33	28.18	27.6	0.06	0.09	0.107	0.062	0.143	0.246
24.4	20.86	20.34	18.46	0.113	0.171	0.237	0.071	0.186	0.256
14.35	6.86	6.57	6.08	0.156	0.343	0.361	0.16	0.279	0.267

Generation Outputs (Case 0)

	G1	G2	G3	G4	G5	G6	G7	G8	G9	G10
T1	0	0	0	0	0	0	0	0	0	0
T2	0	0	0	0	0	0	0	0	0	0
T3	0	0	0	0	0	0	0	0	0	0
T4	0	0	0	0	0	0	0	0	0	0
T5	0	0	0	0	0	0	0	0	0	0
T6	0	0	0	0	0	0	0	0	0	0
T7	0	0	0	0	0	0	0	0	0	0
T8	0	0	68.75	62.87	66.87	60.29	77.43	59.08	63.96	67.18
T9	0	0	114.34	104.57	111.22	100.28	128.78	98.27	106.39	111.73
T10	0	0	116.38	106.43	113.21	102.07	131.08	100.02	108.29	113.72
T11	0	0	122.99	112.47	119.63	107.86	138.52	105.7	114.43	120.18
T12	0	0	167.52	153.2	162.95	146.92	188.68	143.97	155.87	163.69
T13	0	0	138.32	126.5	134.55	121.31	155.79	118.88	128.7	135.16
T14	0	0	153.83	140.68	149.63	134.92	173.26	132.21	143.13	150.32
T15	0	0	129.56	118.49	126.03	113.63	145.93	111.35	120.55	126.6
T16	0	0	134.54	123.04	130.87	118	151.53	115.63	125.18	131.47
T17	0	0	141.35	129.27	137.5	123.97	159.21	121.48	131.52	138.12
T18	0	0	151.29	138.36	147.17	132.69	170.4	130.03	140.77	147.84
T19	0	0	187.5	171.48	182.39	164.45	211.19	161.15	174.46	183.22
T20	0	0	202.33	185.04	196.81	177.46	227.89	173.89	188.26	197.71
T21	0	0	146.87	134.32	142.87	128.82	165.43	126.23	136.66	143.52
T22	0	0	52.82	0	51.38	0	59.5	0	55	51.62
T23	0	0	0	0	0	0	0	0	0	0
T24	0	0	0	0	0	0	0	0	0	0

Generation Outputs (Case 0)

	G11	G12	G13	G14	G15	G16	G17	G18	G19
T1	0	0	289.08	304.1	312.71	320.78	308.83	75	22
T2	0	0	186.82	196.53	202.09	207.31	199.58	75	22
T3	0	0	144.3	151.8	156.1	160.13	154.16	75	22
T4	0	0	111.29	117.08	120.39	123.5	118.9	75	22
T5	0	0	121.27	127.58	131.19	134.57	129.56	75	22
T6	0	0	127.05	133.65	137.43	140.98	135.73	75	22
T7	0	0	286.91	301.83	310.37	318.38	306.51	75	22
T8	77.43	0	283.61	298.35	306.8	314.72	302.99	75	22
T9	128.78	0	311.97	328.19	337.48	346.19	333.29	75	22
T10	131.08	0	313.24	329.53	338.85	347.6	334.65	75	22
T11	138.52	0	317.35	333.85	343.3	352.16	339.03	75	22
T12	188.68	0	345.06	362.99	373.27	382.9	368.63	75	22
T13	155.79	0	326.89	343.88	353.62	362.74	349.22	75	22
T14	173.26	0	336.54	354.03	364.05	373.45	359.53	75	22
T15	145.93	0	321.44	338.15	347.72	356.7	343.4	75	22
T16	151.53	0	324.54	341.41	351.07	360.13	346.71	75	22
T17	159.21	0	328.78	345.87	355.66	364.84	351.24	75	22
T18	170.4	107.92	334.96	352.38	362.35	371.7	357.85	75	22
T19	211.19	133.75	357.49	376.07	386.72	396.7	381.91	75	22
T20	227.89	144.33	366.71	385.78	396.7	406.93	391.77	75	22
T21	165.43	104.77	332.21	349.48	359.37	368.65	354.91	75	22
T22	59.5	0	273.7	287.93	296.08	303.72	292.4	75	22
T23	0	0	203.01	213.56	219.61	225.27	216.88	75	22
T24	0	0	57.04	60.01	61.71	63.3	60.94	75	22

Generation Outputs (Case 0)

	G20	G21	G22	G23	G24	G25	G26	G27	G28	G29
T1	660	219	660	625	300	90	120	100	0	0
T2	660	219	660	625	300	90	120	100	0	0
T3	660	219	660	625	300	90	120	100	0	0
T4	660	219	660	625	300	90	120	100	116.67	52
T5	660	219	660	625	300	90	120	100	175	78
T6	660	219	660	625	300	90	120	100	233.33	104
T7	660	219	660	625	300	90	120	100	291.67	130
T8	660	219	660	625	300	90	120	100	350	156
T9	660	219	660	625	300	90	120	100	408.33	182
T10	660	219	660	625	300	90	120	100	408.33	182
T11	660	219	660	625	300	90	120	100	408.33	182
T12	660	219	660	625	300	90	120	100	116.67	52
T13	660	219	660	625	300	90	120	100	408.33	182
T14	660	219	660	625	300	90	120	100	408.33	182
T15	660	219	660	625	300	90	120	100	408.33	182
T16	660	219	660	625	300	90	120	100	408.33	182
T17	660	219	660	625	300	90	120	100	525	234
T18	660	219	660	625	300	90	120	100	525	234
T19	660	219	660	625	300	90	120	100	525	234
T20	660	219	660	625	300	90	120	100	291.67	130
T21	660	219	660	625	300	90	120	100	233.33	104
T22	660	219	660	625	300	90	120	100	408.33	182
T23	660	219	660	625	300	90	120	100	408.33	182
T24	660	219	660	625	300	90	120	100	350	156

Generation Outputs (Case 0)

	G30	G31	G32	G33	G34	G35	G36	G37	G38
T1	0	132	119.17	82.5	287.83	172.67	74.67	40	44.67
T2	0	144	130	90	261.67	296	128	60	67
T3	0	132	119.17	82.5	235.5	296	128	80	89.33
T4	46	72	65	45	183.17	296	128	120	134
T5	69	84	75.83	52.5	183.17	222	96	80	89.33
T6	92	60	54.17	37.5	235.5	98.67	42.67	140	156.33
T7	115	72	65	45	157	98.67	42.67	240	268
T8	138	108	97.5	67.5	261.67	148	64	240	268
T9	161	108	97.5	67.5	287.83	172.67	74.67	240	268
T10	161	60	54.17	37.5	287.83	296	128	240	268
T11	161	60	54.17	37.5	314	222	96	240	268
T12	46	36	32.5	22.5	314	296	128	180	201
T13	161	12	10.83	7.5	261.67	246.67	106.67	180	201
T14	161	0	0	0	287.83	296	128	60	67
T15	161	36	32.5	22.5	287.83	296	128	80	89.33
T16	161	0	0	0	314	296	128	120	134
T17	207	24	21.67	15	314	296	128	140	156.33
T18	207	0	0	0	314	296	128	100	111.67
T19	207	0	0	0	314	0	0	80	89.33
T20	115	12	10.83	7.5	287.83	0	0	40	44.67
T21	92	12	10.83	7.5	314	246.67	106.67	60	67
T22	161	12	10.83	7.5	314	296	128	220	245.67
T23	161	12	10.83	7.5	261.67	296	128	200	223.33
T24	138	24	21.67	15	314	296	128	200	223.33

Generation Outputs (Case 1)

	G1	G2	G3	G4	G5	G6	G7	G8	G9	G10
T1	0	0	0	0	45	40	48	45	55	0
T2	0	0	0	0	45	40	48	45	0	0
T3	0	0	0	0	45	40	48	45	0	0
T4	0	0	0	0	45	40	48	45	0	0
T5	0	0	0	0	45	40	48	45	0	0
T6	0	0	0	0	45	40	48	45	0	0
T7	0	0	0	0	45	40	48	45	55	0
T8	0	0	68.75	62.87	66.87	60.29	77.43	59.08	63.96	67.18
T9	0	0	114.34	104.57	111.22	100.28	128.78	98.27	106.39	111.73
T10	0	0	116.38	106.43	113.21	102.07	131.08	100.02	108.29	113.72
T11	0	0	122.99	112.47	119.63	107.86	138.52	105.7	114.43	120.18
T12	0	0	158.49	144.95	154.17	139.01	178.51	136.21	147.47	154.87
T13	0	0	131.12	119.92	127.55	115	147.69	112.69	122	128.13
T14	0	0	145.26	132.84	141.3	127.4	163.61	124.84	135.15	141.94
T15	0	0	122.38	111.92	119.04	107.33	137.84	105.18	113.87	119.59
T16	0	0	127.04	116.18	123.58	111.42	143.09	109.19	118.21	124.14
T17	0	0	132.97	121.6	129.34	116.62	149.77	114.28	123.72	129.93
T18	0	0	152.11	139.11	147.96	133.41	171.33	130.73	141.53	148.64
T19	0	0	187.5	171.48	182.39	164.45	211.19	161.15	174.46	183.22
T20	0	0	203.62	186.22	198.07	178.59	229.35	175	189.46	198.98
T21	0	0	154.99	141.74	150.76	135.93	174.56	133.2	144.21	151.45
T22	0	0	0	0	52.88	47.68	61.23	46.72	55	0
T23	0	0	0	0	45	40	48	45	55	0
T24	0	0	0	0	45	40	48	45	55	0

Generation Outputs (Case 1)

	G11	G12	G13	G14	G15	G16	G17	G18	G19
T1	40	0	237.68	250.04	257.11	263.75	253.92	75	22
T2	40	0	145.78	153.36	157.7	161.77	155.74	75	22
T3	40	0	103.26	108.63	111.7	114.59	110.32	75	22
T4	40	0	70.25	73.91	76	77.96	75.05	75	22
T5	40	0	80.23	84.4	86.79	89.03	85.71	75	22
T6	40	0	86	90.48	93.04	95.44	91.88	75	22
T7	40	0	235.52	247.76	254.77	261.35	251.61	75	22
T8	77.43	0	283.61	298.35	306.8	314.72	302.99	75	22
T9	128.78	0	311.97	328.19	337.48	346.19	333.29	75	22
T10	131.08	0	313.24	329.53	338.85	347.6	334.65	75	22
T11	138.52	0	317.35	333.85	343.3	352.16	339.03	75	22
T12	178.51	113.06	339.44	357.09	367.19	376.67	362.63	75	22
T13	147.69	93.54	322.41	339.18	348.78	357.78	344.44	75	22
T14	163.61	103.62	331.21	348.43	358.29	367.53	353.84	75	22
T15	137.84	87.3	316.97	333.45	342.89	351.74	338.63	75	22
T16	143.09	90.62	319.88	336.51	346.03	354.96	341.73	75	22
T17	149.77	94.85	323.56	340.38	350.02	359.05	345.67	75	22
T18	171.33	108.51	335.47	352.91	362.9	372.27	358.39	75	22
T19	211.19	133.75	357.49	376.07	386.72	396.7	381.91	75	22
T20	229.35	145.25	367.52	386.62	397.57	407.82	392.63	75	22
T21	174.56	0	337.26	354.79	364.83	374.25	360.3	75	22
T22	61.23	0	274.66	288.94	297.12	304.79	293.43	75	22
T23	40	0	151.61	159.5	164.01	168.24	161.97	75	22
T24	40	0	0	45	40	48	50	75	22

Generation Outputs (Case 1)

	G20	G21	G22	G23	G24	G25	G26	G27	G28	G29
T1	660	219	660	625	300	90	120	100	0	0
T2	660	219	660	625	300	90	120	100	0	0
T3	660	219	660	625	300	90	120	100	0	0
T4	660	219	660	625	300	90	120	100	116.67	52
T5	660	219	660	625	300	90	120	100	175	78
T6	660	219	660	625	300	90	120	100	233.33	104
T7	660	219	660	625	300	90	120	100	291.67	130
T8	660	219	660	625	300	90	120	100	350	156
T9	660	219	660	625	300	90	120	100	408.33	182
T10	660	219	660	625	300	90	120	100	408.33	182
T11	660	219	660	625	300	90	120	100	408.33	182
T12	660	219	660	625	300	90	120	100	116.67	52
T13	660	219	660	625	300	90	120	100	408.33	182
T14	660	219	660	625	300	90	120	100	408.33	182
T15	660	219	660	625	300	90	120	100	408.33	182
T16	660	219	660	625	300	90	120	100	408.33	182
T17	660	219	660	625	300	90	120	100	525	234
T18	660	219	660	625	300	90	120	100	525	234
T19	660	219	660	625	300	90	120	100	525	234
T20	660	219	660	625	300	90	120	100	291.67	130
T21	660	219	660	625	300	90	120	100	233.33	104
T22	660	219	660	625	300	90	120	100	408.33	182
T23	660	219	660	625	300	90	120	100	408.33	182
T24	660	219	650.15	487.61	300	90	120	100	350	156

Generation Outputs (Case 1)

	G30	G31	G32	G33	G34	G35	G36	G37	G38
T1	0	132	119.17	82.5	287.83	172.67	74.67	40	44.67
T2	0	144	130	90	261.67	296	128	60	67
T3	0	132	119.17	82.5	235.5	296	128	80	89.33
T4	46	72	65	45	183.17	296	128	120	134
T5	69	84	75.83	52.5	183.17	222	96	80	89.33
T6	92	60	54.17	37.5	235.5	98.67	42.67	140	156.33
T7	115	72	65	45	157	98.67	42.67	240	268
T8	138	108	97.5	67.5	261.67	148	64	240	268
T9	161	108	97.5	67.5	287.83	172.67	74.67	240	268
T10	161	60	54.17	37.5	287.83	296	128	240	268
T11	161	60	54.17	37.5	314	222	96	240	268
T12	46	36	32.5	22.5	314	296	128	180	201
T13	161	12	10.83	7.5	261.67	246.67	106.67	180	201
T14	161	0	0	0	287.83	296	128	60	67
T15	161	36	32.5	22.5	287.83	296	128	80	89.33
T16	161	0	0	0	314	296	128	120	134
T17	207	24	21.67	15	314	296	128	140	156.33
T18	207	0	0	0	314	296	128	100	111.67
T19	207	0	0	0	314	0	0	80	89.33
T20	115	12	10.83	7.5	287.83	0	0	40	44.67
T21	92	12	10.83	7.5	314	246.67	106.67	60	67
T22	161	12	10.83	7.5	314	296	128	220	245.67
T23	161	12	10.83	7.5	261.67	296	128	200	223.33
T24	138	24	21.67	15	314	296	128	200	223.33

Generation Outputs (Case 2)

	G1	G2	G3	G4	G5	G6	G7	G8	G9	G10
T1	0	0	0	0	45	40	48	45	55	0
T2	0	0	0	0	45	40	48	45	55	0
T3	0	0	0	0	45	40	48	45	55	0
T4	0	0	0	0	45	40	48	45	55	0
T5	0	0	0	0	45	40	48	45	55	0
T6	0	0	0	0	45	40	48	45	55	0
T7	0	0	0	0	45	40	48	45	55	0
T8	0	0	64.92	59.37	63.15	56.93	73.12	55.79	60.4	63.43
T9	0	0	107.97	98.74	105.03	94.7	121.61	92.79	100.46	105.51
T10	0	0	109.9	100.5	106.9	96.38	123.78	94.45	102.25	107.39
T11	0	0	116.13	106.21	112.97	101.85	130.8	99.81	108.05	113.48
T12	0	0	158.18	144.66	153.87	138.74	178.17	135.95	147.18	154.57
T13	0	0	130.61	119.45	127.05	114.55	147.11	112.25	121.52	127.63
T14	0	0	145.26	132.84	141.3	127.4	163.6	124.84	135.15	141.94
T15	0	0	122.34	111.89	119.01	107.3	137.8	105.15	113.83	119.55
T16	0	0	127.04	116.18	123.58	111.42	143.09	109.19	118.21	124.14
T17	0	0	133.47	122.07	129.83	117.06	150.33	114.71	124.19	130.43
T18	0	0	151.08	138.16	146.96	132.5	170.16	129.84	140.57	147.63
T19	0	0	187.5	171.48	182.39	164.45	211.19	161.15	174.46	183.22
T20	0	0	202.33	185.04	196.81	177.46	227.89	173.89	188.26	197.71
T21	0	0	148.18	135.52	144.14	129.96	166.9	127.35	137.87	144.8
T22	0	0	50	50	45	40	48	45	55	0
T23	0	0	0	0	45	40	48	45	55	0
T24	0	0	0	0	45	40	48	45	55	0

Generation Outputs (Case 2)

	G11	G12	G13	G14	G15	G16	G17	G18	G19
T1	40	40	230.15	242.12	248.97	255.39	245.87	75	22
T2	40	0	135.42	142.46	146.5	150.28	144.68	75	22
T3	40	0	92.91	97.74	100.5	103.1	99.25	75	22
T4	40	0	59.9	63.01	64.8	66.47	63.99	75	22
T5	40	0	69.88	73.51	75.59	77.54	74.65	75	22
T6	40	0	75.65	79.58	81.84	83.95	80.82	75	22
T7	40	0	235.52	247.76	254.77	261.35	251.61	75	22
T8	73.12	46.31	281.23	295.85	304.22	312.07	300.44	75	22
T9	121.61	77.02	308.01	324.02	333.19	341.79	329.05	75	22
T10	123.78	78.39	309.21	325.28	334.49	343.12	330.34	75	22
T11	130.8	82.84	313.09	329.37	338.69	347.43	334.48	75	22
T12	178.17	112.84	339.25	356.89	366.99	376.46	362.43	75	22
T13	147.11	93.17	322.09	338.84	348.43	357.42	344.1	75	22
T14	163.6	103.62	331.21	348.42	358.29	367.53	353.84	75	22
T15	137.8	87.27	316.95	333.43	342.87	351.71	338.61	75	22
T16	143.09	90.62	319.88	336.51	346.03	354.96	341.73	75	22
T17	150.33	95.21	323.88	340.71	350.36	359.4	346	75	22
T18	170.16	107.77	334.83	352.23	362.2	371.55	357.7	75	22
T19	211.19	133.75	357.49	376.07	386.72	396.7	381.91	75	22
T20	227.89	144.33	366.71	385.78	396.7	406.93	391.77	75	22
T21	166.9	105.7	333.03	350.34	360.25	369.55	355.78	75	22
T22	40	40	258.04	271.46	279.14	286.35	275.67	75	22
T23	40	40	144.08	151.57	155.86	159.89	153.93	75	22
T24	40	40	50	45	40	48	50	75	22

Generation Outputs (Case 2)

	G20	G21	G22	G23	G24	G25	G26	G27	G28	G29
T1	660	219	660	625	300	90	120	100	0	0
T2	660	219	660	625	300	90	120	100	0	0
T3	660	219	660	625	300	90	120	100	0	0
T4	660	219	660	625	300	90	120	100	116.67	52
T5	660	219	660	625	300	90	120	100	175	78
T6	660	219	660	625	300	90	120	100	233.33	104
T7	660	219	660	625	300	90	120	100	291.67	130
T8	660	219	660	625	300	90	120	100	350	156
T9	660	219	660	625	300	90	120	100	408.33	182
T10	660	219	660	625	300	90	120	100	408.33	182
T11	660	219	660	625	300	90	120	100	408.33	182
T12	660	219	660	625	300	90	120	100	116.67	52
T13	660	219	660	625	300	90	120	100	408.33	182
T14	660	219	660	625	300	90	120	100	408.33	182
T15	660	219	660	625	300	90	120	100	408.33	182
T16	660	219	660	625	300	90	120	100	408.33	182
T17	660	219	660	625	300	90	120	100	525	234
T18	660	219	660	625	300	90	120	100	525	234
T19	660	219	660	625	300	90	120	100	525	234
T20	660	219	660	625	300	90	120	100	291.67	130
T21	660	219	660	625	300	90	120	100	233.33	104
T22	660	219	660	625	300	90	120	100	408.33	182
T23	660	219	660	625	300	90	120	100	408.33	182
T24	660	219	595.43	446.57	300	90	120	100	350	156

Generation Outputs (Case 2)

	G30	G31	G32	G33	G34	G35	G36	G37	G38
T1	0	132	119.17	82.5	287.83	172.67	74.67	40	44.67
T2	0	144	130	90	261.67	296	128	60	67
T3	0	132	119.17	82.5	235.5	296	128	80	89.33
T4	46	72	65	45	183.17	296	128	120	134
T5	69	84	75.83	52.5	183.17	222	96	80	89.33
T6	92	60	54.17	37.5	235.5	98.67	42.67	140	156.33
T7	115	72	65	45	157	98.67	42.67	240	268
T8	138	108	97.5	67.5	261.67	148	64	240	268
T9	161	108	97.5	67.5	287.83	172.67	74.67	240	268
T10	161	60	54.17	37.5	287.83	296	128	240	268
T11	161	60	54.17	37.5	314	222	96	240	268
T12	46	36	32.5	22.5	314	296	128	180	201
T13	161	12	10.83	7.5	261.67	246.67	106.67	180	201
T14	161	0	0	0	287.83	296	128	60	67
T15	161	36	32.5	22.5	287.83	296	128	80	89.33
T16	161	0	0	0	314	296	128	120	134
T17	207	24	21.67	15	314	296	128	140	156.33
T18	207	0	0	0	314	296	128	100	111.67
T19	207	0	0	0	314	0	0	80	89.33
T20	115	12	10.83	7.5	287.83	0	0	40	44.67
T21	92	12	10.83	7.5	314	246.67	106.67	60	67
T22	161	12	10.83	7.5	314	296	128	220	245.67
T23	161	12	10.83	7.5	261.67	296	128	200	223.33
T24	138	24	21.67	15	314	296	128	200	223.33

Generation Outputs (Case 3)

	G1	G2	G3	G4	G5	G6	G7	G8	G9	G10
T1	0	0	50	50	45	40	48	45	55	45
T2	0	0	50	50	45	40	48	45	55	45
T3	0	0	50	50	45	40	48	45	55	45
T4	0	0	50	50	45	40	48	45	55	45
T5	0	0	50	50	45	40	48	45	55	45
T6	0	0	50	50	45	40	48	45	55	45
T7	0	0	50	50	45	40	48	45	55	45
T8	0	0	64.72	59.19	62.95	56.76	72.89	55.62	60.21	63.24
T9	0	0	107.63	98.43	104.69	94.39	121.22	92.5	100.14	105.17
T10	0	0	109.46	100.11	106.48	96	123.29	94.08	101.85	106.96
T11	0	0	115.66	105.77	112.5	101.44	130.27	99.4	107.61	113.02
T12	0	0	157.33	143.89	153.04	137.99	177.21	135.22	146.39	153.74
T13	0	0	129.87	118.77	126.33	113.9	146.28	111.62	120.84	126.91
T14	0	0	144.42	132.08	140.48	126.67	162.66	124.12	134.38	141.12
T15	0	0	121.58	111.19	118.27	106.63	136.94	104.49	113.12	118.81
T16	0	0	126.28	115.48	122.83	110.75	142.23	108.53	117.49	123.39
T17	0	0	132.69	121.35	129.07	116.38	149.45	114.04	123.46	129.66
T18	0	0	150.89	137.99	146.77	132.33	169.95	129.68	140.39	147.44
T19	0	0	187.52	171.49	182.4	164.46	211.2	161.16	174.47	183.24
T20	0	0	202.29	185	196.77	177.42	227.84	173.86	188.22	197.67
T21	0	0	146.35	133.84	142.36	128.36	164.84	125.78	136.17	143.01
T22	0	0	50	50	45	40	48	45	55	45
T23	0	0	50	50	45	40	48	45	55	45
T24	0	0	50	50	45	40	48	45	55	45

Generation Outputs (Case 3)

	G11	G12	G13	G14	G15	G16	G17	G18	G19
T1	40	40	202.85	213.4	219.44	225.1	216.71	75	22
T2	40	40	100.59	105.82	108.82	111.63	107.47	75	22
T3	40	40	58.08	61.1	62.83	64.45	62.05	75	22
T4	40	40	50	45	40	48	50	75	22
T5	40	40	50	45	40	48	50	75	22
T6	40	40	50	45	40	48	50	75	22
T7	40	40	200.69	211.12	217.1	222.7	214.4	75	22
T8	72.89	46.16	281.1	295.72	304.09	311.93	300.31	75	22
T9	121.22	76.77	307.8	323.8	332.96	341.55	328.83	75	22
T10	123.29	78.08	308.94	325	334.2	342.82	330.05	75	22
T11	130.27	82.5	312.79	329.05	338.37	347.1	334.16	75	22
T12	177.21	112.23	338.72	356.33	366.41	375.87	361.86	75	22
T13	146.28	92.64	321.64	338.36	347.93	356.91	343.61	75	22
T14	162.66	103.02	330.69	347.88	357.72	366.96	353.28	75	22
T15	136.94	86.73	316.48	332.93	342.35	351.19	338.1	75	22
T16	142.23	90.08	319.4	336	345.51	354.43	341.22	75	22
T17	149.45	94.65	323.39	340.2	349.83	358.86	345.48	75	22
T18	169.95	107.63	334.71	352.11	362.07	371.42	357.58	75	22
T19	211.2	133.76	357.5	376.08	386.72	396.7	381.92	75	22
T20	227.84	144.3	366.69	385.75	396.67	406.9	391.74	75	22
T21	164.84	104.4	331.89	349.14	359.02	368.29	354.56	75	22
T22	40	40	249.57	262.55	269.98	276.94	266.62	75	22
T23	40	40	116.79	122.86	126.33	129.59	124.76	75	22
T24	40	40	50	45	40	48	50	75	22

Generation Outputs (Case 3)

	G20	G21	G22	G23	G24	G25	G26	G27	G28	G29
T1	660	219	660	625	300	90	120	100	0	0
T2	660	219	660	625	300	90	120	100	0	0
T3	660	219	660	625	300	90	120	100	0	0
T4	660	219	660	525.17	300	90	120	100	116.67	52
T5	660	219	660	578.17	300	90	120	100	175	78
T6	660	219	660	608.83	300	90	120	100	233.33	104
T7	660	219	660	625	300	90	120	100	291.67	130
T8	660	219	660	625	300	90	120	100	350	156
T9	660	219	660	625	300	90	120	100	408.33	182
T10	660	219	660	625	300	90	120	100	408.33	182
T11	660	219	660	625	300	90	120	100	408.33	182
T12	660	219	660	625	300	90	120	100	116.67	52
T13	660	219	660	625	300	90	120	100	408.33	182
T14	660	219	660	625	300	90	120	100	408.33	182
T15	660	219	660	625	300	90	120	100	408.33	182
T16	660	219	660	625	300	90	120	100	408.33	182
T17	660	219	660	625	300	90	120	100	525	234
T18	660	219	660	625	300	90	120	100	525	234
T19	660	219	660	625	300	90	120	100	525	234
T20	660	219	660	625	300	90	120	100	291.67	130
T21	660	219	660	625	300	90	120	100	233.33	104
T22	660	219	660	625	300	90	120	100	408.33	182
T23	660	219	660	625	300	90	120	100	408.33	182
T24	660	219	512.57	384.43	300	90	120	100	350	156

Generation Outputs (Case 3)

	G30	G31	G32	G33	G34	G35	G36	G37	G38
T1	0	132	119.17	82.5	287.83	172.67	74.67	40	44.67
T2	0	144	130	90	261.67	296	128	60	67
T3	0	132	119.17	82.5	235.5	296	128	80	89.33
T4	46	72	65	45	183.17	296	128	120	134
T5	69	84	75.83	52.5	183.17	222	96	80	89.33
T6	92	60	54.17	37.5	235.5	98.67	42.67	140	156.33
T7	115	72	65	45	157	98.67	42.67	240	268
T8	138	108	97.5	67.5	261.67	148	64	240	268
T9	161	108	97.5	67.5	287.83	172.67	74.67	240	268
T10	161	60	54.17	37.5	287.83	296	128	240	268
T11	161	60	54.17	37.5	314	222	96	240	268
T12	46	36	32.5	22.5	314	296	128	180	201
T13	161	12	10.83	7.5	261.67	246.67	106.67	180	201
T14	161	0	0	0	287.83	296	128	60	67
T15	161	36	32.5	22.5	287.83	296	128	80	89.33
T16	161	0	0	0	314	296	128	120	134
T17	207	24	21.67	15	314	296	128	140	156.33
T18	207	0	0	0	314	296	128	100	111.67
T19	207	0	0	0	314	0	0	80	89.33
T20	115	12	10.83	7.5	287.83	0	0	40	44.67
T21	92	12	10.83	7.5	314	246.67	106.67	60	67
T22	161	12	10.83	7.5	314	296	128	220	245.67
T23	161	12	10.83	7.5	261.67	296	128	200	223.33
T24	138	24	21.67	15	314	296	128	200	223.33

Publications

Journal Publications

Bian, Y., Wyman-Pain, H., Li, F., Bhakar, R., Mishra, S., & Padhy, N. P. (2018). Demand Side Contributions for System Inertia in the GB Power System. *IEEE Transactions on Power Systems*, 33(4), 3521-3530.

Wyman-Pain, H., Bian, Y., Thomas, C., & Li, F. (2018). The economics of different generation technologies for frequency response provision. *Applied Energy*, 222, 554-563.

Journal Under Review

Bian, Y., Zhang, Z., & Li, F. Inertia-Dependent Frequency-related Constraints for the System Operation Planning. *IEEE Transactions on Power Systems.* (Under review)

Bian, Y., Wyman-Pain, H., & Li, F. Pricing for System Inertia Base on the Equivalent Primary Frequency Response. *IEEE Transactions on Power Systems.* (Under review)

Conference Publications

Bian, Y., Wang, H., Wyman-Pain, H., Xu, M., & Li, F. (2017, November). Availability of CHPs to provide primary frequency response in the great Britain power system. In *Energy Internet and Energy System Integration (EI2), 2017 IEEE Conference on* (pp. 1-6). IEEE.

Bian, Y., Wang, H., Wyman-Pain, H., Gu, C., & Li, F. (2017). Frequency Response in the GB Power System from Responsive CHPs. *Energy Procedia*, 105, 2302-2309.

Wyman-Pain, H., Bian, Y., Williams, S., Xu, M., & Li, F. (2017, July). An assessment of energy deficits in the future electricity system of the United Kingdom with a significant penetration of intermittent renewable generators. In *Power & Energy Society General Meeting, 2017 IEEE* (pp. 1-5). IEEE.

Wyman-Pain, H., Thomas, C., Bian, Y., & Li, F. (2017). An economic analysis of part loading generators with a focus on the provision of frequency response. *Energy Procedia*, 142, 2580-2585.

References

[1] Prabha Kundur, Neal Balu, and Mark Lauby. *Power System Stability and Control*, volume 7. McGraw-Hill New York, 1994.

[2] Colin Bayliss and Brian Hardy. *Transmission and Distribution electrical engineering*. Elsevier, 2012.

[3] National Grid. Historic Frequency Data [Online]. Available: `https://www.nationalgrid.com/uk/electricity/balancing-services/frequency-response-services/historic-frequency-data`. Accessed September 5, 2018.

[4] National Grid. System Operability Framework 2014 [Online]. Available: `https://www.nationalgrid.com/sites/default/files/documents/35435-SOF%202014%20Final.pdf`. Accessed August 15, 2015.

[5] National Grid. System Operability Framework 2015 [Online]. Available: `https://www.nationalgrid.com/sites/default/files/documents/44046-SOF%202015%20Full%20Document.pdf`. Accessed August 15, 2016.

[6] Met Office. An overview of global surface temperatures in 2017 [Online]. Available: `https://www.metoffice.gov.uk/research/news/2018/global-surface-temperatures-in-2017`. Accessed June 25, 2018.

[7] United Nations Framework Convention on Climate Change (UNFCCC). Kyoto Protocol to the United Nations Framework Convention on Climate Change [Online]. Available: `https://unfccc.int/sites/default/files/kpeng.pdf`. Accessed June 25, 2018.

[8] International Energy Agency (IEA). World Energy Outlook 2016 [Online]. Available: `https://webstore.iea.org/download/direct/202?fileName=WEO2016.pdf`. Accessed June 25, 2018.

[9] European Commission. The 2020 Climate and Energy Package [Online]. Available: https://ec.europa.eu/clima/policies/strategies/2020_en. Accessed June 25, 2018.

[10] Department for Business, Energy & Industrial Strategy. Climate Change Act 2008 [Online]. Available: https://www.legislation.gov.uk/ukpga/2008/27/pdfs/ukpga_20080027_en.pdf. Accessed June 25, 2018.

[11] International Energy Agency (IEA). CO2 Emissions from Fuel Combustion Highlights 2017 [Online]. Available: https://www.iea.org/publications/freepublications/publication/CO2EmissionsfromFuelCombustionHighlights2017.pdf. Accessed June 25, 2018.

[12] Department for Business, Energy & Industrial Strategy. Digest of United Kingdom Energy Statistics 2011 [online]. Available: http://webarchive.nationalarchives.gov.uk/20120403141252/https://www.decc.gov.uk/assets/decc/11/stats/publications/dukes/2312-dukes-2011--full-document-excluding-cover-pages.pdf. Accessed June 25, 2018.

[13] Department for Business, Energy & Industrial Strategy. Digest of United Kingdom Energy Statistics 2018 [online]. Available: http://webarchive.nationalarchives.gov.uk/20120403141252/https://www.decc.gov.uk/assets/decc/11/stats/publications/dukes/2312-dukes-2011--full-document-excluding-cover-pages.pdf. Accessed July 30, 2018.

[14] Ronan Doherty, Alan Mullane, Gillian Nolan, Daniel J. Burke, Alexander Bryson, and Mark O'Malley. An assessment of the impact of wind generation on system frequency control. *IEEE Transactions on Power Systems*, 25(1):452–460, 2010.

[15] Janaka Ekanayake and Nick Jenkins. Comparison of the response of doubly fed and fixed-speed induction generator wind turbines to changes in network frequency. *IEEE Transactions on Energy Conversion*, 19(4):800–802, 2004.

[16] Rogério G. de Almeida and J. A. Peças Lopes. Participation of doubly fed induction wind generators in system frequency regulation. *IEEE Transactions on Power Systems*, 22(3):944–950, 2007.

[17] Francesco Baccino, Francesco Conte, Samuele Grillo, Stefano Massucco, and Federico Silvestro. An optimal model-based control technique to improve wind farm

participation to frequency regulation. *IEEE Transactions on Sustainable Energy*, 6(3):993–1003, 2015.

[18] Claudia Rahmann and Alfredo Castillo. Fast frequency response capability of photovoltaic power plants: The necessity of new grid requirements and definitions. *Energies*, 7(10):6306–6322, 2014.

[19] C. Rahmann, V. Vittal, J. Ascui, and J. Haas. Mitigation control against partial shading effects in large-scale pv power plants. *IEEE Transactions on Sustainable Energy*, 7(1):173–180, 2016.

[20] National Grid. Security and Quality of Supply Standards [Online]. Available: `http://www2.nationalgrid.com/UK/Industry-information/Electricity-codes/SQSS/The-SQSS/`. Accessed February 5, 2016.

[21] Johan Morren, Sjoerd W. H. de Haan, Wil L. Kling, and J. A. Ferreira. Wind turbines emulating inertia and supporting primary frequency control. *IEEE Transactions on Power Systems*, 21(1):433–434, 2006.

[22] Inmaculada Martinez Sanz, Balarko Chaudhuri, and Goran Strbac. Inertial response from offshore wind farms connected through dc grids. *IEEE Transactions on Power Systems*, 30(3):1518–1527, 2015.

[23] Yi Wang, Jianhui Meng, Xiangyu Zhang, and Lie Xu. Control of pmsg-based wind turbines for system inertial response and power oscillation damping. *IEEE Transactions on Sustainable Energy*, 6(2):565–574, 2015.

[24] Toshio Inoue, Haruhito Taniguchi, Yasuyuki Ikeguchi, and Kiyoshi Yoshida. Estimation of power system inertia constant and capacity of spinning-reserve support generators using measured frequency transients. *IEEE Transactions on Power Systems*, 12(1):136–143, 1997.

[25] D. R. Bobo, D. M. Mauzy, and F. J. Trefny. Economic generation dispatch with responsive spinning reserve constraints. In *Power Industry Computer Application Conference, 1993. Conference Proceedings*, pages 299–303. IEEE, 1993.

[26] José F. Restrepo and Francisco D. Galiana. Unit commitment with primary frequency regulation constraints. *IEEE Transactions on Power Systems*, 20(4):1836–1842, 2005.

[27] Ronan Doherty, Gillian Lalor, and Mark O'Malley. Frequency control in competitive electricity market dispatch. *IEEE Transactions on Power Systems*, 20(3):1588–1596, 2005.

[28] Prabha Kundur, John Paserba, Venkat Ajjarapu, Göran Andersson, Anjan Bose, Claudio Canizares, Nikos Hatziargyriou, David Hill, Alex Stankovic, and Carson Taylor. Definition and classification of power system stability. *IEEE Transactions on Power Systems*, 19(2):1387–1401, 2004.

[29] Hassan Bevrani. *Robust power system frequency control*, volume 85. Springer, 2009.

[30] Paul M. Anderson and Aziz A. Fouad. *Power system control and stability*. John Wiley & Sons, 2008.

[31] Mustafa Kayikçi and Jovica V. Milanovic. Dynamic contribution of DFIG-based wind plants to system frequency disturbances. *IEEE Transactions on Power Systems*, 24(2):859–867, 2009.

[32] James S. Thorp, Charles E. Seyler, and Arun G. Phadke. Electromechanical wave propagation in large electric power systems. *IEEE Transactions on Circuits and Systems I: Fundamental Theory and Applications*, 45(6):614–622, 1998.

[33] Vladimir Terzija. Adaptive underfrequency load shedding based on the magnitude of the disturbance estimation. *IEEE Transactions on Power Systems*, 21(3):1260–1266, 2006.

[34] Shu-Jen Tsai, Li Zhang, Arun G Phadke, Yilu Liu, Michael R Ingram, Sandra C Bell, Ian S Grant, Dale T Bradshaw, David Lubkeman, and Le Tang. Frequency sensitivity and electromechanical propagation simulation study in large power systems. *IEEE Transactions on Circuits and Systems I: Regular Papers*, 54(8):1819–1828, 2007.

[35] Tianya Li, Gerard Ledwich, Yateendra Mishra, Joe H. Chow, and Arash Vahidnia. Wave aspect of power system transient stability—Part I: Finite approximation. *IEEE Transactions on Power Systems*, 32(4):2493–2500, 2017.

[36] Kamalanath Samarakoon, Janaka Ekanayake, and Nick Jenkins. Investigation of domestic load control to provide primary frequency response using smart meters. *IEEE Transactions on Smart Grid*, 3(1):282–292, 2012.

[37] Meng Cheng, Jianzhong Wu, Stephen J. Galsworthy, Carlos E. Ugalde-Loo, Nikola Gargov, William W. Hung, and Nick Jenkins. Power system frequency response from the control of bitumen tanks. *IEEE Transactions on Power Systems*, 31(3):1769–1778, 2016.

[38] Tharangika Bambaravanage, Asanka Rodrigo, and Sisil Kumarawadu. *Modeling, Simulation, and Control of a Medium-Scale Power System*. Springer, 2018.

[39] Karel De Brabandere, Bruno Bolsens, Jeroen Van den Keybus, Achim Woyte, Johan Driesen, and Ronnie Belmans. A voltage and frequency droop control method for parallel inverters. *IEEE Transactions on Power Electronics*, 22(4):1107–1115, 2007.

[40] National Grid. Frequency response services [Online]. Available: `https://www.nationalgrideso.com/balancing-services/frequency-response-services`. Accessed September 5, 2018.

[41] NERC. United States Mandatory Standards Subject to Enforcement [Online]. Available: `https://www.nerc.com/pa/stand/Pages/ReliabilityStandardsUnitedStates.aspx?jurisdiction=United%20States`. Accessed June 25, 2018.

[42] ENTSO-E. Emergency and Restoration [Online]. Available: `https://www.entsoe.eu/network_codes/er/`. Accessed June 25, 2018.

[43] Prabhat Kumar and Dwarka P. Kothari. Recent philosophies of automatic generation control strategies in power systems. *IEEE Transactions on Power Systems*, 20(1):346–357, 2005.

[44] Ertuğrul Çam. Application of fuzzy logic for load frequency control of hydroelectrical power plants. *Energy Conversion and management*, 48(4):1281–1288, 2007.

[45] Surya Prakash and S. K. Sinha. Application of artificial intelligence in load frequency control of interconnected power system. *International Journal of Engineering, Science and Technology*, 3(4), 2011.

[46] Haluk Gozde, M. Cengiz Taplamacioglu, and Ilhan Kocaarslan. Comparative performance analysis of artificial bee colony algorithm in automatic generation control for interconnected reheat thermal power system. *International Journal of Electrical Power & Energy Systems*, 42(1):167–178, 2012.

[47] ENTSO-E. ENTSO-E Member Companies [Online]. Available: https://www.entsoe.eu/about/inside-entsoe/members/. Accessed June 25, 2018.

[48] Ofgem. The GB Electricity Transmission Network [Online]. Available: https://www.ofgem.gov.uk/electricity/transmission-networks/gb-electricity-transmission-network. Accessed June 25, 2018.

[49] National Grid. Mandatory response services (MFR) [Online]. Available: https://www.nationalgrideso.com/balancing-services/frequency-response-services/mandatory-response-services. Accessed September 5, 2018.

[50] National Grid. Firm frequency response (FFR) [Online]. Available: https://www.nationalgrideso.com/balancing-services/frequency-response-services/firm-frequency-response-ffr. Accessed September 5, 2018.

[51] National Grid. Enhanced frequency response (EFR) [Online]. Available: https://www.nationalgrideso.com/balancing-services/frequency-response-services/enhanced-frequency-response-efr. Accessed September 5, 2018.

[52] Ofgem. Changes to the Distribution Code and Engineering Recommendation G59: Frequency Changes during Large Disturbances and their Impact on the Total System [Online]. Available: https://www.ofgem.gov.uk/publications-and-updates/. Accessed February 5, 2016.

[53] National Grid. Frequency Changes during Large Disturbances and their Impact on the Total System [Online]. Available: http://www.nationalgrid.com/NR/rdonlyres/D3F18F81-BFE8-4BA1-8B82-CCD6CD0A0A4F/62018/GC0035IndustryConsultationv10.pdf/. Accessed February 5, 2016.

[54] RenewableUK. Offshore Wind Development Rounds [Online]. Available: https://web.archive.org/web/20140201235019/http://www.renewableuk.com/en/renewable-energy/wind-energy/offshore-wind/development-rounds.cfm. Accessed June 25, 2018.

[55] National Grid. Future Energy Scenario 2015 [Online]. Available: http://fes.nationalgrid.com/fes-document/. Accessed August 24, 2015.

[56] National Grid. Future Energy Scenario 2017 [Online]. Available: http://fes.nationalgrid.com/fes-document/. Accessed June 24, 2018.

[57] ELEXON. Elexon - Load Profiling [Online]. Available: http://www.elexon.co.uk/reference/technical-operations/profiling/. Accessed April 2, 2015.

[58] Ofgem. Distribution Code: DC0079 - Frequency Changes during Large Disturbances and their Impact on the Total System [Online]. Available: https://www.ofgem.gov.uk/system/files/docs/2018/05/dc0079_d.pdf. Accessed February 5, 2018.

[59] Set Muller, M. Deicke, and Rik W. De Doncker. Doubly fed induction generator systems for wind turbines. *IEEE Industry Applications Magazine*, 8(3):26–33, 2002.

[60] Nayeem Rahmat Ullah, Torbjörn Thiringer, and Daniel Karlsson. Temporary primary frequency control support by variable speed wind turbines—potential and applications. *IEEE Transactions on Power Systems*, 23(2):601–612, 2008.

[61] Feng Liu, Zhangwei Liu, Shengwei Mei, Wei Wei, and Yaxin Yao. ESO-based inertia emulation and rotor speed recovery control for dfigs. *IEEE Transactions on Energy Conversion*, 32(3):1209–1219, 2017.

[62] Andrea Bonfiglio, Marco Invernizzi, Alessandro Labella, and Renato Procopio. Design and implementation of a variable synthetic inertia controller for wind generating units. *IEEE Transactions on Power Systems*, 2018.

[63] Yannick Phulpin. Communication-free inertia and frequency control for wind generators connected by an HVDC-link. *IEEE Transactions on Power Systems*, 27(2):1136–1137, 2012.

[64] B. Silva, C. L. Moreira, L. Seca, Y. Phulpin, and J. A. Pecas Lopes. Provision of inertial and primary frequency control services using offshore multiterminal HVDC networks. *IEEE Transactions on Sustainable Energy*, 3(4):800–808, 2012.

[65] Nilanjan Ray Chaudhuri, Rajat Majumder, and Balarko Chaudhuri. System frequency support through multi-terminal DC (MTDC) grids. *IEEE Transactions on Power Systems*, 28(1):347–356, 2013.

[66] Yujun Li, Zeren Zhang, Yong Yang, Yingyi Li, Hairong Chen, and Zheng Xu. Coordinated control of wind farm and vsc–hvdc system using capacitor energy and kinetic energy to improve inertia level of power systems. *International Journal of Electrical Power & Energy Systems*, 59:79–92, 2014.

[67] Oluwole Daniel Adeuyi, Marc Cheah-Mane, Jun Liang, and Nick Jenkins. Fast frequency response from offshore multiterminal vsc–hvdc schemes. *IEEE Transactions on Power Delivery*, 32(6):2442–2452, 2017.

[68] Pascal Mercier, Rachid Cherkaoui, and Alexandre Oudalov. Optimizing a battery energy storage system for frequency control application in an isolated power system. *IEEE Transactions on Power Systems*, 24(3):1469–1477, 2009.

[69] Gauthier Delille, Bruno Francois, and Gilles Malarange. Dynamic frequency control support by energy storage to reduce the impact of wind and solar generation on isolated power system's inertia. *IEEE Transactions on Sustainable Energy*, 3(4):931–939, 2012.

[70] Yunfeng Wen, Chuangxin Guo, Daniel S. Kirschen, and Shufeng Dong. Enhanced security-constrained OPF with distributed battery energy storage. *IEEE Transactions on Power Systems*, 30(1):98–108, 2015.

[71] Bolun Xu, Yuanyuan Shi, Daniel S Kirschen, and Baosen Zhang. Optimal battery participation in frequency regulation markets. *IEEE Transactions on Power Systems*, 2018.

[72] Weifeng Li, Pengwei Du, and Ning Lu. Design of a new primary frequency control market for hosting frequency response reserve offers from both generators and loads. *IEEE Transactions on Smart Grid*, 2017.

[73] David P. Chassin, Zhenyu Huang, Matthew K. Donnelly, Candee Hassler, Enrique Ramirez, and Cody Ray. Estimation of WECC system inertia using observed frequency transients. *IEEE Transactions on Power Systems*, 20(2):1190–1192, 2005.

[74] Peter Wall, Francisco Gonzalez-Longatt, and Vladimir Terzija. Estimation of generator inertia available during a disturbance. In *Power and Energy Society General Meeting, 2012 IEEE*, pages 1–8. Citeseer, 2012.

[75] P. Wall, P. Regulski, Z. Rusidovic, and V. Terzija. Inertia estimation using PMUs in a laboratory. In *Innovative Smart Grid Technologies Conference Europe (ISGT-Europe), 2014 IEEE PES*, pages 1–6. IEEE, 2014.

[76] Peter Wall and Vladimir Terzija. Simultaneous estimation of the time of disturbance and inertia in power systems. *IEEE Transaction on Power Delivery*, 29(4):2018–2031, 2014.

[77] Govind Chavan, Matthew Weiss, Aranya Chakrabortty, Subhashish Bhattacharya, Armando Salazar, and Farrokh-Habibi Ashrafi. Identification and predictive analysis of a multi-area WECC power system model using synchrophasors. *IEEE Transactions on Smart Grid*, 8(4):1977–1986, 2017.

[78] Jose David Lara-Jimenez, Juan M. Ramırez, and Fernando Mancilla-David. Allocation of PMUs for power system-wide inertial frequency response estimation. *IET Generation, Transmission & Distribution*, 11(11):2902–2911, 2017.

[79] Phillip M. Ashton, Christopher S. Saunders, Gareth A. Taylor, Alex M. Carter, and Martin E. Bradley. Inertia estimation of the GB power system using synchrophasor measurements. *IEEE Transactions on Power Systems*, 30(2):701–709, 2015.

[80] Walter O. Stadlin. Economic allocation of regulating margin. *IEEE Transactions on Power Apparatus and Systems*, (4):1776–1781, 1971.

[81] Miguel A. Ortega-Vazquez and Daniel S. Kirschen. Estimating the spinning reserve requirements in systems with significant wind power generation penetration. *IEEE Transactions on Power Systems*, 24(1):114–124, 2009.

[82] Juan M. Morales, Antonio J Conejo, and Juan Pérez-Ruiz. Economic valuation of reserves in power systems with high penetration of wind power. *IEEE Transactions on Power Systems*, 24(2):900–910, 2009.

[83] Tsung-Ying Lee. Optimal spinning reserve for a wind-thermal power system using EIPSO. *IEEE Transactions on Power Systems*, 22(4):1612–1621, 2007.

[84] Yunfeng Wen, Wenyuan Li, Gang Huang, and Xuan Liu. Frequency dynamics constrained unit commitment with battery energy storage. *IEEE Transactions on Power Systems*, 31(6):5115–5125, 2016.

[85] Héctor Chávez, Ross Baldick, and Sandip Sharma. Governor rate-constrained opf for primary frequency control adequacy. *IEEE Transactions on Power Systems*, 29(3):1473–1480, 2014.

[86] Fei Teng, Vincenzo Trovato, and Goran Strbac. Stochastic scheduling with inertia-dependent fast frequency response requirements. *IEEE Transactions on Power Systems*, 31(2):1557–1566, 2016.

[87] Hamed Ahmadi and Hassan Ghasemi. Security-constrained unit commitment with linearized system frequency limit constraints. *IEEE Transactions on Power Systems*, 29(4):1536–1545, 2014.

[88] Yen-Yu Lee and Ross Baldick. A frequency-constrained stochastic economic dispatch model. *IEEE Transactions on Power Systems*, 28(3):2301–2312, 2013.

[89] Saleh Y. Abujarad, M. W. Mustafa, and J. J. Jamian. Recent approaches of unit commitment in the presence of intermittent renewable energy resources: A review. *Renewable and Sustainable Energy Reviews*, 70:215–223, 2017.

[90] Fei Teng, Yunfei Mu, Hongjie Jia, Jianzhong Wu, Pingliang Zeng, and Goran Strbac. Challenges on primary frequency control and potential solution from EVs in the future GB electricity system. *Applied energy*, 194:353–362, 2017.

[91] Vivek Prakash, Kailash Chand Sharma, Rohit Bhakar, Har Pal Tiwari, and Furong Li. Frequency response constrained modified interval scheduling under wind uncertainty. *IEEE Transactions on Sustainable Energy*, 9(1):302–310, 2018.

[92] Thaís de Fátima Araújo and Wadaed Uturbey. Performance assessment of PSO, DE and hybrid PSO-DE algorithms when applied to the dispatch of generation and demand. *International Journal of Electrical Power & Energy Systems*, 47:205–217, 2013.

[93] S. Goleijani, T. Ghanbarzadeh, F. Sadeghi Nikoo, and M. Parsa Moghaddam. Reliability constrained unit commitment in smart grid environment. *Electric Power Systems Research*, 97:100–108, 2013.

[94] Ning Zhang, Zhaoguang Hu, Daihong Dai, Shuping Dang, Mingtao Yao, and Yuhui Zhou. Unit commitment model in smart grid environment considering carbon emissions trading. *IEEE Transactions on Smart Grid*, 7(1):420–427, 2016.

[95] Fulin Zhuang and Frank D. Galiana. Towards a more rigorous and practical unit commitment by Lagrangian relaxation. *IEEE Transactions on Power Systems*, 3(2):763–773, 1988.

[96] Chenchen Yuan, Chenghong Gu, Furong Li, Bless Kuri, and Roderick W Dunn. New problem formulation of emission constrained generation mix. *IEEE Transactions on Power Systems*, 28(4):4064–4071, 2013.

[97] Erik Ela, Vahan Gevorgian, Aidan Tuohy, Brendan Kirby, Michael Milligan, and Mark O'Malley. Market designs for the primary frequency response ancillary

service—Part I: Motivation and design. *IEEE Transactions on Power Systems*, 29(1):421–431, 2014.

[98] R. Pearmine, Y. H. Song, T. G. Williams, and A. Chebbo. Identification of a load–frequency characteristic for allocation of spinning reserves on the British electricity grid. *IEE Proceedings-Generation, Transmission and Distribution*, 153(6):633–638, 2006.

[99] James W. Taylor and Matthew B. Roberts. Forecasting frequency-corrected electricity demand to support frequency control. *IEEE Transactions on Power Systems*, 31(3):1925–1932, 2016.

[100] National Grid. Electricity Ten Year Statement 2013 [Online]. Available: `http://www2.nationalgrid.com/UK/Industry-information/Future-of-Energy/Electricity-Ten-Year-Statement/`. Accessed February 5, 2016.

[101] National Grid. Electricity Ten Year Statement 2014 [Online]. Available: `https://www.nationalgrid.com/sites/default/files/documents/37790-ETYS%202014.pdf`. Accessed June 25, 2018.

[102] National Grid. Demand Data 2017 [Online]. Available: `https://www.nationalgrid.com/uk/electricity/market-operations-and-data/data-explorer/`. Accessed May 5, 2018.

[103] MathWorks. Polynomial curve fitting - polyfit [Online]. Available: `https://uk.mathworks.com/help/matlab/ref/polyfit.html?s_tid=srchtitle`. Accessed September 5, 2017.

[104] Eduard Muljadi, Vahan Gevorgian, Mohit Singh, and Surya Santoso. *Understanding inertial and frequency response of wind power plants*. IEEE, 2012.

[105] Peter Wall, Francisco González-Longatt, and Vladimir Terzija. Demonstration of an inertia constant estimation method through simulation. In *Universities Power Engineering Conference (UPEC), 2010 45th International*, pages 1–6. IEEE, 2010.

[106] Emmanuel B. Agamloh. Power and efficiency measurement of motor-variable-frequency drive systems. *IEEE Transactions on Industry Applications*, 53(1):766–773, 2017.

[107] Brendan J. Kirby, Jim Dyer, Carlos Martinez, Rahmat A. Shoureshi, Ross Guttromson, and Jeff Dagle. *Frequency control concerns in the North American electric power system.* United States. Department of Energy, 2003.

[108] I. A. Erinmez, D. O. Bickers, G. F. Wood, and W. W. Hung. NGC experience with frequency control in England and Wales-provision of frequency response by generators. In *Power Engineering Society 1999 Winter Meeting, IEEE*, volume 1, pages 590–596. IEEE, 1999.

[109] F. Gonzalez-Longatt. Frequency control and inertial response schemes for the future power networks. In *Large Scale Renewable Power Generation*, pages 193–231. Springer, 2014.

[110] Electricity National Control Centre. Historic frequency data [Online]. Available: `https://www.nationalgrideso.com/balancing-services/frequency-response-services/historic-frequency-data`. Accessed February 5, 2015.

[111] Amar Sahay. *Applied regression and modeling: a computer integrated approach.* Business Expert Press, 2016.

[112] Siemens. Turn down the power [Online]. Available: `http://www.industry.usa.siemens.com/drives/us/en/energy-efficiency/Pages/Turn-Down-the-Power.aspx`. Accessed August, 2017.

[113] EPSRC. Centre for Power Electronics [Online]. Available: `http://www.powerelectronics.ac.uk/research/drives.aspx`. Accessed August, 2017.

[114] Dimitris Bertsimas, Eugene Litvinov, Xu Andy Sun, Jinye Zhao, and Tongxin Zheng. Adaptive robust optimization for the security constrained unit commitment problem. *IEEE Transactions on Power Systems*, 28(1):52–63, 2013.

[115] IBM. CPLEX Optimizer [Online]. Available: `https://www.ibm.com/analytics/cplex-optimizer`. Accessed March 20, 2017.

[116] Tao Li and Mohammad Shahidehpour. Price-based unit commitment: A case of Lagrangian relaxation versus mixed integer programming. *IEEE Transactions on Power Systems*, 20(4):2015–2025, 2005.

[117] Tong Wu, Mark Rothleder, Ziad Alaywan, and Alex D. Papalexopoulos. Pricing energy and ancillary services in integrated market systems by an optimal power flow. *IEEE Transactions on Power Systems*, 19(1):339–347, 2004.

[118] Pengwei Du and Julia Matevosyan. Forecast system inertia condition and its impact to integrate more renewables. *IEEE Transactions on Smart Grid*, 9(2):1531–1533, 2018.

[119] Weerakorn Ongsakul and Nit Petcharaks. Unit commitment by enhanced adaptive Lagrangian relaxation. *IEEE Transactions on Power Systems*, 19(1):620–628, 2004.

[120] George Papaefthymiou and Bernd Klockl. MCMC for wind power simulation. *IEEE Transactions on Energy Conversion*, 23(1):234–240, 2008.

[121] Huazhang Huang and C. Y. Chung. Coordinated damping control design for DFIG-based wind generation considering power output variation. *IEEE Transactions on Power Systems*, 27(4):1916–1925, 2012.

[122] National Centers for Environmental Information. Hourly/Sub-Hourly Observational Data Map [Online]. Available: `https://gis.ncdc.noaa.gov/maps/ncei/cdo/hourly`. Accessed March 20, 2018.

[123] Mariano Ventosa, Alvaro Baıllo, Andrés Ramos, and Michel Rivier. Electricity market modeling trends. *Energy Policy*, 33(7):897–913, 2005.

[124] Zhi Zhou, Fei Zhao, and Jianhui Wang. Agent-based electricity market simulation with demand response from commercial buildings. *IEEE Transactions on Smart Grid*, 2(4):580–588, 2011.

[125] Jan Awrejcewicz. *Ordinary Differential Equations and Mechanical Systems*. Springer, 2014.

[126] Ravi P. Agarwal and Donal O'Regan. *Ordinary and partial differential equations: with special functions, Fourier series, and boundary value problems*. Springer Science & Business Media, 2008.